

Stable Signatures for Dynamic Graphs and Dynamic Metric Spaces via Zigzag Persistence

Woojin Kim¹ and Facundo Mémoli²

¹Department of Mathematics, The Ohio State University, kim.5235@osu.edu

²Department of Mathematics and Department of Computer Science and Engineering, The Ohio State University, memoli@math.osu.edu

April 11, 2022

Abstract

When studying flocking/swarming behaviors in animals one is interested in quantifying and comparing the dynamics of the clustering induced by the coalescence and disbanding of animals in different groups. In a similar vein, studying the dynamics of social networks leads to the problem of characterizing groups/communities as they form and disperse throughout time.

Motivated by this, we study the problem of obtaining persistent homology based summaries of time-dependent data. Given a finite dynamic graph (DG), we first construct a zigzag persistence module arising from linearizing the dynamic transitive graph naturally induced from the input DG. Based on standard results, we then obtain a persistence diagram or barcode from this zigzag persistence module. We prove that these barcodes are stable under perturbations in the input DG under a suitable distance between DGs that we identify.

More precisely, our stability theorem can be interpreted as providing a lower bound for the distance between DGs. Since it relies on barcodes, and their bottleneck distance, this lower bound can be computed in polynomial time from the DG inputs.

Since DGs can be given rise by applying the Rips functor (with a fixed threshold) to dynamic metric spaces, we are also able to derive related stable invariants for these richer class of dynamic objects.

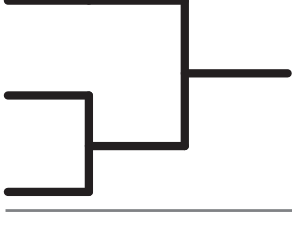
Along the way, we propose a summarization of dynamic graphs that captures their time-dependent clustering features which we call formigrams. These set-valued functions generalize the notion of dendrogram, a prevalent tool for hierarchical clustering. In order to elucidate the relationship between our distance between two DGs and the bottleneck distance between their associated barcodes, we exploit recent advances in the stability of zigzag persistence due to Botnan and Lesnick, and to Bjerkevik.

Contents

1	Introduction	3
2	Proof strategy for Theorem 1.1	7
3	Preliminaries	7
3.1	Category theory elements	7
3.2	Zigzag modules and their decompositions	9
3.3	Levelset zigzag persistence	11
4	Dynamic graphs (DGs)	12
5	Formigrams	13
5.1	Formigrams and their barcodes	13
5.2	From DGs to formigrams	18
5.3	The Reeb graph of a formigram	18
6	Metrics for DGs and formigrams	20
6.1	A distance between DGs	20
6.2	A distance between formigrams	23
7	The effect of smoothing operations	26
8	Dynamic directed graphs (DDGs)	29
8.1	From DDGs to formigrams	29
8.2	A distance between DDGs	30
8.3	Stability of clustering	31
9	Analysis of dynamic metric spaces (DMSs)	31
9.1	DMSs	32
9.2	From DMSs to DGs	33
9.3	The λ -slack interleaving distance between DMSs	34
10	Discussion	37
11	Details and Proofs	38
11.1	Details from Section 6	39
11.1.1	Details from Section 6.1	39
11.1.2	Details from Section 6.2	40
11.2	Details from Section 2	41
11.2.1	Interleavings and the bottleneck distance	42
11.2.2	\mathbf{U} -indexed diagrams induced by formigrams	42
11.2.3	Colimits of diagrams induced by formigrams	44
11.2.4	The Reeb cosheaf functor \mathcal{C}	45
11.3	Details from Section 7	46
11.4	Details from Section 9	49
11.4.1	Details from Section 9.2	49
11.4.2	Details from Section 9.3	50
11.4.3	The maximal groups [10] of DMSs and their clustering barcodes	53
11.5	Details from Section 10	54
11.5.1	Zigzag simplicial filtrations and their barcodes	54

1 Introduction

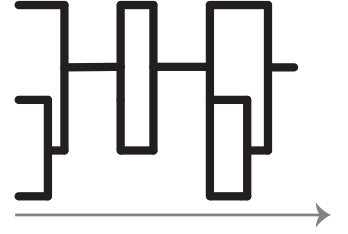
One of the most frequent tasks in data analysis consists of finding clusters in datasets. The most commonplace scenario is that of *static* datasets, which are often modeled as finite metric spaces (X, d_X) . There are two main formulations for this problem: flat and hierarchical clustering. In flat clustering, one aims at computing a single partition of X which subsumes intrinsic structure present in the data [34]. In hierarchical clustering, the goal is to find a hierarchical family of partitions X that captures multi-scale features present in the dataset. These hierarchical families of partitions are called *dendrograms* (see figure on the left) and from a graph theoretic perspective, they are planar, hence their visualization is straightforward. We study a related but different problem: clustering of *dynamic* data. We model dynamic datasets as time-varying (directed) graphs or time-varying finite



metric spaces and study a simple generalization of the notion of dendrogram which we call *formigram* (see figure on the right)– a combination of the words *formicarium*¹ and *diagram*. Whereas dendrograms are useful for modeling situations when data points *aggregate* along a certain scale parameter, formigrams are better suited for representing phenomena when data points may also separate or *disband* and then regroup at different parameter values.

One motivation for considering this scenario comes from the study and characterization of *flocking/swarming/herding* behavior of animals [4, 28, 29, 32, 42, 50, 53, 58], convoys [35], moving clusters [36], or mobile groups [33, 59].

As mentioned above, dendrograms can be represented by planar graphs, a fact that makes them very useful for exploratory data analysis due to their straightforward visualization. Formigrams, in contrast, are not always planar, so even if we argue that they arise naturally in the context of dynamic data clustering, more simplification is desirable in order to easily visualize the information they contain. We do this by associating zigzag persistent homology barcodes/diagrams [12] to formigrams. We prove that the resulting signatures turn



out to be (1) stable to perturbations of the input dynamic data and (2) still informative. The so called Single Linkage Hierarchical Clustering method [34] produces dendrograms from finite metric spaces in a stable manner: namely, if the input static datasets are close in the Gromov-Hausdorff sense, then the output dendrograms will also be close [14]. More generally, higher dimensional analogues of this result have also been established: the bottleneck distance between the persistence diagrams produced by the Rips filtration applied to two finite metric spaces is stable in the Gromov-Hausdorff sense [18]. In this paper we study to what extent one can export similar results to the case of dynamic datasets.

Overview of our results. We define a *dynamic graph* (DG) \mathcal{G}_X as a time series of graphs on a (potential) vertex set X induced by consecutive elementary graph operations: addition/deletion of vertices/edges. Regarding this sequence \mathcal{G}_X as a zigzag simplicial filtration (consisting solely of 1-dimensional simplicial complexes), we consider the 0-th (zigzag persistent) homology barcode of \mathcal{G}_X as a summary of clustering information of \mathcal{G}_X (see Figure 1). We show that the 0-th homology barcodes are stable invariants of dynamic graphs in terms of the bottleneck distance (between barcodes) [19] and the interleaving distance (between DGs), which we will define (Definition 6.9):

Theorem 1.1 (Stability theorem). Let $\mathcal{G}_X, \mathcal{G}_Y$ be any DGs over non-empty finite sets X and Y , respectively. Let $\text{dgm}_0(\mathcal{G}_X), \text{dgm}_0(\mathcal{G}_Y)$ be their *clustering barcodes*, respectively. Then,

$$d_B(\text{dgm}_0(\mathcal{G}_X), \text{dgm}_0(\mathcal{G}_Y)) \leq 2 d_1^{\text{dynG}}(\mathcal{G}_X, \mathcal{G}_Y).$$

¹A formicarium or ant farm is an enclosure for keeping ants under semi-natural conditions [61].

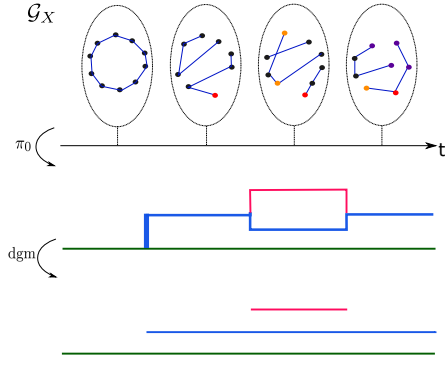


Figure 1: A dynamic graph (DG) \mathcal{G}_X (first row) is converted into a formigram (second row), and into a barcode (third row), summarizing its clustering information: In the first row, some different colors are assigned to vertices of \mathcal{G}_X according to their birth time.

Theorem 1.1 extends to the stability theorem regarding dynamic directed graphs (DDGs) and dynamic metric spaces (DMSs) (Theorems 8.11 and 9.21).

Along the way we introduce the notion of *formigrams*, both as a summary (akin to dendrograms) of the dynamic clustering behavior of a DG (see the second row of Figure 1) and as an object whose algebraic interpretation (via its zigzag persistence barcode) is parsimonious. Also, we define a notion of distance d_1^F between formigrams (Definition 6.26), which mediates between d_1^{dynG} and the bottleneck distance between barcodes. We remark that recent stability results for zigzag persistence due to Botnan and Lesnick [8] are essential to prove Theorems 1.1, 8.11, and 9.21. In addition, we present negative results about the extension of Theorem 9.21 to higher dimensional homology (Section 10).

An announcement of some of our results in Sections 5, 6, and 9 has appeared in [37]. A webpage dedicated to illustrating our theoretical framework via synthetic flocking models can be found at <https://research.math.osu.edu/networks/formigrams/>.

Overview of related work. In what follows, we review related work about characterizing or summarizing time-varying geometric data via persistent homology methods.

Vineyards as a signature for dynamic point clouds. In the same way that we associate persistence diagrams to any finite metric space by constructing filtrations such as the Čech or Rips filtration, we can also associate time-parametrized stacks of persistence diagrams, called *vineyards* [20], to any time-dependent metric data set. To the best of our knowledge, in [47] E. Munch first proved the stability of vineyards derived from dynamic point clouds in \mathbf{R}^d by defining metrics both for vineyards and for dynamic point clouds. Munch defined the distance between vineyards to be the integral of the bottleneck distance over time and the distance between dynamic point clouds in \mathbf{R}^d to be the integral of the Hausdorff distance over time. By doing so, a stability result is directly obtained [47, Theorem 17, Section 3] via the standard stability result of [18].

On the other hand, the nature of the barcodes that we will associate to dynamic graphs or dynamic metric spaces is distinct from that of vineyards.² While a vineyard is a stack of persistence diagrams where each persistence diagram retains the *multi-scale* topological information of a dynamic metric space *at a specific time*, what we will assign to a dynamic graph or dynamic metric space is a single diachronic persistence diagram: (1) for a dynamic graph, this diachronic persistence diagram reflects the evolution throughout time of its clustering features, and (2) for a dynamic metric space and fixed spatial scale $\delta \geq 0$, the diachronic persistence diagram reflects the evolution throughout time of the topology corresponding to the scale δ .

Dynamic graphs. M. Hajij et al. [30] provide a visualization of the structural changes in time-varying graphs using persistent homology. They embed each graph appearing in a sequence of graphs into a metric space, and then compute persistent homology of its corresponding Rips filtration. This process yields a collection C of time-stamped persistence diagrams. By applying classical multidimensional scaling, the collection C is turned into a real-valued time series that depicts the structural changes of the sequence of graphs.

Dynamic cubical complexes. R. González-Díaz et al. devise the so-called *spatiotemporal barcode* as a visual tool to encode the lifespan of connected components on an image sequence over time [27]. Given any

²A priori, there is no canonical way to associate a persistence diagram to a graph, and hence there is no canonical way to associate a vineyard to a dynamic graph.

binary image sequence, they construct a large cubical complex consisting of a *spatial subcomplex* and a *temporal subcomplex*. They filter this whole complex to obtain a spatiotemporal barcode. In contrast to [27], we will interrelate spatial complexes by inclusion maps and will obtain zigzag persistence barcodes directly.

Trajectory grouping structures. Let \mathcal{X} be a set of points having piecewise linear trajectories with time-stamped vertices in Euclidean space \mathbf{R}^d . Buchin and et al. [10] provided explicit algorithms for studying the grouping structure of \mathcal{X} . This was subsequently enriched in [40, 55, 56, 57]. In [10], a *group* (or cluster) is defined according to three different parameters: the size m of the group, the spatial cohesion parameter ε , and the time duration δ of the group. Namely, a set $G \subset \mathcal{X}$ forms an (m, ε, δ) -*group* during a time interval I if and only if (1) G contains at least m points, (2) the length of I is not less than δ and (3) for any two points $x, x' \in G$ and time $t \in I$, there is a chain $x = x_0, x_1, \dots, x_n = x'$ of points in \mathcal{X} such that any two consecutive ones are at distance $\leq \varepsilon$.

From the set \mathcal{X} of moving points, the authors of [10] construct a Reeb graph-like structure $\mathcal{R}_{\mathcal{X}}$ which is closely related to the Reeb graph of a *formigram* derived from \mathcal{X} that we introduce (Definition 5.4, Propositions 5.16, 9.5). The edges of $\mathcal{R}_{\mathcal{X}}$ are labeled by *maximal groups*, and they call $\mathcal{R}_{\mathcal{X}}$ together with these labels the *trajectory grouping structure* of \mathcal{X} , enabling the visualization of the life span of maximal groups. See Section 11.4.3 for comments on the relationship between the maximal groups of [10] and our clustering barcodes of DMSs.

Also, the authors of [10] propose a method (tuned by a temporal parameter α) for smoothing out their grouping structures. In short, this process consists of ignoring interruptions of disbanding/merging events in the original grouping structure of duration at most α .

Biological aggregation. Topological data analysis ideas have recently been used in studies of aggregation models for biological systems. In [54] the authors employ a certain 2D-plot of Betti numbers depending on both time and a scale parameter (which they use for constructing a Rips complex) in order to extract insights about the global behavior of aggregations. In [21] the authors explore zigzag persistent homology from a computational perspective in order to cluster different swarming behaviors of fish. They construct a certain time dependent simplicial complex by estimating at any given time how many individuals in the population of fish are visiting the different cells in a fixed triangulation of the area inside which they swim.³ Their model differs from ours in that we consider time-dependent (metric) Rips complexes induced by the configuration of points/particles at any given time.

Other work. Other work on constructing and maintaining simplified representations of time dependent data appears in [25] where the authors study Reeb graphs for dynamic data, in [60] where the authors study exploration/visualization techniques for tracking features of time varying data, in [49] where the authors study the computation and visualization of time dependent merge trees, and in [23, 24] where the authors discuss algorithmic complexity of certain problems related to clustering time dependent data.

Contributions. Our work provides a common framework that brings together ideas from [10, 57] and [21, 54].

- We define the notion of formigrams, as a generalization of dendrograms and treegrams [14, 52]. We observe that a formigram arises from a zigzag simplicial filtration as an analogue to the fact that a dendrogram arises from a simplicial filtration, both encoding clustering features of the given filtrations. In particular, formigrams can represent points which are born at a certain time and later die. This flexibility enables formigrams to encode clustering features of dynamic data consisting of both points with finite lifespan and points with infinite lifespan.
- For the analysis of DGs, DDGs and DMSs, we identify a condition that is required on DGs, DDGs, and DMSs, called *tameness*, to turn them into formigrams. Specifically, this sort of condition is not identified

³In fact they filter their fixed simplicial complex by a time dependent density function.

in [10] in the process to turn trajectory data into trajectory grouping structures. This condition is crucial to obtain barcodes from DGs, DDGs and DMSs. Barcodes not only provide succinct (planar) graphical summaries that can be computed in polynomial time [45], but also that they enable the (poly-time computable) quantification of the distance between any two time-varying data sets via the lower bound provided by our stability theorems (Theorems 1.1, 8.11, and 9.21).

- We identify precise notions of distance between pairs of DGs, DDGs, and DMSs. We expect these metric will be useful to people working in related fields. The desire to obtain such a precise quantification of the difference between two dynamic clusterings was already made explicit in [10, Section 6].

These distance admit poly-time computable lower bounds in terms of the bottleneck distance between the zigzag persistence diagrams/barcodes associated to DGs, DDGs, and DMSs, respectively. These lower bounds can then be used in applications where one may want to classify different flocking/swarming behaviors (see our experiments [39]). Dually, our results establish the stability/robustness of our methods for clustering DGs, DDGs, and DMSs – a property of chief importance for applications. Furthermore, we construct a precise notion of distance between formigrams (Definition 6.26, which is inspired by [22] and comes together with the stability results given in Theorem 6.32 and Proposition 11.9).

- In line with the ideas of the α -smoothing operation on grouping structures in [10], we further clarify how the α -smoothed grouping structure (the α -smoothed-out formigram in our language) is obtained via the computation of finest common coarsening of partitions (Section 6.2) and thereby precisely characterize what is the effect of the α -smoothing process on the barcode of formigrams (Proposition 7.1). Our work establishes a connection between this α -smoothing of grouping structures with the notion of Reeb graph smoothing studied in [22].

Organization. In Section 2, we outline the proof of our main stability result. Section 3 introduces some categories and functors that we will consider, and also contains a review of zigzag persistence. Section 4 introduces the notion of dynamic graph. Section 5 introduces the notions of formigrams, their barcodes, and their Reeb graphs. In particular, we also discuss how to turn any dynamic graph into a formigram. Section 6 introduces suitable notions of distance between dynamic graphs and between formigrams. The construction of both distances depends on the notion of smoothing operation, which will be discussed in Section 7 more in detail. Sections 8 and 9 introduce the notions of dynamic directed graphs and dynamic metric spaces and suitable notions of distance between. We will see that the clustering features of dynamic directed graphs, and dynamic metric spaces can also be encoded into formigrams, Reeb graphs, and barcodes in a stable way. In Section 10, we discuss high dimensional homology barcodes of dynamic metric spaces, and computational experiments. Some details and proofs pertaining to Sections 6 - 10 are deferred to Section 11.

Conventions. We declare some conventions that we will follow throughout this paper.

- X, Y, Z and W will stand for non-empty finite sets unless there is any other specification.
- We fix a field \mathbb{F} and only consider vector spaces over \mathbb{F} whenever they arise.
- The topology on any finite set will be the discrete topology.

Acknowledgements. This work was partially supported by NSF grants IIS-1422400, CCF-1526513, DMS-1723003, and CCF-1740761. We thank Zane Smith for providing an example of non-planar formigram in Example 5.21. Also, we thank Michael Lesnick for useful comments about the paper and for suggesting a proof strategy for Proposition 11.21.

2 Proof strategy for Theorem 1.1

In this section we discuss the proof of Theorem 1.1 from a broad outlook. This proof invokes several ideas and results due to Botnan and Lesnick [8] regarding the stability of zigzag persistence, and also a recent improvement by Bjerkevik [5]. In the course of sketching the proof of Theorem 1.1 we will refer to the diagram shown in Figure 2.

Sketch of Proof of Theorem 1.1. The stability theorem (Theorem 1.1) is established by proving that each one of the four successive processes $\boxed{A} \rightarrow \boxed{B} \rightarrow \boxed{C} \rightarrow \boxed{D} \rightarrow \boxed{E}$ illustrated in Figure 2 is stable with respect to the metrics d_1^{dynG} , d_1^F , d_I , $d_{B,2}$, d_B , respectively. Let \mathcal{G}_X and \mathcal{G}_Y be any DGs over X and Y , respectively. Let $\theta_X := \pi_0(\mathcal{G}_X)$ and $\theta_Y := \pi_0(\mathcal{G}_Y)$ (Definition 5.15 and Proposition 5.16). Then, we have

$$\begin{aligned}
& d_B(\text{dgm}(\theta_X), \text{dgm}(\theta_Y)) \\
&= d_B(\mathcal{L}_0(\mathbf{Reeb}(\theta_X)), \mathcal{L}_0(\mathbf{Reeb}(\theta_Y))) && \text{Proposition 5.22} \\
&\leq 2 d_I(E_{\mathbf{Sets}}(\theta_X), E_{\mathbf{Sets}}(\theta_Y)) && \text{Corollary 11.19} \\
&\leq 2 d_1^F(\theta_X, \theta_Y) && \text{Proposition 11.9} \\
&\leq 2 d_1^{\text{dynG}}(\mathcal{G}_X, \mathcal{G}_Y) && \text{Theorem 6.32,}
\end{aligned}$$

where $\mathcal{L}_0(\mathbf{Reeb}(\theta_X))$ and $\mathcal{L}_0(\mathbf{Reeb}(\theta_Y))$ are the 0-th levelset barcodes of the Reeb graphs of the formigrams θ_X and θ_Y , respectively (see Sections 3.3, 5.1). \square

3 Preliminaries

We now introduce some categories and functors that we will consider throughout the paper (Section 3.1). We also review the notions of zigzag modules (Section 3.2) and levelset zigzag persistence (Section 3.3).

3.1 Category theory elements

Given any category \mathbf{C} , we will denote the collection of objects in \mathbf{C} by $\text{Ob}(\mathbf{C})$. Any non-empty set with a partial order determines a *poset*. Given a poset \mathbf{P} , we call any subset \mathbf{Q} of \mathbf{P} with the partial order obtained by restricting that of \mathbf{P} to \mathbf{Q} a *sub-poset of \mathbf{P}* . We will consider the following categories and functors. Consult [43] for general definitions related to category theory.

1. Any poset \mathbf{P} will be considered as a category: Objects are elements in \mathbf{P} . For any $p, q \in \mathbf{P}$, there exists a unique morphism $p \rightarrow q$ if and only if $p \leq q$. Therefore, $p \leq q$ in \mathbf{P} will denote the unique morphism $p \rightarrow q$. Any sub-poset \mathbf{Q} of \mathbf{P} is a full subcategory of \mathbf{P} .
2. The category **Sets** consists of sets with functions.
3. The category **Vec** consists of finite-dimensional vector spaces over \mathbb{F} with linear maps.
4. The category **Met** of finite metric spaces with 1-Lipschitz maps [15].
5. The category **Top** of topological spaces with continuous maps.
6. The category **Simp** of abstract simplicial complexes with simplicial maps (consult [48]).
7. The category **Graph** consists of the following:
 - Objects: pairs $G_X = (X, E_X)$ consisting of a vertex set X and an edge set E_X , where E_X is a collection of two-point multisets consisting of points in X . Specifically, for any $x \in X$, the multiset $\{x, x\}$ can be included in E_X , implying the existence of the self-loop at x in G_X . However, there can be no multiple edges that connect the same two vertices.

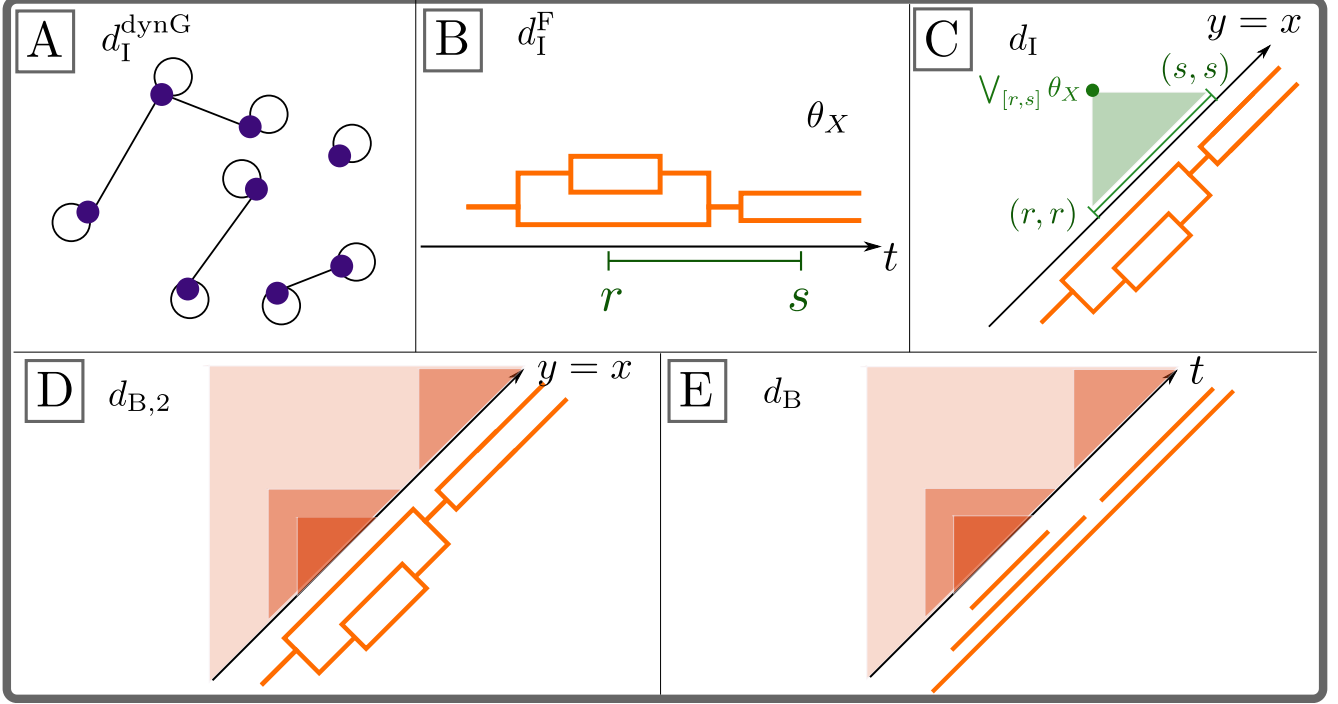


Figure 2: The four successive processes $\boxed{\text{A}} \rightarrow \boxed{\text{B}} \rightarrow \boxed{\text{C}} \rightarrow \boxed{\text{D}} \rightarrow \boxed{\text{E}}$ taking a DG to its clustering barcode over the real line \mathbf{R} (\mathbf{R} stands for time). Suppose that a DG \mathcal{G}_X over X is given, as illustrated in panel $\boxed{\text{A}}$ (Definition 4.1). For $x, x' \in X$ and $t \in \mathbf{R}$, x and x' belong to the same block of the sub-partition $\theta_X(t) := \pi_0(\mathcal{G}_X(t))$ of X if and only if x and x' belong to the same connected components. Stacking up these sub-partitions across time gives rise to a *formigram* $\theta_X = \pi_0(\mathcal{G}_X)$, as illustrated in panel $\boxed{\text{B}}$ (Definition 5.4, Definition 5.15, Proposition 5.16). Next, we extend θ_X to the upper-half $\mathbf{U} = \{(x, y) \in \mathbf{R}^2 : x \leq y\}$ of the Euclidean plane via the finest common coarsening of sub-partitions of X over real intervals (Definition 6.17) as depicted in panel $\boxed{\text{C}}$: For $r \leq s$, the sub-partition associated to $(r, s) \in \mathbf{U}$ is the finest common coarsening of the collection $\{\theta_X(t) : r \leq t \leq s\}$ of sub-partitions of X . This gives rise to a functor $E_{\mathbf{Sets}}(\theta_X) : \mathbf{U} \rightarrow \mathbf{Sets}$ (Definition 11.8). Composing the free functor $\mathfrak{V}_{\mathbb{F}} : \mathbf{Sets} \rightarrow \mathbf{Vec}$ (item 18 in Section 3.1) with $E_{\mathbf{Sets}}(\theta_X)$ on the left yields a 2-D persistence module $E_{\mathbf{Vec}}(\theta_X)$ (Definition 11.8). By virtue of Proposition 11.17 together with [8, Theorem 4.7, (i)] $E_{\mathbf{Vec}}(\theta_X)$ is *block decomposable*. Each block factor of $E_{\mathbf{Vec}}(\theta_X)$ is a convex region touching the line $y = x$ as depicted in panel $\boxed{\text{D}}$. The intersections of those regions with the line $y = x$ constitute the barcode $\text{dgm}(\theta_X)$ of θ_X via the identification $(t, t) \leftrightarrow t$ as illustrated in panel $\boxed{\text{E}}$ (Proposition 11.23). At each step of $\boxed{\text{A}}, \boxed{\text{B}}, \boxed{\text{C}}, \boxed{\text{D}}, \boxed{\text{E}}$, we have a metric $d_I^{\text{dynG}}, d_I^F, d_I, d_{B,2}, d_B$, respectively (Definitions 6.9, 6.26, 11.6, [8, Section 2.3], and Definition 11.7), in order. Theorem 1.1 basically follows from the stability of each of the processes $\boxed{\text{A}} \rightarrow \boxed{\text{B}} \rightarrow \boxed{\text{C}} \rightarrow \boxed{\text{D}} \rightarrow \boxed{\text{E}}$ with respect to the involved metrics.

- Morphisms: given any graphs $G_X = (X, E_X)$ and $G_Y = (Y, E_Y)$ over vertex sets X and Y respectively, a map $f : X \rightarrow Y$ will be said to be a *graph morphism* if $\{x, x'\} \in E_X$ implies $\{f(x), f(x')\} \in E_Y$.

There exists the canonical functor $F : \mathbf{Graph} \rightarrow \mathbf{Simp}$ sending each graph G_X to the 1-dimensional simplicial complex which is obtained by getting rid of all self-loops in G_X .

8. The category **Digraph** consists of the following:

- Objects: pairs $\overrightarrow{G_X} = (X, A_X)$ consisting of a vertex set X and a directed edge set A_X , where A_X is a subset of $X \times X$ (thus, self-loops are allowed).
- Morphisms: given any digraphs $\overrightarrow{G_X} = (X, A_X)$ and $\overrightarrow{G_Y} = (Y, A_Y)$ over vertex sets X and Y respectively, a map $f : X \rightarrow Y$ will be said to be a *digraph morphism* if $(x, x') \in A_X$ implies $(f(x), f(x')) \in A_Y$.

9. The poset \mathbf{R}^n with order $(a_1, a_2, \dots, a_n) \leq (b_1, b_2, \dots, b_n)$ if and only if $a_i \leq b_i$ for all $1 \leq i \leq n$.

10. The poset $\mathbf{R}^{\text{op}} \times \mathbf{R}$ where $(a_1, a_2) \leq (b_1, b_2)$ if and only if $a_1 \geq b_1$ and $a_2 \leq b_2$ for the usual order \leq on \mathbf{R} .

11. The poset \mathbf{U} is the sub-poset of $\mathbf{R}^{\text{op}} \times \mathbf{R}$ consisting of objects (a, b) with $a \leq b$.

12. The poset \mathbf{ZZ} is the sub-poset of $\mathbf{R}^{\text{op}} \times \mathbf{R}$ given by $\mathbf{ZZ} := \{(k, l) : k \in \mathbf{Z}, l \in \{k, k-1\}\}$.

13. For two categories \mathbf{C} and \mathbf{D} , the category $\mathbf{C}^{\mathbf{D}}$ stands for the category of functors from \mathbf{D} to \mathbf{C} with objects functors $\mathbf{C} \rightarrow \mathbf{D}$ and arrows natural transformations.

14. For two functors $F, G : \mathbf{C} \rightarrow \mathbf{D}$, we write $F \cong G$ whenever F and G are naturally isomorphic, i.e. there exists a natural transformation $\tau : F \rightarrow G$ such that $\tau_c : F(c) \rightarrow G(c)$ is invertible for each $c \in \text{Ob}(\mathbf{C})$ (see [43, p.16] for details).

15. For $\delta \geq 0$, $\mathcal{R}_\delta : \mathbf{Met} \rightarrow \mathbf{Simp}$ is the δ -Rips functor defined as follows: Given any finite metric space (X, d_X) , $\mathcal{R}_\delta(X, d_X)$ is the abstract simplicial complex on the set X where $X \supset \sigma \in \mathcal{R}_\delta(X, d_X)$ if and only if $\text{diam}(\sigma) \leq \delta$. For any arrow $f : (X, d_X) \rightarrow (Y, d_Y)$ in \mathbf{Met} , $\mathcal{R}_\delta(f) : \mathcal{R}_\delta(X) \rightarrow \mathcal{R}_\delta(Y)$ is defined to be the same map as f and this is a simplicial map since f is distance non-increasing map.

16. For $\delta \geq 0$, $\mathcal{R}_\delta^1 : \mathbf{Met} \rightarrow \mathbf{Graph}$ is the δ -Rips graph functor, i.e. for any finite metric space (X, d_X) , $\mathcal{R}_\delta^1(X, d_X)$ is the graph on the vertex set X with the edge set $E_X = \{\{x, x'\} : d_X(x, x') \leq \delta\}$ (note that by definition every vertex x of the graph $\mathcal{R}_\delta^1(X, d_X)$ has the self-loop $\{x, x\}$ in E_X).

17. For each $k \in \mathbf{Z}_+$, we have the k -th simplicial homology functor $H_k : \mathbf{Simp} \rightarrow \mathbf{Vec}$ and the k -th singular homology functor $H_k : \mathbf{Top} \rightarrow \mathbf{Vec}$ with coefficients in the field \mathbb{F} . Consult [31, 48] for a general reference.

18. We will use the free functor $\mathfrak{V}_{\mathbb{F}} : \mathbf{Sets} \rightarrow \mathbf{Vec}$, see Chapter IV of [43] for a general reference. Namely, given a set S , $\mathfrak{V}_{\mathbb{F}}(S)$ consists of formal linear combinations $\sum_i a_i s_i$ ($a_i \in \mathbb{F}$, $s_i \in S$) of finite terms of elements in S over the field \mathbb{F} . Also, given a set map $f : S \rightarrow T$, $\mathfrak{V}_{\mathbb{F}}(f)$ is the linear map from $\mathfrak{V}_{\mathbb{F}}(S)$ to $\mathfrak{V}_{\mathbb{F}}(T)$ obtained by linearly extending f .

3.2 Zigzag modules and their decompositions

We generally follow the notation/definition from [8] in the following. For \mathbf{P} a poset and \mathbf{C} an arbitrary category, $F : \mathbf{P} \rightarrow \mathbf{C}$ a functor, and $s, t \in \mathbf{P}$, let $F_s := F(s)$. Also, let $\varphi_F(s, t) : F_s \rightarrow F_t$ denote the morphism $F(s \leq t)$. We refer to the morphisms $\varphi_F(s, t) : F_s \rightarrow F_t$ for $s \leq t$ in \mathbf{P} as *internal maps* of F in the case the morphisms in \mathbf{C} are maps. Also, any functor $F : \mathbf{P} \rightarrow \mathbf{Vec}$ is called a **P-indexed module**.

Definition 3.1 (Intervals, [8]). Given a poset \mathbf{P} , an *interval* \mathcal{I} of \mathbf{P} is any subset $\mathcal{I} \subset \mathbf{P}$ such that

1. \mathcal{I} is non-empty.

2. If $r, t \in \mathcal{J}$ and $r \leq s \leq t$, then $s \in \mathcal{J}$.
3. (connectivity) For any $s, t \in \mathcal{J}$, there is a sequence $s = s_0, s_1, \dots, s_l = t$ of elements of \mathcal{J} with s_i and s_{i+1} comparable for $0 \leq i \leq l-1$.

For \mathcal{J} an interval of \mathbf{P} , the *interval module* $I^{\mathcal{J}} : \mathbf{P} \rightarrow \mathbf{Vec}$ is the \mathbf{P} -indexed module where

$$I_t^{\mathcal{J}} = \begin{cases} \mathbb{F} & \text{if } t \in \mathcal{J}, \\ 0 & \text{otherwise.} \end{cases} \quad \varphi_{I^{\mathcal{J}}}(s, t) = \begin{cases} \text{id}_{\mathbb{F}} & \text{if } s, t \in \mathcal{J}, s \leq t, \\ 0 & \text{otherwise.} \end{cases}$$

Let F, G be \mathbf{P} -indexed modules. The *direct sum* $F \oplus G$ of F and G is the \mathbf{P} -indexed module defined as follows: for all $s \in \mathbf{P}$, $(F \oplus G)_s := F_s \oplus G_s$ and for all $s \leq t$ in \mathbf{P} , the linear map $\varphi_{F \oplus G}(s, t) : (F \oplus G)_s \rightarrow (F \oplus G)_t$ is defined by

$$\varphi_{F \oplus G}(s, t)(v, w) := (\varphi_F(s, t)(v), \varphi_G(s, t)(w))$$

for all $(v, w) \in (F \oplus G)_s$. We say a \mathbf{P} -indexed module F is *decomposable* if F is (naturally) isomorphic to $G_1 \oplus G_2$ for some non-trivial \mathbf{P} -indexed modules G_1 and G_2 and we denote it by $F \cong G_1 \oplus G_2$ (this notation is defined in item 14 in Section 3.1). Otherwise, we say that F is *indecomposable*.

Proposition 3.2 (Proposition 2.2 in [8]). $I^{\mathcal{J}}$ is indecomposable.

Recall that a *multiset* is a generalized notion of a set in that a multiset allows multiple instances of the multiset's elements (but the order of the elements does not matter). We call the number of instances of an element in a specific multiset the *multiplicity* of the element. For example, $A = \{x, x, y\}$ is a multiset and the multiplicity of x is two. Also, this multiset A is distinct from the multiset $\{x, y\}$.

A \mathbf{P} -indexed module F is *interval decomposable* if there exists a multiset $\mathcal{B}(F)$ of intervals in \mathbf{P} such that

$$F \cong \bigoplus_{\mathcal{J} \in \mathcal{B}(F)} I^{\mathcal{J}}.$$

It is well-known that, by the theorem of Azumaya-Krull-Remak-Schmidt [1], such a decomposition is unique up to a permutation of the terms in the direct sum. Therefore, the multiset $\mathcal{B}(F)$ is unique if F is interval decomposable since a multiset does not care about the order of its elements. We call $\mathcal{B}(F)$ the *barcode* of F .

Remark 3.3. In this paper, we are mainly interested in \mathbf{ZZ} -indexed modules $F : \mathbf{ZZ} \rightarrow \mathbf{Vec}$ such that for all $s \in \mathbf{ZZ}$, F_s is a finite dimensional vector space. We refer to such F simply as *zigzag modules*. Note that every zigzag module F has a unique barcode [7], and we denote its barcode by $\text{dgm}(F)$.

Remark 3.4. Notation introduced in [8] is useful to describe barcodes of zigzag modules: Letting $<$ denote the strict partial order on \mathbf{Z}^2 (not on $\mathbf{Z}^{\text{op}} \times \mathbf{Z}$), any intervals of \mathbf{ZZ} fall into the four types as follows:

$$\begin{aligned} \langle b, d \rangle_{\mathbf{ZZ}} &:= \{(i, j) \in \mathbf{ZZ} : (b, b) < (i, j) < (d, d)\} && \text{for } b < d \in \mathbf{Z} \cup \{-\infty, \infty\}, \\ [b, d]_{\mathbf{ZZ}} &:= \{(i, j) \in \mathbf{ZZ} : (b, b) \leq (i, j) < (d, d)\} && \text{for } b < d \in \mathbf{Z} \cup \{\infty\}, \\ \langle b, d \rangle_{\mathbf{ZZ}} &:= \{(i, j) \in \mathbf{ZZ} : (b, b) < (i, j) \leq (d, d)\} && \text{for } b < d \in \mathbf{Z} \cup \{-\infty\}, \\ [b, d]_{\mathbf{ZZ}} &:= \{(i, j) \in \mathbf{ZZ} : (b, b) \leq (i, j) \leq (d, d)\} && \text{for } b \leq d \in \mathbf{Z}. \end{aligned}$$

See Figure 3 for examples. Specifically, we let $\langle b, d \rangle_{\mathbf{ZZ}}$ denote any of the above sets without specifying its type.

Theorem 3.5 ([7]). Any zigzag module $F : \mathbf{ZZ} \rightarrow \mathbf{Vec}$ is decomposed as

$$F \cong \bigoplus_{j \in J} I^{\langle b_j, d_j \rangle_{\mathbf{ZZ}}}$$

for some index set J uniquely up to a permutation of the terms in the direct sum. Thus we have the barcode $\text{dgm}(F) = \{\langle b_j, d_j \rangle_{\mathbf{ZZ}} : j \in J\}$ of F .

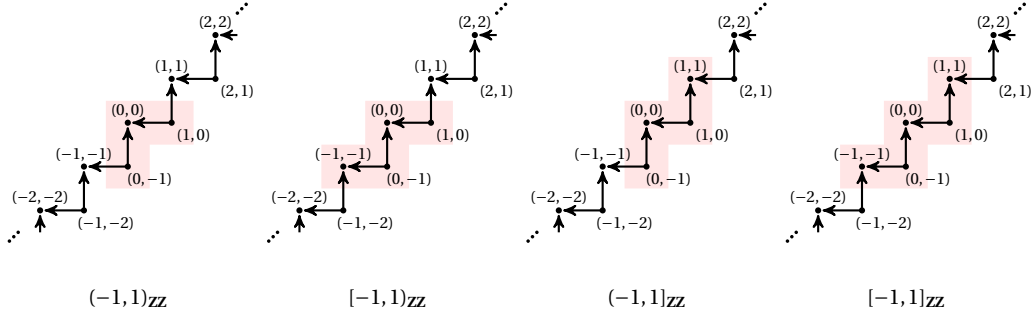


Figure 3: The points falling into the shaded regions comprise the intervals $(-1, 1)_{\mathbf{ZZ}}$, $[-1, 1)_{\mathbf{ZZ}}$, $(-1, 1]_{\mathbf{ZZ}}$ and $[-1, 1]_{\mathbf{ZZ}}$ of the poset \mathbf{ZZ} , respectively in order.

3.3 Levelset zigzag persistence

We review the notion of levelset zigzag persistence for functions of *Morse type* from [8, 13].

Definition 3.6 (Morse type functions). Let T be a topological space. We say that a continuous function $f : T \rightarrow \mathbf{R}$ is of *Morse type* if

- (i) There exists a strictly increasing function $\mathcal{G} : \mathbf{Z} \rightarrow \mathbf{R}$ such that $\lim_{i \rightarrow +\infty} \mathcal{G}(i) = \infty$, $\lim_{i \rightarrow -\infty} \mathcal{G}(i) = -\infty$ and such that for each open interval $I_i = (\mathcal{G}(i), \mathcal{G}(i+1))$ there exist a topological space Y_i and a homeomorphism $h_i : I_i \times Y_i \rightarrow f^{-1}(I_i)$ with $f \circ h_i$ being the projection $I_i \times Y_i \rightarrow I_i$.
- (ii) Each homeomorphism $h_i : I_i \times Y_i \rightarrow f^{-1}(I_i)$ extends to a continuous function

$$\bar{h}_i : \bar{I}_i \times Y_i \rightarrow f^{-1}(\bar{I}_i),$$

where \bar{I}_i denotes the closure of I_i .

- (iii) For all $t \in \mathbf{R}$ and $k \in \mathbf{Z}_+$, $\dim H_k(f^{-1}(t)) < \infty$.

Let $f : T \rightarrow \mathbf{R}$ be any function of Morse type and let $\mathcal{G} : \mathbf{Z} \rightarrow \mathbf{R}$ be any strictly increasing function as in Definition 3.6 (i). For $i \in \mathbf{Z}$, let $c_i := \mathcal{G}(i)$ and pick any $s_i \in (c_i, c_{i+1})$. Then, we have the following diagram in the category **Top**:

$$\begin{array}{ccccccc} & & f^{-1}([s_{-2}, s_{-1}]) & & f^{-1}([s_{-1}, s_0]) & & f^{-1}([s_0, s_1]) & & \\ & \nearrow & & \nwarrow & \nearrow & & \nwarrow & & \\ \mathbb{T}_f : & \cdots & & & & & & & \cdots \\ & & & f^{-1}(s_{-1}) & & f^{-1}(s_0) & & & \end{array} \quad (1)$$

where all the arrows stand for inclusions. By virtue of the product structure between critical values c_i , the topological spaces that appear in the diagram of $H_k(\mathbb{T}_f)$ are independent of the choice of intermediate values s_i . For $k \in \mathbf{Z}_+$, by applying the k -th singular homology functor $H_k : \mathbf{Top} \rightarrow \mathbf{Vec}$ (with coefficients in the field \mathbb{F}) to \mathbb{T}_f , we obtain:

$$\begin{array}{ccccccc} & & H_k(f^{-1}([s_{-2}, s_{-1}])) & & H_k(f^{-1}([s_{-1}, s_0])) & & H_k(f^{-1}([s_0, s_1])) & & \\ & \nearrow & & \nwarrow & \nearrow & & \nwarrow & & \\ H_k(\mathbb{T}_f) : & \cdots & & & & & & & \cdots \\ & & & H_k(f^{-1}(s_{-1})) & & H_k(f^{-1}(s_0)) & & & \end{array} \quad (2)$$

For each $i \in \mathbb{Z}$, let us index $H_k(f^{-1}[s_{i-1}, s_i])$ and $H_k(f^{-1}(s_i))$ by (i, i) and $(i+1, i)$ in \mathbb{ZZ} , respectively. Then, $H_k(\mathbb{T}_f)$ can be seen as a functor $\mathbb{ZZ} \rightarrow \mathbf{Vec}$ and thus by Theorem 3.5, $H_k(\mathbb{T}_f)$ admits a barcode $\text{dgm}(H_k(\mathbb{T}_f))$. Let $c_{-\infty} := -\infty$ and $c_{\infty} := \infty$. We obtain the k -th levelset barcode $\mathcal{L}_k(T, f)$ of the pair (T, f) by the following substitution rule (see Remark 3.4):

$$\begin{array}{ccc} \text{dgm}(H_k(\mathbb{T}_f)) & & \mathcal{L}_k(T, f) \\ \hline (m, n)_{\mathbb{ZZ}} & \leftrightarrow & (c_m, c_n) \\ [m, n]_{\mathbb{ZZ}} & \leftrightarrow & [c_m, c_n] \\ (m, n]_{\mathbb{ZZ}} & \leftrightarrow & (c_m, c_n] \\ [m, n]_{\mathbb{ZZ}} & \leftrightarrow & [c_m, c_n]. \end{array} \quad (3)$$

Definition 3.7 (Levelset barcodes). Let T be a topological space and let $f : T \rightarrow \mathbf{R}$ be of Morse type. For each $k \in \mathbb{Z}_+$, the k -th levelset barcode of the pair (T, f) is defined as the multiset described above which we henceforth denote by $\mathcal{L}_k(T, f)$.

4 Dynamic graphs (DGs)

In this section we define *dynamic graphs* as a model for time varying graph theoretic structures. For a set X , let $\text{pow}(X)$ be the power set of X and let $\text{pow}_2(X) = \{X' : X' \text{ is a multiset consisting of elements in } X \text{ with } |X'| = 2\}$. Note that given any graph $G_X = (X, E_X)$, its edge set E_X is an element of $\text{pow}(\text{pow}_2(X))$.

Definition 4.1 (Dynamic graphs). A *dynamic graph* (DG) \mathcal{G}_X over X is a pair of maps

$$V_X(\cdot) : \mathbf{R} \rightarrow \text{pow}(X) \quad \text{and} \quad E_X(\cdot) : \mathbf{R} \rightarrow \text{pow}(\text{pow}_2(X)),$$

satisfying the conditions below. By $\text{crit}(\mathcal{G}_X)$ we denote the union of the set of points of discontinuity of $V_X(\cdot)$ and the set of points of discontinuity of $E_X(\cdot)$. We call the elements of $\text{crit}(\mathcal{G}_X)$ the *critical points* of \mathcal{G}_X . We require $\mathcal{G}_X = (V_X(\cdot), E_X(\cdot))$ to satisfy the following:

- (i) (Self-loops) For all $t \in \mathbf{R}$ and for all $x \in V_X(t)$, $\{x, x\} \in E_X(t)$.
- (ii) (Tameness) The set $\text{crit}(\mathcal{G}_X)$ is locally finite.⁴
- (iii) (Lifespan of vertices) for every $x \in X$, the set $I_x := \{t \in \mathbf{R} : x \in V_X(t)\}$, said to be the *lifespan* of x , is a non-empty interval.
- (iv) (Comparability) for every $t \in \mathbf{R}$, it holds that

$$V_X(t - \varepsilon) \subset V_X(t) \supset V_X(t + \varepsilon) \text{ and } E_X(t - \varepsilon) \subset E_X(t) \supset E_X(t + \varepsilon)$$

for all sufficiently small $\varepsilon > 0$ (concisely, we will re-write this as $\mathcal{G}_X(t - \varepsilon) \subset \mathcal{G}_X(t) \supset \mathcal{G}_X(t + \varepsilon)$).

In plain words, a DG can be regarded as a graph that is subjected to a sequence of updates such as addition/deletion of vertices/edges.

Remark 4.2 (Comments on Definition 4.1). We remark the following:

- (i) The ‘self-loops’ condition of Definition 4.1 (i) is introduced for purely technical reasons since it helps ease notation in defining a distance between DGs in Section 6.
- (ii) Definition 4.1 (iv) implies that \mathcal{G}_X is locally maximum at critical points. Namely, for any $c \in \text{crit}(\mathcal{G}_X)$, at least one of the inclusions $\mathcal{G}_X(c - \varepsilon) \subset \mathcal{G}_X(c) \supset \mathcal{G}_X(c + \varepsilon)$ is strict for all sufficiently small $\varepsilon > 0$.

⁴To say that $A \subset \mathbf{R}$ is locally finite means that for any bounded interval $I \subset \mathbf{R}$, the cardinality of $I \cap A$ is finite.

- (iii) (Lifespan of vertices and edges) Definition 4.1 (iii), (iv) together implies that the lifespan of vertices in a DG are non-empty closed intervals. Also, Definition 4.1 (iii) implies that the lifespan of edges in a DG are a (possibly empty) union of closed intervals.

Example 4.3 (Special cases). (i) (Saturated DGs) Given a DG $\mathcal{G}_X = (V_X(\cdot), E_X(\cdot))$, if $V_X(\cdot) \equiv X$, then we will call \mathcal{G}_X *saturated*. In plain words, all the vertices of a saturated DG are always present in the time series of graphs (but edges that are connecting two different vertices can flicker over time).

- (ii) (Constant DGs) A saturated DG $\mathcal{G}_X = (V_X(\cdot), E_X(\cdot))$ is a *constant* DG, if it satisfies the additional condition that $E_X(\cdot)$ is constant. Note that \mathcal{G}_X is constant if and only if $\text{crit}(\mathcal{G}_X) = \emptyset$.

We specify the notion of isomorphism in the class of DGs.

Definition 4.4 (Isomorphism for DGs). Two DGs $\mathcal{G}_X = (V_X(\cdot), E_X(\cdot))$ and $\mathcal{G}_Y = (V_Y(\cdot), E_Y(\cdot))$ are isomorphic if there exists a bijection $\varphi : X \rightarrow Y$ such that for all $t \in \mathbf{R}$, $V_X(t) = \varphi(V_Y(t))$ and $\{x, x'\} \in E_X(t)$ if and only if $\{\varphi(x), \varphi(x')\} \in E_Y(t)$. In words, the map φ serves as a graph isomorphism between \mathcal{G}_X and \mathcal{G}_Y for all time.

5 Formigrams

The goal of this section is to construct dendrogram-like structures that are able to represent the clustering information of time-varying metric spaces, graphs/networks, or point clouds. Towards this goal we introduce the notion of *formigrams*.

5.1 Formigrams and their barcodes

We begin with introducing notation that will be widely used throughout the rest of the paper.

Partitions and sub-partitions. We call any partition P of a subset X' of X a *sub-partition* of X (in particular, any partition of the empty set is defined as the empty set). In this case we call X' the *underlying set of P* .

Definition 5.1 (Collection of (sub-)partitions). Let X be a non-empty finite set.

- (i) By $\mathcal{P}^{\text{sub}}(X)$, we denote the set of *all sub-partitions of X* , i.e.

$$\mathcal{P}^{\text{sub}}(X) := \{P : \exists X' \subset X, P \text{ is a partition of } X'\}.$$

- (ii) By $\mathcal{P}(X)$, we denote the subcollection of $\mathcal{P}^{\text{sub}}(X)$ consisting solely of partitions of the *whole X* .

Given $P, Q \in \mathcal{P}^{\text{sub}}(X)$, by $P \leq Q$ we mean “ P is finer than or equal to Q ”, i.e. for all $B \in P$, there exists $C \in Q$ such that $B \subset C$.

Dendrograms, treegrams, and formigrams. Recall the notion of dendrogram [14]:

Definition 5.2 (Dendrogram). A *dendrogram* over a finite set X is any function $\theta_X : \mathbf{R}_+ \rightarrow \mathcal{P}(X)$ such that the following properties hold: (1) $\theta_X(0) = \{\{x\} : x \in X\}$, (2) if $t_1 \leq t_2$, then $\theta_X(t_1) \leq \theta_X(t_2)$, (3) there exists $T > 0$ such that $\theta_X(t) = \{X\}$ for $t \geq T$, (4) for all t there exists $\epsilon > 0$ s.t. $\theta_X(s) = \theta_X(t)$ for $s \in [t, t + \epsilon]$ (right-continuity).

Dendrograms can be generalized to treegrams, which were introduced in [52] as a visual representation for hierarchical clustering of networks. In contrast to dendrograms, treegrams allow each point in their underlying sets to have different “birth” times (see Figure 4 for a pair of illustrative examples).

Definition 5.3 (Treegram). A *treegram* over a finite set X is any function $\theta_X : \mathbf{R} \rightarrow \mathcal{P}^{\text{sub}}(X)$ such that the following properties hold: (1) if $t_1 \leq t_2$, then $\theta_X(t_1) \leq \theta_X(t_2)$, (2) (boundedness) there exists $T > 0$ such that $\theta_X(t) = \{X\}$ for $t \geq T$ and $\theta_X(t)$ is empty for $t \leq -T$. (3) for all t there exists $\epsilon > 0$ s.t. $\theta_X(s) = \theta_X(t)$ for $s \in [t, t + \epsilon]$ (right-continuity).

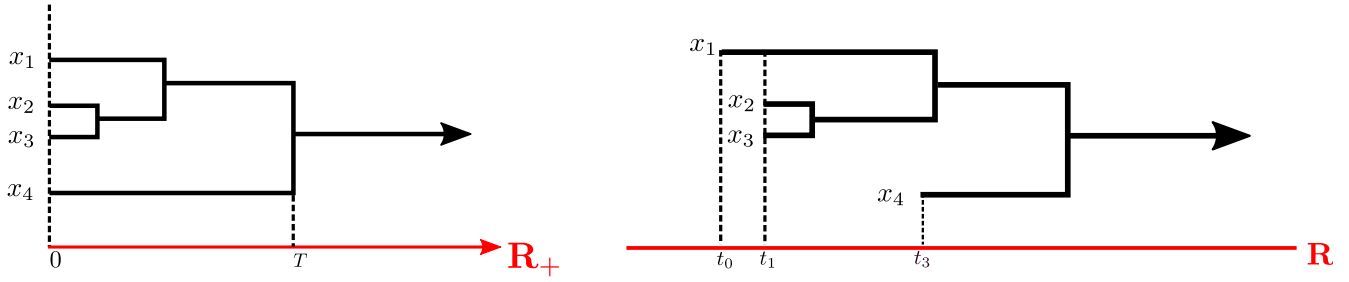


Figure 4: For the set $X = \{x_1, x_2, x_3, x_4\}$, an example of dendrogram (Left) and an example of treegram (Right) over X .

Although the notions of dendrogram or treegram are useful when representing the output of a hierarchical clustering method (i.e. when partitions only become coarser with the increase of a parameter), in order to represent the diverse clustering behaviors of dynamic datasets we need a more flexible concept allowing for possible refinement of partitions. Here we suggest a “zigzag like” notion of dendrograms that we call *formigram*.⁵ We allow partitions to become finer sometimes, but require that partitions defined by a formigram change only finitely many times in any finite interval.

Definition 5.4 (Formigram). A *formigram* over a finite set X is any function $\theta_X : \mathbf{R} \rightarrow \mathcal{P}^{\text{sub}}(X)$ such that:

- (i) (Tameness) the set $\text{crit}(\theta_X)$ of points of discontinuity of θ_X is locally finite. We call the elements of $\text{crit}(\theta_X)$ the *critical points* of θ_X .
- (ii) (Interval lifespan) for every $x \in X$, the set $I_x := \{t \in \mathbf{R} : x \in B \in \theta_X(t)\}$, said to be the *lifespan* of x , is a non-empty closed interval,
- (iii) (Comparability) for every point $c \in \mathbf{R}$ it holds that $\theta_X(c - \varepsilon) \leq \theta_X(c) \geq \theta_X(c + \varepsilon)$ for all sufficiently small $\varepsilon > 0$.⁶

Note that for $t \in \mathbf{R}$, $\theta_X(t)$ is a sub-partition of X , so that its underlying set could be a strict subset of X . Also, note that Definition 5.4 generalizes both Definitions 5.2 and 5.3.⁷ Specifically, a formigram over a finite set X can have an element $x \in X$ that disappears at some $t \in \mathbf{R}$, in contrast to dendrograms or treegrams. Also, if θ_X is right-continuous on the whole \mathbf{R} , then $\theta_X(t)$ can only get coarser as t increases, just as dendrograms/treegrams. Just as in the case of dendrograms/treegrams, we can also graphically represent formigrams by drawing their *Reeb graphs*, see Figures 5 and 6 for the intuition. See Definition 5.18 for the precise definition.

Remark 5.5 (Special cases). (i) (Saturated formigram) Given a formigram $\theta_X : \mathbf{R} \rightarrow \mathcal{P}^{\text{sub}}(X)$, if its image is confined to $\mathcal{P}(X) \subset \mathcal{P}^{\text{sub}}(X)$, then we will call θ_X *saturated*.

- (ii) (Constant formigram) Let θ_X be a saturated formigram over X . If in addition $\text{crit}(\theta_X)$ is empty, then θ_X is said to be *constant*.

Example 5.6. Let $X = \{x_1, x_2, x_3\}$ and define a saturated formigram θ_X over X as follows: $\theta_X(t) = \{X\}$ for $t \in (-\infty, 2] \cup [17, \infty)$, $\theta_X(t) = \{\{x_1, x_2\}, \{x_3\}\}$ for $t \in (2, 6]$, $\theta_X(t) = \{\{x_1\}, \{x_2\}, \{x_3\}\}$ for $t \in (6, 10) \cup (15, 17)$, and $\theta_X(t) = \{\{x_1\}, \{x_2, x_3\}\}$ for $t \in [10, 15]$. See Figure 5.

Example 5.7. Let $X = \{x_1, x_2, x_3\}$ and consider the formigram θ_X over X defined as in Figure 6.

⁵The name formigram is a combination of the words formicarium and diagram.

⁶If θ_X is not continuous at c , then at least one of the relations of $\theta_X(c - \varepsilon) \leq \theta_X(c) \geq \theta_X(c + \varepsilon)$ would be strict for small $\varepsilon > 0$. But if c is a continuity point of θ_X , then $\theta_X(c - \varepsilon) = \theta_X(c) = \theta_X(c + \varepsilon)$ for small $\varepsilon > 0$.

⁷In order to regard a dendrogram $\theta_X : \mathbf{R}_+ \rightarrow \mathcal{P}(X)$ as a formigram, trivially extend θ_X to the whole \mathbf{R} : for $t \in (-\infty, 0)$, let $\theta_X(t) := \emptyset \in \mathcal{P}^{\text{sub}}(X)$ by definition.

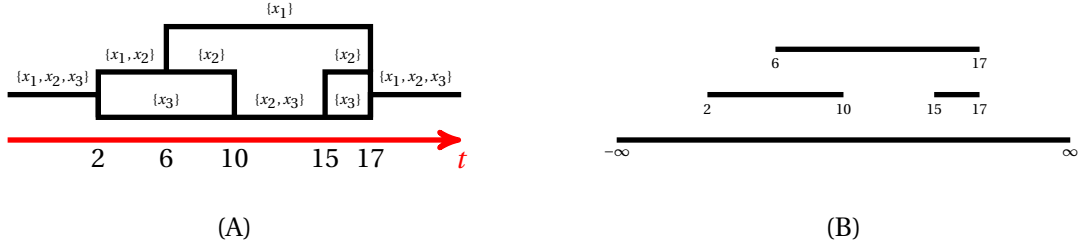


Figure 5: (A) The Reeb graph of θ_X enriched with the labels from Example 5.6. Note that $\text{crit}(\theta_X) = \{2, 6, 10, 15, 17\}$. (B) The barcode $\text{dgm}(\theta_X)$ of θ_X (see details in Example 5.12). For each $t \in \mathbf{R}$, the number of blocks in $\theta_X(t)$ is equal to the number of intervals containing t in $\text{dgm}(\theta_X)$.

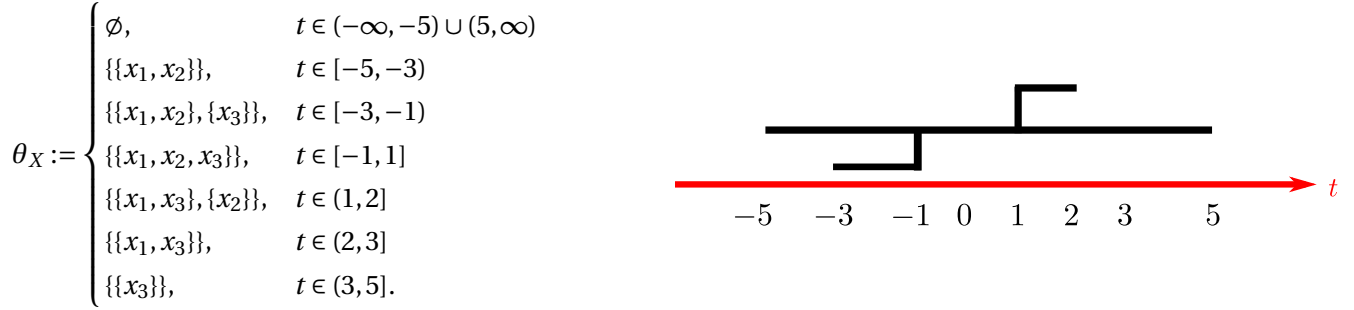


Figure 6: Left: The specification of the formigram θ_X from Example 5.7. Right: The Reeb graph $\text{Reeb}(\theta_X)$ of θ_X . The lifespans of x_1, x_2 and x_3 are $[-5, 3], [-5, 2]$ and $[-3, 5]$, respectively. Note that the death of x_2 at $t = 2$ is reflected in $\text{Reeb}(\theta_X)$, whereas the death of x_3 at $t = 3$ is not.

Definition 5.8 (Merging, disbanding, birth, and death events). Let θ_X be a formigram over X and let $t_0 \in \text{crit}(\theta_X)$. Take any sufficiently small $\varepsilon > 0$ such that $\{t_0\} = [t_0 - \varepsilon, t_0 + \varepsilon] \cap \text{crit}(\theta_X)$.⁸

- (i) We say that a *merging event* occurs at $t_0 \in \mathbf{R}$ if there exist two different blocks $A, B \in \theta_X(t_0 - \varepsilon)$ and $C \in \theta_X(t_0)$ such that $A \cup B \subset C$.
- (ii) We say that a *disbanding event* occurs at $t_0 \in \mathbf{R}$ if there exist two different blocks $A, B \in \theta_X(t_0 + \varepsilon)$ and $C \in \theta_X(t_0)$ such that $A \cup B \subset C$.
- (iii) We say that a *birth event* occurs at $t_0 \in \mathbf{R}$ if there exists $x \in X$ that belongs to the underlying set of the sub-partition $\theta_X(t_0)$, but does not belong to the underlying set of the sub-partition $\theta_X(t_0 - \varepsilon)$.
- (iv) We say that a *death event* occurs at $t_0 \in \mathbf{R}$ if there exists $x \in X$ that belongs to the underlying set of $\theta_X(t_0)$, but does not belong to $\theta_X(t_0 + \varepsilon)$.

For example, for the formigram from Example 5.6 (Figure 5), disbanding events occur at $t = 2, 6, 15$, and merging events occur at $t = 10, 17$. Also, for the formigram from Example 5.7 (Figure 6), a birth event occurs at $t = -3$ and death events occur at $t = 2, 3$.

The barcode of a formigram. Reeb graphs of formigrams can sometimes be difficult to visualize (see Example 5.21), which motivates us to turn formigrams into barcodes (which are readily visualizable) via considerations related to zigzag persistence [12].

We now define the barcode of a formigram precisely. Recall Definition 5.1. Given any $P, Q \in \mathcal{P}^{\text{sub}}(X)$ with $P \leq Q$, the *canonical map* from P to Q is defined as follows: each block $A \in P$ is sent to the unique block $B \in Q$ such that $A \subset B$.

⁸This is possible by virtue of the tameness of θ_X (Definition 5.4 (i)).

Let θ_X be a formigram over X . Let $\mathfrak{C}(\theta_X)$ be the collection of sets $C = \{c_i \in \mathbf{R} : i \in \mathbf{Z}\}$ such that $\cdots < c_{i-1} < c_i < c_{i+1} < \cdots$, $\lim_{i \rightarrow +\infty} c_i = +\infty$, $\lim_{i \rightarrow -\infty} c_i = -\infty$, and $\text{crit}(\theta_X) \subset C$. Also, for each $C \in \mathfrak{C}(\theta_X)$, define the collection $\text{Subdiv}(C)$ of sets $S = \{s_i \in \mathbf{R} : i \in \mathbf{Z}\}$ such that $s_i \in (c_i, c_{i+1})$ for all $i \in \mathbf{Z}$. Pick *any* $C \in \mathfrak{C}(\theta_X)$ and $S \in \text{Subdiv}(C)$, and let

$$K := C \cup S = \{\cdots < c_{i-1} < s_{i-1} < c_i < s_i < c_{i+1} < \cdots\}. \quad (4)$$

Any K arising in this way is called an *indexing set* for θ_X . We have the following chain of canonical maps:

$$\begin{array}{ccccccc} & & \theta_X(c_{i-1}) & & \theta_X(c_i) & & \theta_X(c_{i+1}) \\ & \nearrow & & \nwarrow & \nearrow & \nwarrow & \nearrow \\ \cdots & & & & & & \cdots \\ & & \theta_X(s_{i-1}) & & \theta_X(s_i) & & \end{array} \quad (5)$$

By applying the free functor $\mathfrak{V}_{\mathbb{F}} : \mathbf{Sets} \rightarrow \mathbf{Vec}$ (Section 3.1, item 18) to this diagram, we obtain the following diagram in \mathbf{Vec} .

$$\mathbb{V}_{\theta_X} : \begin{array}{ccccccc} & & V_{c_{i-1}} & & V_{c_i} & & V_{c_{i+1}} \\ & \nearrow & & \nwarrow & \nearrow & \nwarrow & \nearrow \\ \cdots & & & & & & \cdots \\ & & V_{s_{i-1}} & & V_{s_i} & & \end{array} \quad (6)$$

where V_{c_j}, V_{s_j} are the vector spaces generated over \mathbb{F} by the elements of $\theta_X(c_j)$ and $\theta_X(s_j)$ for all $j \in \mathbf{Z}$, respectively.

We regard \mathbb{V}_{θ_X} as a \mathbf{ZZ} -indexed module by identifying the indexing set K of diagram (6) with the poset \mathbf{ZZ} via the following bijection:

$$f_K : K \rightarrow \mathbf{ZZ} \text{ such that, } c_i \mapsto (i, i), \text{ and } s_i \mapsto (i+1, i) \text{ for } i \in \mathbf{Z}.$$

Then by Theorem 3.5, \mathbb{V}_{θ_X} can be decomposed as

$$\mathbb{V}_{\theta_X} \cong \bigoplus_{j \in J} I^{\langle b_j, d_j \rangle \mathbf{ZZ}}$$

for some index set J . Note that each interval $\langle b_j, d_j \rangle \mathbf{ZZ}$ in \mathbf{ZZ} for $j \in J$ has the corresponding *interval* $f_K^{-1}(\langle b_j, d_j \rangle \mathbf{ZZ})$ in K which consists of consecutive elements of K . Define the multiset $\text{dgm}_K(\mathbb{V}_{\theta_X}) := \{\{f_K^{-1}(\langle b_j, d_j \rangle \mathbf{ZZ}) : j \in J\}\}$ consisting of intervals of K .

We write $[c_i, c_j]_K$, $[c_i, s_j]_K$, $[s_i, c_j]_K$, $[s_i, s_j]_K$ for some $i, j \in \mathbf{Z}$ to denote finite intervals of K : for example, for $i \leq j$, $[c_i, c_j]_K$ is defined to be the set $\{c_i, s_i, c_{i+1}, \dots, s_{j-1}, c_j\} \subset K$ and similarly for the other types $[c_i, s_j]_K$, $[s_i, c_j]_K$, and $[s_i, s_j]_K$. For infinite intervals of K , we use $(-\infty, \infty)_K (= K)$, $(-\infty, c_i]_K$, $(-\infty, s_i]_K$, $[c_i, \infty)_K$, and $[s_i, \infty)_K$.

Let $\mathbf{Int}(K)$ and $\mathbf{Int}(\mathbf{R})$ be the collection of all intervals of K and the collection of all intervals of \mathbf{R} , respectively. Define the map

$$\Psi_K : \mathbf{Int}(K) \rightarrow \mathbf{Int}(\mathbf{R})$$

as indicated in the following diagram:

$\mathbf{Int}(K)$	$\mathbf{Int}(\mathbf{R})$	$\mathbf{Int}(K)$	$\mathbf{Int}(\mathbf{R})$
$[c_i, c_j]_K \mapsto [c_i, c_j]$	for $i \leq j$	$(-\infty, \infty)_K \mapsto (-\infty, \infty)$	
$[c_i, s_j]_K \mapsto [c_i, c_{j+1})$	for $i \leq j$	$(-\infty, c_i]_K \mapsto (-\infty, c_i]$	
$[s_i, c_j]_K \mapsto (c_i, c_j]$	for $i < j$	$(-\infty, s_i]_K \mapsto (-\infty, c_{i+1})$	
$[s_i, s_j]_K \mapsto (c_i, c_{j+1})$	for $i \leq j$	$[c_i, \infty)_K \mapsto [c_i, \infty)$	
		$[s_i, \infty)_K \mapsto (c_i, \infty)$	

(7)

Let $\Psi_K \circ \text{dgm}_K(\mathbb{V}_{\theta_X}) := \{\{\Psi_K(f_K^{-1}(\langle b_j, d_j \rangle \mathbf{zz})) : j \in J\}\}$, which is a multiset consisting of intervals of \mathbf{R} (this construction is similar to the one given in [13]). Note that the indexing set $K = C \cup S$ in equation (4) is not uniquely specified. However, as long as $C \in \mathfrak{C}(\theta_X)$ and $S \in \text{Subdiv}(C)$, the choice of K does not affect the resulting multiset $\Psi_K \circ \text{dgm}_K(\mathbb{V}_{\theta_X})$:

Proposition 5.9 (Invariance to indexing set). For any formigram θ_X over X , let $C, C' \in \mathfrak{C}(\theta_X)$ and let $S \in \text{Subdiv}(C)$, and let $S' \in \text{Subdiv}(C')$. For the diagrams \mathbb{V}_{θ_X} and \mathbb{V}'_{θ_X} constructed as in (6) with respect to $K = C \cup S$ and $K' = C' \cup S'$ respectively, we have $\Psi_K \circ \text{dgm}_K(\mathbb{V}_{\theta_X}) = \Psi_{K'} \circ \text{dgm}_{K'}(\mathbb{V}'_{\theta_X})$.

The proof of Proposition 5.9 is elementary but lengthy, hence we omit it. By virtue of Proposition 5.9, we have:

Definition 5.10 (Barcode of a formigram). Let θ_X be a formigram over X . The *barcode of formigram* θ_X is defined as the multiset $\Psi_K \circ \text{dgm}_K(\mathbb{V}_{\theta_X})$ described as above and denoted by $\text{dgm}(\theta_X)$.

Note that given a formigram $\theta_X : \mathbf{R} \rightarrow \mathcal{P}^{\text{sub}}(X)$, one can directly compute the barcode of θ_X via the process described above together with zigzag persistence decomposition algorithm given in [12] (in particular without ever referring to the Reeb graph of θ_X). However, as Figure 5 indicates, the barcode of a formigram θ_X can also be interpreted as the 0-th levelset barcode of the Reeb graph of the formigram θ_X . See Section 5.3 for details.

Example 5.11 (Barcode of a constant formigram). Suppose that θ_X is a constant formigram over X , i.e. $\theta_X \equiv P$ for some $P \in \mathcal{P}(X)$ (Remark 5.5). Let $m := |P|$. Then, the zigzag module \mathbb{V}_{θ_X} associated to θ_X from (6) is isomorphic to

$$\mathbb{V}_{\theta_X} : \quad \cdots \quad \begin{array}{c} \mathbb{F}^m \\ \nearrow \quad \nwarrow \\ \mathbb{F}^m \end{array} \quad \begin{array}{c} \mathbb{F}^m \\ \nwarrow \quad \nearrow \\ \mathbb{F}^m \end{array} \quad \begin{array}{c} \mathbb{F}^m \\ \nearrow \quad \nwarrow \\ \mathbb{F}^m \end{array} \quad \cdots \quad (8)$$

where each arrow stands for the identity map on \mathbb{F}^m . Therefore, $\text{dgm}(\theta_X)$ consists exactly of m copies of $(-\infty, \infty)$.

Example 5.12. Consider the formigram θ_X from Example 5.6, which has finite set of critical points $\text{crit}(\theta_X) = \{2, 6, 10, 15, 17\}$. Fix an indexing set $K = C \cup S$ for θ_X where $C = \{c_i \in \mathbf{R} : i \in \mathbf{Z}\}$ such that $c_1 = 2, c_2 = 6, c_3 = 10, c_4 = 15, c_5 = 17$, and $S \in \text{Subdiv}(C)$. Let \mathbb{V}_{θ_X} be the zigzag module associated to θ_X given by (6). Via the algorithm given in [12], one can prove that $\text{dgm}_K(\mathbb{V}_{\theta_X}) = \{(-\infty, \infty)_K, [s_1, s_2]_K, [s_2, s_4]_K, [s_4, s_4]_K\}$. Therefore, by table (7), one has

$$\text{dgm}(\theta_X) = \{(-\infty, \infty), (c_1, c_3), (c_2, c_5), (c_4, c_5)\} = \{(-\infty, \infty), (2, 10), (6, 17), (15, 17)\},$$

as illustrated in Figure 5.

Remark 5.13 (Barcode of a saturated formigram). Let θ_X be a saturated formigram over X . Then, $\text{dgm}(\theta_X)$ consists solely of open intervals, as seen already in Example 5.12. This can be proved by the following observation (we omit the detailed proof): Let \mathbb{V}_{θ_X} be the zigzag module associated to θ_X given by (6). Then, every morphism in \mathbb{V}_{θ_X} is surjective, which prevents $\text{dgm}_K(\mathbb{V}_{\theta_X})$ from containing intervals that have endpoints in $C = \{c_i : i \in \mathbf{Z}\}$, and in turn prevents $\text{dgm}(\theta_X)$ from containing (half) closed intervals.

Remark 5.14 (Interpretation of barcodes of formigrams). Let θ_X be a formigram over X .

- (i) Any interval of the form (a, b) in $\text{dgm}(\theta_X)$ stands for a pair of events consisting of a disbanding event of a group at $t = a$ and a merging event of some number $N \geq 2$ of groups at $t = b$.
- (ii) Any interval of the form $[a, b)$ in $\text{dgm}(\theta_X)$ stands for a pair of events consisting of a birth event of a group (possibly a single point) at $t = a$ and a merging event of some number $N \geq 2$ of groups at $t = b$.
- (iii) Any interval of the form $(a, b]$ in $\text{dgm}(\theta_X)$ stands for a pair of events consisting of a disbanding event of a group at $t = a$ and a death event of a group (possibly a single point) at $t = b$.
- (iv) Any interval of the form $[a, b]$ in $\text{dgm}(\theta_X)$ stands for a pair of events consisting of a birth event of a group at $t = a$ and a death event of a group at $t = b$.

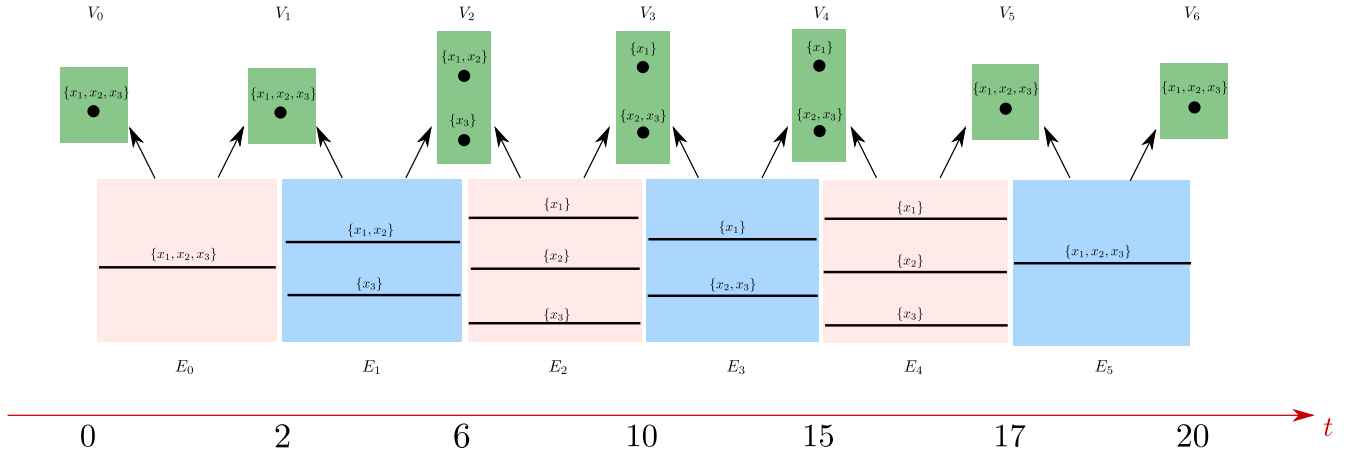


Figure 7: The construction of the Reeb graph of the formigram θ_X from Example 5.6 over the interval $[0, 20]$ (cf. Figure 5 (A) and [22, Figure 6]).

5.2 From DGs to formigrams

In this section we describe the process that associates a (certain) formigram to any DG. Recall the category **Graph** from Section 3.1, item 7.

Definition 5.15 (Path component functor $\pi_0 : \mathbf{Graph} \rightarrow \mathbf{Sets}$). Given any graph $G_X = (X, E_X)$, define the partition $\pi_0(X, E_X) := X / \sim$ of X where \sim stands for the equivalence relation on X defined by $x \sim x'$ if and only if there exists a sequence $x = x_1, x_2, \dots, x_n = x'$ of points in X such that $\{x_i, x_{i+1}\} \in E_X$ for each $i \in \{1, \dots, n-1\}$. In words, the relation \sim on X is the transitive closure of the adjacency relation of the graph G_X .

Note that any graph morphism $f : G_X = (X, E_X) \rightarrow G_Y = (Y, E_Y)$ induces a set map $\pi_0(f) : \pi_0(G_X) \rightarrow \pi_0(G_Y)$ sending each block $B \in \pi_0(G_X)$ to the unique block $C \in \pi_0(G_Y)$ such that $f(B) \subset C$.

We can turn any DG into a formigram:

Proposition 5.16. Let $\mathcal{G}_X = (V_X(\cdot), E_X(\cdot))$ be a DG. Then, the function $\pi_0(\mathcal{G}_X) : \mathbf{R} \rightarrow \mathcal{P}^{\text{sub}}(X)$ defined by $\pi_0(\mathcal{G}_X)(t) = \pi_0(\mathcal{G}_X(t))$ for $t \in \mathbf{R}$ satisfies all the conditions in Definition 5.4, therefore it is a formigram.

Proof. Since any DG \mathcal{G}_X satisfies Definition 4.1 (ii), (iii), and (iv), $\pi_0(\mathcal{G}_X)$ necessarily satisfies Definition 5.4 (i), (ii), and (iii). \square

5.3 The Reeb graph of a formigram

Adapting notions and notation from [22], we rigorously define the Reeb graph of a formigram. The Reeb graph of a formigram $\theta_X : \mathbf{R} \rightarrow \mathcal{P}^{\text{sub}}(X)$ illustrates the evolution of partitions $t \mapsto \theta_X(t)$. While the Reeb graph of any dendrogram is always a *rooted tree* and thus planar, the Reeb graph of a generic formigram is not always necessarily planar: it is possible that it exhibits some loops because both merging and disbanding of blocks could happen over time in contrast to dendrograms, which only exhibit merging events.

Definition 5.17 (**R-graphs and their isomorphisms**). (i) Let T be a topological space and let $f : T \rightarrow \mathbf{R}$ be of Morse type (Definition 3.6). If the topological spaces Y_i as in Definition 3.6 (i) are finite sets of points with the discrete topology, then the pair (T, f) is said to be an **R-graph** [22].

(ii) Any two **R-graphs** $(S, f), (T, g)$ are said to be *isomorphic* if there is a homeomorphism $\phi : S \rightarrow T$ such that $f = g \circ \phi$.

Now, we are ready to rigorously define *the Reeb graph of a formigram* (see Figure 7 for an illustration):

Definition 5.18 (The Reeb graph of a formigram). Let θ_X be a formigram over X .

- (i) (The Reeb graph of θ_X over a finite interval) Given a closed finite interval $I = [a, b] \subset \mathbf{R}$, By the *Reeb graph of θ_X over I* , we mean the \mathbf{R} -graph (\mathbb{X}_I, f_I) over I that is constructed as follows:

Step 1 Consider $(\text{crit}(\theta_X) \cap [a, b]) \cup \{a, b\} = \{a = c_0 < c_1 < \dots < c_n = b\}$,

Step 2 for each $0 \leq i \leq n-1$, pick any $s_i \in (c_i, c_{i+1})$,

Step 3 for $0 \leq i \leq n$, we specify a finite set of vertices $V_i := \theta_X(c_i)$, which lie over c_i ,

Step 4 for $0 \leq i \leq n-1$, we specify a finite set of edges $E_i := \theta_X(s_i)$ which lie over the interval $[c_i, c_{i+1}]$,

Step 5 for $0 \leq i \leq n-1$, we define left and right attaching maps $l_i : E_i \rightarrow V_i$ and $r_i : E_i \rightarrow V_{i+1}$ by sending each block $e \in E_i$ to the blocks in V_i and V_{i+1} which contain e , respectively.

The space \mathbb{X}_I is the quotient of the disjoint union of the spaces $V_i \times \{c_i\}$ and $E_i \times [c_i, c_{i+1}]$ with respect to the identifications $(l_i(e), c_i) \sim (e, c_i)$ and $(r_i(e), c_{i+1}) \sim (e, c_{i+1})$, with the map f_I being the projection onto the second factor.

- (ii) (The Reeb graph of θ_X) For each $n \in \mathbf{Z}$, let $(\mathbb{X}_{I_n}, f_{I_n})$ be the Reeb graph of θ_X over the interval $I_n := [n, n+1]$. By the *Reeb graph $\mathbf{Reeb}(\theta_X)$ of a formigram θ_X* , we will refer to the \mathbf{R} -graph $(\mathbb{X}_{\theta_X}, f_{\theta_X}) := \cup_{n \in \mathbf{Z}} (\mathbb{X}_{I_n}, f_{I_n})$, formed by the concatenation of $(\mathbb{X}_{I_n}, f_{I_n})$, for all $n \in \mathbf{Z}$.

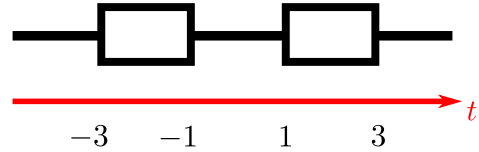
Remark 5.19 (Comments about Definition 5.18). Regarding the Reeb graph of a formigram, it is noteworthy that each vertex and each edge of the Reeb graph of a formigram over X correspond to a specific non-empty subset of X .

The following example shows that two different non-isomorphic formigrams can have the same Reeb graph.

Example 5.20 (Non-isomorphic formigrams with the same Reeb graph). Let $X = \{x_1, x_2\}$ and $Y = \{y_1, y_2, y_3\}$. Define formigrams θ_X, θ_Y over X, Y , respectively as follows:

$$\theta_X(t) := \begin{cases} \{\{x_1\}, \{x_2\}\}, & t \in (-3, -1) \cup (1, 3) \\ \{\{x_1, x_2\}\}, & \text{otherwise,} \end{cases}$$

$$\theta_Y(t) := \begin{cases} \{\{y_1, y_2\}, \{y_3\}\}, & t \in (-3, -1) \\ \{\{y_1\}, \{y_2, y_3\}\}, & t \in (1, 3) \\ \{\{y_1, y_2, y_3\}\}, & \text{otherwise.} \end{cases}$$



Then, both θ_X and θ_Y have the same Reeb graph depicted on the right.

Reeb graphs of formigrams are not always planar:

Example 5.21 (A non-planar formigram). Consider a formigram θ_X over the set $X = \{x_i\}_{i=1}^3 \cup \{y_i\}_{i=1}^3 \cup \{z_i\}_{i=1}^3$ given by:

$$\theta_X(t) := \begin{cases} \{\{x_1, x_2, x_3\}, \{y_1, y_2, y_3\}, \{z_1, z_2, z_3\}\}, & t \in (-\infty, 1] \\ \{\{x_1\}, \{x_2\}, \{x_3\}, \{y_1\}, \{y_2\}, \{y_3\}, \{z_1\}, \{z_2\}, \{z_3\}\}, & t \in (1, 2) \\ \{\{x_1, y_1, z_1\}, \{x_2, y_2, z_2\}, \{x_3, y_3, z_3\}\}, & t \in [2, \infty). \end{cases}$$

See Figure 8 for the Reeb graph of θ_X : the graph has the complete bipartite graph $K_{3,3}$ as a minor, which implies that it is not planar by Kuratowski's theorem [6].

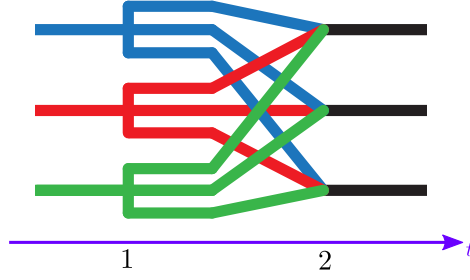


Figure 8: The Reeb graph $\mathbf{Reeb}(\theta_X)$ of the formigram θ_X in Example 5.21.

Another interpretation of the barcode of a formigram. As Figure 5 suggests, the Reeb graph of a formigram is closely related to its barcode. We now clarify this relationship.

Let θ_X be a formigram over X and let $(\mathbb{X}_{\theta_X}, f_{\theta_X}) := \mathbf{Reeb}(\theta_X)$ (Definition 5.18 (ii)). The tameness of θ_X (Definition 5.4 (i)) ensures that the map $f_{\theta_X} : \mathbb{X}_{\theta_X} \rightarrow \mathbf{R}$ is of Morse type (Definition 3.6), and hence the 0-th levelset barcode $\mathcal{L}_0(\mathbf{Reeb}(\theta_X))$ of $\mathbf{Reeb}(\theta_X)$ is well-defined (Definition 3.7). It is not difficult to check that $\mathcal{L}_0(\mathbf{Reeb}(\theta_X))$ defined in Section 3.3 coincides with $\text{dgm}(\theta_X)$ described in Section 5.1:

Proposition 5.22. Let θ_X be a formigram over X . Then,

$$\text{dgm}(\theta_X) = \mathcal{L}_0(\mathbf{Reeb}(\theta_X)).$$

Proposition 5.22 implies that barcodes of formigrams entirely depend on their Reeb graphs. Therefore, the barcodes of the formigrams θ_X and θ_Y in Example 5.20 are identical.

6 Metrics for DGs and formigrams

In this section we define metrics for DGs and formigrams respectively via smoothing operations. Ideas on smoothing similar objects have appeared in [10, 22]. The construction of our metric is inspired by both the interleaving distance for zigzag persistence modules [8] and the interleaving distance for Reeb graphs [22].

6.1 A distance between DGs

The main goal of this section is to introduce the notion of the ε -smoothing of DGs, as well as a (pseudo) metric on the collection of DGs.

Pullback of a (dynamic) graph. Let $G_X = (X, E_X)$ be any graph and let Z be any set. For any map $\varphi : Z \rightarrow X$, the pullback $G_Z := \varphi^* G_X$ of G_X via φ is the graph on the vertex set Z with the edge set $E_Z = \{\{z, z'\} : \{\varphi(z), \varphi(z')\} \in E_X\}$.

Definition 6.1 (Pullback of a DG). Let $\mathcal{G}_X = (V_X(\cdot), E_X(\cdot))$ be a DG and let Z be any set. For any map $\varphi : Z \rightarrow X$, the *pullback* $\mathcal{G}_Z := \varphi^* \mathcal{G}_X$ of \mathcal{G}_X via φ is a DG over Z defined as follows: for all $t \in \mathbf{R}$, $\mathcal{G}_Z(t)$ is the graph on the vertex set $V_Z(t) = \varphi^{-1}(V_X(t))$ with the edge set $E_Z(t) = \{\{z, z'\} : \{\varphi(z), \varphi(z')\} \in E_X(t)\}$.

Interconnecting DGs via tripods. We first establish a method for interconnecting any two DGs via a *tripod*, which has been utilized for constructing a distance between filtered spaces [44] and a distance between Reeb graphs [2].

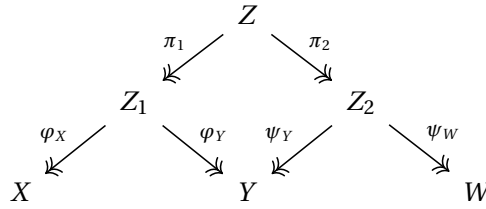
Definition 6.2 (Tripod). Let X and Y be any two sets. A *tripod* R between X and Y is a pair of surjections from another set Z to X and Y , respectively. Namely, R can be expressed as the diagram $R : X \xleftarrow{\varphi_X} Z \xrightarrow{\varphi_Y} Y$.

Definition 6.3 (Comparison between two DGs via a tripod). Let $\mathcal{G}_X = (V_X(\cdot), E_X(\cdot))$, $\mathcal{G}_Y = (V_Y(\cdot), E_Y(\cdot))$ be any two DGs and let $R : X \xleftarrow{\varphi_X} Z \xrightarrow{\varphi_Y} Y$ be any tripod between X and Y . We write $\mathcal{G}_X \xrightarrow{R} \mathcal{G}_Y$ if for all $t \in \mathbf{R}$, $\varphi_X^* \mathcal{G}_X(t)$ is a subgraph of $\varphi_Y^* \mathcal{G}_Y(t)$, i.e. the vertex set and the edge set of $\varphi_X^* \mathcal{G}_X(t)$ are subsets of those of $\varphi_Y^* \mathcal{G}_Y(t)$, respectively.

Remark 6.4. In Definition 6.3, $\mathcal{G}_X \xrightarrow{R} \mathcal{G}_Y$ implies that for all $t \in \mathbf{R}$, any function $f : X \rightarrow Y$ satisfying $\{(x, f(x)) : x \in X\} \subset \varphi_Y \circ \varphi_X^{-1}$ gives rise to a graph morphism from $\mathcal{G}_X(t)$ to $\mathcal{G}_Y(t)$. However, the converse is not true in general.

For any sets X, Y and W , consider any two tripods $R_1 : X \xleftarrow{\varphi_X} Z_1 \xrightarrow{\varphi_Y} Y$ and $R_2 : Y \xleftarrow{\psi_Y} Z_2 \xrightarrow{\psi_W} W$. Consider the set $Z := \{(z_1, z_2) \in Z_1 \times Z_2 : \varphi_Y(z_1) = \psi_Y(z_2)\}$ and let $\pi_1 : Z \rightarrow Z_1$ and $\pi_2 : Z \rightarrow Z_2$ be the canonical projections to the first and the second coordinate, respectively. We define the tripod

$$R_2 \circ R_1 : X \xleftarrow{\omega_X} Z \xrightarrow{\omega_W} W, \text{ where } \omega_X = \varphi_X \circ \pi_1, \omega_W = \psi_W \circ \pi_2 \text{ (see the diagram below)}. \quad (9)$$



Remark 6.5. Let $\mathcal{G}_X = (V_X(\cdot), E_X(\cdot))$, $\mathcal{G}_Y = (V_Y(\cdot), E_Y(\cdot))$, and $\mathcal{G}_W = (V_W(\cdot), E_W(\cdot))$ be any three DGs. Let R_1 be any tripod between X and Y and let R_2 be any tripod between Y and W . If $\mathcal{G}_X \xrightarrow{R_1} \mathcal{G}_Y$ and $\mathcal{G}_Y \xrightarrow{R_2} \mathcal{G}_W$, then it is easy to check that $\mathcal{G}_X \xrightarrow{R_2 \circ R_1} \mathcal{G}_W$.

A distance between DGs. In order to define our distance between DGs, we begin by introducing the following notation:

- For any set $A \subset \mathbf{R}$ and any $t \in \mathbf{R}$, let $A + t := \{a + t : a \in A\}$.
- When $A \subset \mathbf{R}$ is a (closed) interval, i.e. $A = [a, b]$, then for $\varepsilon \geq 0$, we define $A^\varepsilon := [a - \varepsilon, b + \varepsilon]$.
- For any $t \in \mathbf{R}$ and $\varepsilon \geq 0$, let $[t]^\varepsilon$ denote the interval $[t - \varepsilon, t + \varepsilon] \subset \mathbf{R}$.

As an ingredient for defining our distance between DGs, we introduce the notion of ε -smoothing of DGs for $\varepsilon \geq 0$. The intuition is that ε -smoothed-out DGs will be oblivious to ephemeral disconnections between their vertices.

Definition 6.6 (Time-interlevel smoothing of DGs). Let $\mathcal{G}_X = (V_X(\cdot), E_X(\cdot))$ be any DG.

(i) Let $I \subset \mathbf{R}$ be an interval. We define $\bigcup_I \mathcal{G}_X := \left(\bigcup_{t \in I} V_X(t), \bigcup_{t \in I} E_X(t) \right)$.

(ii) Let $\varepsilon \geq 0$. The ε -smoothing $S_\varepsilon \mathcal{G}_X$ of \mathcal{G}_X is defined as follows:

$$S_\varepsilon \mathcal{G}_X(t) = \bigcup_{[t]^\varepsilon} \mathcal{G}_X \text{ for } t \in \mathbf{R}.$$

Proposition 6.7 below will be proved in Section 11.1.1.

Proposition 6.7. The time-dependent graph $S_\varepsilon \mathcal{G}_X$ introduced in Definition 6.6 (ii) is indeed a DG, i.e. $S_\varepsilon \mathcal{G}_X$ satisfies all the conditions in Definition 4.1.

We observe the following, which will be useful later on.

Proposition 6.8. Let $\mathcal{G}_X = (V_X(\cdot), E_X(\cdot))$ and $\mathcal{G}_Y = (V_Y(\cdot), E_Y(\cdot))$ be any two DGs.

- (i) For any $\varepsilon_1, \varepsilon_2 \geq 0$, we have $S_{\varepsilon_2}(S_{\varepsilon_1}\mathcal{G}_X) = S_{\varepsilon_1+\varepsilon_2}\mathcal{G}_X$ (cf. [22, Proposition 4.13]).
- (ii) Let R be any tripod between X and Y , and let $\varepsilon \geq 0$. If $\mathcal{G}_X \xrightarrow{R} \mathcal{G}_Y$, then $S_\varepsilon\mathcal{G}_X \xrightarrow{R} S_\varepsilon\mathcal{G}_Y$.

We omit the proof of Proposition 6.8. Now, we are ready to define the interleaving distance on DGs.

Definition 6.9 (Interleaving distance between DGs). Any two DGs $\mathcal{G}_X = (V_X(\cdot), E_X(\cdot))$ and $\mathcal{G}_Y = (V_Y(\cdot), E_Y(\cdot))$ are said to be ε -interleaved if there exists a tripod R between X and Y such that

$$\mathcal{G}_X \xrightarrow{R} S_\varepsilon\mathcal{G}_Y \quad \text{and} \quad \mathcal{G}_Y \xrightarrow{R} S_\varepsilon\mathcal{G}_X.$$

We call any such R an ε -tripod between \mathcal{G}_X and \mathcal{G}_Y . The *interleaving distance* $d_1^{\text{dynG}}(\mathcal{G}_X, \mathcal{G}_Y)$ between \mathcal{G}_X and \mathcal{G}_Y is defined as the infimum of $\varepsilon \geq 0$ for which there exists an ε -tripod between \mathcal{G}_X and \mathcal{G}_Y . If there is no ε -tripod between \mathcal{G}_X and \mathcal{G}_Y for any $\varepsilon \geq 0$, then we declare $d_1^{\text{dynG}}(\mathcal{G}_X, \mathcal{G}_Y) = +\infty$.

Theorem 6.10. d_1^{dynG} in Definition 6.9 is an extended pseudo metric on DGs.

See Section 11.1.1 for the proof of Theorem 6.10.

Theorem 6.11 (Complexity of d_1^{dynG}). Fix $\rho \in (1, 6)$. Then, it is not possible to compute a ρ -approximation to $d_1^{\text{dynG}}(\mathcal{G}_X, \mathcal{G}_Y)$ between DGs in time polynomial in $|X|, |Y|, |\text{crit}(\mathcal{G}_X)|$, and $|\text{crit}(\mathcal{G}_Y)|$, unless $P = NP$.

We prove Theorem 6.11 in Section 11.1.1 by showing that the computation of the Gromov-Hausdorff distance between finite metric spaces is amount to the computation of the interleaving distance d_1^{dynG} between DGs.

Remark 6.12. In Definition 6.9, the condition $\mathcal{G}_X \xrightarrow{R} S_\varepsilon\mathcal{G}_Y$ is equivalent to the following: For $z, z' \in Z$ with $\varphi_X(z) = x$, $\varphi_X(z') = x'$, $\varphi_Y(z) = y$ and $\varphi_Y(z') = y'$,

- (i) if $x \in V_X(t)$, then there is $s \in [t]^\varepsilon$ such that $y \in V_Y(s)$.
- (ii) if $\{x, x'\} \in E_X(t)$, then there is $s \in [t]^\varepsilon$ such that $\{y, y'\} \in E_Y(s)$.

Let X and Y be any two sets and let $R: X \xleftarrow{\varphi_X} Z \xrightarrow{\varphi_Y} Y$ be any tripod between X and Y . For any $A \subset X$, we define $R(A) := \varphi_Y \circ \varphi_X^{-1}(A)$. Also, for any $B \subset Y$, we define $R(B) := \varphi_X \circ \varphi_Y^{-1}(B)$.

Remark 6.13 (When does d_1^{dynG} vanish?). Let $\mathcal{G}_X = (V_X(\cdot), E_X(\cdot))$, $\mathcal{G}_Y = (V_Y(\cdot), E_Y(\cdot))$ be any two DGs. Then $d_1^{\text{dynG}}(\mathcal{G}_X, \mathcal{G}_Y) = 0$ if and only if there exists a tripod $R: X \xleftarrow{\varphi_X} Z \xrightarrow{\varphi_Y} Y$ such that for each $t \in \mathbf{R}$: (1) whenever any $A \subset X$ is such that the induced subgraph on A of $\mathcal{G}_X(t)$ is complete, the induced subgraph on $R(A)$ of $\mathcal{G}_Y(t)$ is also complete, and symmetrically (2) whenever any $B \subset Y$ is such that the induced subgraph on B of $\mathcal{G}_Y(t)$ is complete, the induced subgraph on $R(B)$ of $\mathcal{G}_X(t)$ is also complete. Examples include the case when \mathcal{G}_X and \mathcal{G}_Y are isomorphic (Definition 4.4).

Let $\mathcal{G}_X = (V_X(\cdot), E_X(\cdot))$ be a saturated DG (Example 4.3 (i)). For $\varepsilon \geq 0$, we call \mathcal{G}_X ε -complete if its ε -smoothing $S_\varepsilon\mathcal{G}_X$ satisfies the following: for all $t \in \mathbf{R}$, $S_\varepsilon\mathcal{G}_X(t)$ is the complete graph on X , i.e. $\{x, x'\} \in E_X(t)$ for all $x, x' \in X$. In particular, $S_\varepsilon\mathcal{G}_X$ is constant.

Proposition 6.14 (A sufficient condition for a pair of DGs to be interleaved). Let $\mathcal{G}_X = (V_X(\cdot), E_X(\cdot))$ and $\mathcal{G}_Y = (V_Y(\cdot), E_Y(\cdot))$ be any two DGs that are ε_1 -complete and ε_2 -complete, respectively. Then, $d_1^{\text{dynG}}(\mathcal{G}_X, \mathcal{G}_Y) \leq \max\{\varepsilon_1, \varepsilon_2\}$.

Proof. It is easy to check that any tripod R between X and Y is a $(\max\{\varepsilon_1, \varepsilon_2\})$ -tripod between \mathcal{G}_X and \mathcal{G}_Y . \square

6.2 A distance between formigrams

In this section we introduce the ε -smoothing operation for formigrams, as well as a (pseudo) metric on the collection of all formigrams. This metric quantifies the structural difference between two grouping/disbanding behaviors over time.

Finest common coarsening of sub-partitions. For a set X , we define the notion of *finest common coarsening* in $\mathcal{P}^{\text{sub}}(X)$ (see Definition 5.1). Recall that there exists the canonical one-to-one correspondence between the collection of all equivalence relations on X and the collection of all partitions $\mathcal{P}(X)$ of X . We will extend this correspondence in a certain way.

Definition 6.15 (Sub-equivalence relation). Let X be a non-empty set. Let \sim be any equivalence relation on any subset $X' \subset X$.⁹ We call the relation \sim a *sub-equivalence relation on X* . We also call X' the *underlying set* of \sim , which is identical to $\{x \in X : (x, x) \in \sim\}$.

Clearly, any equivalence relation on X is also a sub-equivalence relation with underlying set X .

There is the canonical one-to-one correspondence between the collection of all sub-equivalence relations on X and the collection $\mathcal{P}^{\text{sub}}(X)$ of all sub-partitions of X (Definition 5.1): Any sub-equivalence relation \sim on X corresponds to the sub-partition P with underlying set $X' = \{x \in X : (x, x) \in \sim\}$ such that $x \sim y$ iff x and y belong to the same block $B \in P$. Reciprocally, to any sub-partition P of X , one can associate the unique sub-equivalence relation \sim_P on X defined by $x \sim_P y$ if and only if x and y belong to the same block $B \in P$.

For an index set I , suppose that $\{\sim_i \subset X \times X : i \in I\}$ is a collection of sub-equivalence relations on X . The *sub-equivalence closure* of the collection $\{\sim_i \subset X \times X : i \in I\}$ is defined to be the minimal sub-equivalence relation containing \sim_i for all $i \in I$:

Definition 6.16 (Sub-equivalence closure). Let X be a finite set. For an index set I , suppose that $\{\sim_i \subset X \times X : i \in I\}$ is a collection of sub-equivalence relations on X . By the *sub-equivalence closure* \sim of $\{\sim_i \subset X \times X : i \in I\}$, we mean the transitive closure of the relation $\cup_{i \in I} \sim_i$ on X .

Definition 6.17 (Finest common coarsening). Let $\{P_i\}_{i \in I}$ be any subcollection of $\mathcal{P}^{\text{sub}}(X)$. For each $i \in I$, let \sim_i be the sub-equivalence relation on X corresponding to P_i . By $\bigvee_{i \in I} P_i$, we mean the sub-partition of X corresponding to the sub-equivalence closure of the collection $\{\sim_i \subset X \times X : i \in I\}$.

Example 6.18. Let $X = \{x, y, z, w\}$. For $P_1 = \{\{x\}, \{y, z\}\}$, $P_2 = \{\{y, z\}\}$, and $P_3 = \{\{x, w\}\}$ in $\mathcal{P}^{\text{sub}}(X)$, we have:

- (i) $\bigvee_{i=1}^2 P_i = \{\{x\}, \{y, z\}\} \in \mathcal{P}^{\text{sub}}(X)$, and
- (ii) $\bigvee_{i=1}^3 P_i = \{\{x, w\}, \{y, z\}\} \in \mathcal{P}(X)$.

Remark 6.19 (A property of finest common coarsenings). For any subcollection $\{P_i\}_{i \in I}$ of $\mathcal{P}^{\text{sub}}(X)$, let $Q := \bigvee_{i \in I} P_i$ be the finest common coarsening of $\{P_i\}_{i \in I}$. Then,

- (i) $P_i \leq Q$ for all i , and
- (ii) if R is a sub-partition of X such that $P_i \leq R$ for all $i \in I$, then $Q \leq R$.

We will re-interpret the notion of finest common coarsening from the perspective of category theory in Section 11.2.3.

Pullback of a sub-partition/formigram. Let X and Z be any two sets and let $P_X \in \mathcal{P}^{\text{sub}}(X)$. For any map $\varphi : Z \rightarrow X$, the *pullback* $P_Z := \varphi^* P_X$ of P_X via φ is the sub-partition of Z defined as $P_Z = \{\varphi^{-1}(B) : B \in P_X\}$. Let θ_X be a formigram over X . Then the *pullback* of θ_X via φ is the formigram $\theta_Z := \varphi^* \theta_X$ over Z defined as $\theta_Z(t) = \varphi^* \theta_X(t)$ for all $t \in \mathbf{R}$.

⁹In particular, the unique equivalence relation on the empty set \emptyset is \emptyset .

The interleaving distance between formigrams. We now define the distance between formigrams in an manner analogous to Definition 6.9. To this end, we first establish a method for interconnecting any two formigrams with possibly different underlying sets via a tripod.

Definition 6.20 (Comparison between two formigrams via a tripod). Let θ_X, θ_Y be any two formigrams over X and Y , respectively. Given any tripod $R: X \xleftarrow{\varphi_X} Z \xrightarrow{\varphi_Y} Y$ between X and Y (Definition 6.2), we write $\theta_X \xrightarrow{R} \theta_Y$ if for each $t \in \mathbf{R}$, $\varphi_X^* \theta_X(t) \leq \varphi_Y^* \theta_Y(t)$ in $\mathcal{P}^{\text{sub}}(Z)$.

Recall that for any sets X and Y , a multivalued map $\varphi: X \rightrightarrows Y$ is a relation between X and Y such that for all $x \in X$, there exists (a not necessarily unique) $y \in Y$ with $(x, y) \in \varphi$. For $x \in X$, the *image* $\varphi(x)$ of x is defined to be the set $\{y \in Y : (x, y) \in \varphi\}$.

Definition 6.21 (Partition morphism). For any two sets X and Y , let $P_X \in \mathcal{P}(X)$ and $P_Y \in \mathcal{P}(Y)$. Any multivalued map $\varphi: X \rightrightarrows Y$ (or map $\varphi: X \rightarrow Y$) is said to be a *partition morphism between P_X and P_Y* if for any $x, x' \in X$ belonging to the same block of P_X , their images $\varphi(x), \varphi(x')$ are included in the same block of P_Y (note that $\varphi(x), \varphi(x')$ can be sets containing more than one element). In this case, we write $P_X \leq_\varphi P_Y$.

If $P_X \leq_\varphi P_Y$, then there exists the canonical induced map $\varphi^*: P_X \rightarrow P_Y$ defined by sending each block $B \in P_X$ to the block $C \in P_Y$ such that $\varphi(B) \subset C$.

Notation: Let θ_X be a formigram over the set X . For each $t \in \mathbf{R}$, we will denote the underlying set of $\theta_X(t)$ by $U_{\theta_X}(t) \subset X$.

Remark 6.22. Let θ_X, θ_Y be any two formigrams over X and Y respectively and let $R: X \xleftarrow{\varphi_X} Z \xrightarrow{\varphi_Y} Y$ be any tripod between X and Y . Then the condition $\theta_X \xrightarrow{R} \theta_Y$ holds if and only if the following hold: Fix any $t \in \mathbf{R}$.

- (i) If $z \in Z$ with $\varphi_X(z) = x$, $\varphi_Y(z) = y$ and $x \in U_{\theta_X}(t)$, then $y \in U_{\theta_Y}(t)$.
- (ii) For the multivalued map $\varphi := \varphi_Y \circ \varphi_X^{-1}: X \rightrightarrows Y$, the restriction $\varphi|_{U_{\theta_X}(t)}: U_{\theta_X}(t) \rightrightarrows U_{\theta_Y}(t)$ of φ to $U_{\theta_X}(t)$ is a partition morphism between $\theta_X(t)$ and $\theta_Y(t)$.

Exploiting the fact that any formigram is a “deck” of (sub-)partitions of a specific set, we now introduce a smoothing operation on formigrams.

Definition 6.23 (Time-interlevel smoothing of formigrams). Let θ_X be a formigram over X .

- (i) Let $I \subset \mathbf{R}$ be an interval. We define $\bigvee_I \theta_X$ to be the finest common coarsening of $\{\theta_X(t) : t \in I\}$.
- (ii) Let $\varepsilon \geq 0$. The ε -smoothing $S_\varepsilon \theta_X$ of θ_X is defined as

$$(S_\varepsilon \theta_X)(t) = \bigvee_{[t]^\varepsilon} \theta_X \text{ for } t \in \mathbf{R}.$$

Proposition 6.24. $S_\varepsilon \theta_X$, as defined in Definition 6.23(ii), is indeed a formigram, i.e. $S_\varepsilon \theta_X$ satisfies all the conditions in Definition 5.4.

The proof of Proposition 6.24 is similar to that of Proposition 6.7 so we omit it. The following proposition is analogous to Proposition 6.8.

Proposition 6.25. Let θ_X and θ_Y be any two formigrams over X and Y , respectively.

- (i) For any $\varepsilon_1, \varepsilon_2 \geq 0$, we have $S_{\varepsilon_2}(S_{\varepsilon_1} \theta_X) = S_{\varepsilon_1 + \varepsilon_2} \theta_X$ (cf. [22, Proposition 4.13]).
- (ii) Let R be any tripod between X and Y , and let $\varepsilon \geq 0$. If $\theta_X \xrightarrow{R} \theta_Y$, then $S_\varepsilon \theta_X \xrightarrow{R} S_\varepsilon \theta_Y$.

Proof. We only prove (i). Let $t \in \mathbf{R}$. By definition, $(S_{\varepsilon_2}(S_{\varepsilon_1}\theta_X))(t) = \bigvee_{[t]^{\varepsilon_2}} S_{\varepsilon_1}\theta_X$ and $S_{\varepsilon_1+\varepsilon_2}\theta_X(t) = \bigvee_{[t]^{\varepsilon_1+\varepsilon_2}} \theta_X$. First, we show that $\bigvee_{[t]^{\varepsilon_2}} S_{\varepsilon_1}\theta_X \leq \bigvee_{[t]^{\varepsilon_1+\varepsilon_2}} \theta_X$ in $\mathcal{D}^{\text{sub}}(X)$. Let $s \in [t]^{\varepsilon_2}$. The interval $[s - \varepsilon_1, s + \varepsilon_1]$ is a subset of $[t]^{\varepsilon_1+\varepsilon_2}$ and thus $S_{\varepsilon_1}\theta_X(s) = \bigvee_{[s-\varepsilon_1, s+\varepsilon_1]} \theta_X$ refines $\bigvee_{[t]^{\varepsilon_1+\varepsilon_2}} \theta_X$. Since this holds for each $s \in [t]^{\varepsilon_2}$, it must hold that $\bigvee_{[t]^{\varepsilon_2}} S_{\varepsilon_1}\theta_X \leq \bigvee_{[t]^{\varepsilon_1+\varepsilon_2}} \theta_X$ (Remark 6.19 (ii)).

Next we verify that $\bigvee_{[t]^{\varepsilon_1+\varepsilon_2}} \theta_X \leq \bigvee_{[t]^{\varepsilon_2}} S_{\varepsilon_1}\theta_X$ in $\mathcal{D}^{\text{sub}}(X)$. Pick any $s \in [t]^{\varepsilon_1+\varepsilon_2}$. Then, there is $r \in [t]^{\varepsilon_2}$ such that the subinterval $[r - \varepsilon_1, r + \varepsilon_1]$ of $[t]^{\varepsilon_1+\varepsilon_2}$ contains s . Then, we have $\theta_X(s) \leq S_{\varepsilon_1}\theta_X(r) \leq \bigvee_{[t]^{\varepsilon_2}} S_{\varepsilon_1}\theta_X$. Since this holds for any $s \in [t]^{\varepsilon_1+\varepsilon_2}$, the finest common coarsening $\bigvee_{[t]^{\varepsilon_1+\varepsilon_2}} \theta_X$ refines $\bigvee_{[t]^{\varepsilon_2}} S_{\varepsilon_1}\theta_X$, as desired (Remark 6.19 (ii)). \square

Now, we define a distance between formigrams which is inspired by the interleaving distance for Reeb graphs [22].

Definition 6.26 (Interleaving distance between formigrams). Let θ_X and θ_Y be any two formigrams over X and Y , respectively. θ_X and θ_Y are said to be ε -interleaved if there exists a tripod R between X and Y such that

$$\theta_X \xrightarrow{R} S_{\varepsilon}\theta_Y \quad \text{and} \quad \theta_Y \xrightarrow{R} S_{\varepsilon}\theta_X.$$

We call any such R an ε -tripod between θ_X and θ_Y . The interleaving distance $d_1^F(\theta_X, \theta_Y)$ between θ_X and θ_Y is defined as the infimum of $\varepsilon \geq 0$ for which there exists an ε -tripod between θ_X and θ_Y . If there is no ε -tripod between θ_X and θ_Y for any $\varepsilon \geq 0$, then we declare $d_1^F(\theta_X, \theta_Y) = +\infty$.

Theorem 6.27. d_1^F in Definition 6.26 is an extended pseudo metric on formigrams.

The proof of Theorem 6.27 is similar to that of Theorem 6.10 and thus we omit it.

Remark 6.28 (d_1^F is not the interleaving distance for Reeb graphs). Recall Example 5.20. Since θ_X and θ_Y have the same Reeb graph, they are not discriminated by the interleaving distance for Reeb graphs [22]. However, one can check that $d_1^F(\theta_X, \theta_Y) = 1$. Indeed, any tripod R between X and Y fails to be an ε -tripod for $\varepsilon < 1$ and the tripod $R: X \xleftarrow{\varphi_X} Z \xrightarrow{\varphi_Y} Y$ which is defined as follows is an 1-tripod between θ_X and θ_Y : Let $Z = \{(x_1, y_1), (x_2, y_2), (x_2, y_3)\} \subset X \times Y$ and let φ_X and φ_Y be the canonical projections to the first coordinate and the second coordinate, respectively.

Remark 6.29 (Properties of d_1^F). (1) d_1^F between dendrograms agrees with (twice) the Gromov-Hausdorff distance between their associated ultrametrics (Proposition 11.4), and (2) constant factor approximations to d_1^F cannot be obtained in polynomial time (Theorem 11.5).

Proposition 6.30 (Basic observations). In Definition 6.26, the condition $\theta_X \xrightarrow{R} S_{\varepsilon}\theta_Y$ (recall Remark 6.22) is equivalent to the following: For any $z, z' \in Z$ with $\varphi_X(z) = x$, $\varphi_X(z') = x'$, $\varphi_Y(z) = y$ and $\varphi_Y(z') = y'$,

- (i) for any $t \in \mathbf{R}$, if x is in the underlying set of $\theta_X(t)$, then there must exist $s \in [t]^{\varepsilon}$ such that y is in the underlying set of $\theta_Y(s)$.
- (ii) for any interval $I \subset \mathbf{R}$, if $\{x, x'\} \subset B \in \bigvee_I \theta_X$, then there must exist $C \in \bigvee_{I^{\varepsilon}} \theta_Y$ such that $\{y, y'\} \subset C$.

Proof. Suppose that $\theta_X \xrightarrow{R} S_{\varepsilon}\theta_Y$. We will show that (i) and (ii) are the conditions corresponding to Remark 6.22 (i) and (ii), respectively. First, it is easy to check that (i) is the condition corresponding to Remark 6.22 (i). Next, let us show that (ii) is the condition corresponding to Remark 6.22 (ii). Namely, we wish to show that the following two conditions are equivalent:

- (ii) For any $z, z' \in Z$ with $\varphi_X(z) = x$, $\varphi_X(z') = x'$, $\varphi_Y(z) = y$ and $\varphi_Y(z') = y'$, and for any interval $I \subset \mathbf{R}$, if $\{x, x'\} \subset B \in \bigvee_I \theta_X$, then there must exist $C \in \bigvee_{I^{\varepsilon}} \theta_Y$ such that $\{y, y'\} \subset C$.
- (ii)' Consider the multivalued map $\varphi := \varphi_Y \circ \varphi_X^{-1}: X \rightrightarrows Y$ and pick any $t \in \mathbf{R}$. Then the restriction $\varphi|_{U_{\theta_X}(t)}: U_{\theta_X}(t) \rightrightarrows U_{S_{\varepsilon}\theta_Y}(t)$ of φ to $U_{\theta_X}(t)$ is a partition morphism between $\theta_X(t)$ and $S_{\varepsilon}\theta_Y(t)$.

Suppose that (ii) holds. Then by choosing interval I to be any singleton interval $\{t\} \subset \mathbf{R}$, one can see that (ii)' holds. Let us prove that (ii)' implies (ii). Let I be any interval of \mathbf{R} . Let $z, z' \in Z$ with $\varphi_X(z) = x$, $\varphi_X(z') = x'$, $\varphi_Y(z) = y$ and $\varphi_Y(z') = y'$. Also, suppose that x, x' belong to the same block B of $\bigvee_I \theta_X$, which is the finest common coarsening of $\{\theta_X(t) : t \in I\}$. By Definitions 6.16 and 6.17, there exist sequences $x = x_0, x_1, \dots, x_n = x'$ in X and t_0, t_1, \dots, t_{n-1} in I such that x_i, x_{i+1} belong to the same block of $\theta_X(t_i)$ for each $i = 0, \dots, n-1$. Then there exists a corresponding sequence $y = y_0, y_1, \dots, y_n = y'$ in Y such that $y_i \in \varphi(x_i)$ for $i = 0, \dots, n$. For each i , since $\varphi|_{U_{\theta_X}(t_i)}$ is a partition morphism from $\theta_X(t_i)$ to $S_\varepsilon \theta_Y(t_i)$, y_i and y_{i+1} belong to the same block of $S_\varepsilon \theta_Y(t_i)$. Since $S_\varepsilon \theta_X(t_i) = \bigvee_{[t_i]^\varepsilon} \theta_X$, there exist sequences $y_i = y_{i0}, y_{i1}, \dots, y_{ii_m} = y_{i+1}$ in Y and $s_{i0}, s_{i1}, \dots, s_{i(i_m-1)}$ in $[t_i]^\varepsilon$ such that y_{ik} and $y_{i(k+1)}$ belong to the same block of $\theta_X(s_{ik})$ for $k = 0, \dots, i_m - 1$. In particular, observe that $[t_i]^\varepsilon \subset I^\varepsilon$. By concatenating and re-indexing the sequences in Y and \mathbf{R} above respectively, we have shown the following: there are sequences $y = y_0, \dots, y_N = y'$ in Y and t_0, \dots, t_{N-1} in I^ε such that y_i and y_{i+1} belong to the same block of $\theta_X(t_l)$ for $l = 0, \dots, N-1$. This implies that y and y' belong to the same block of $\bigvee_{I^\varepsilon} \theta_Y$, as desired. \square

We characterize the distance between any two constant formigrams:

Proposition 6.31 (Interleaving of constant formigrams). For some finite sets X and Y , consider any two constant formigrams $\theta_X \equiv P_X \in \mathcal{P}(X)$ and $\theta_Y \equiv P_Y \in \mathcal{P}(Y)$. Then, either $d_1^F(\theta_X, \theta_Y) = 0$ or $d_1^F(\theta_X, \theta_Y) = \infty$. Specifically, $d_1^F(\theta_X, \theta_Y) = 0$ if and only if $|P_X| = |P_Y|$.

Proposition 6.31 will be proved in Section 11.1.2.

The stability result. DGs are mapped into formigrams via the path connected functor π_0 (Definition 5.15) in a stable manner:

Theorem 6.32 (π_0 is 1-Lipschitz). Let $\mathcal{G}_X = (V_X(\cdot), E_X(\cdot))$ and $\mathcal{G}_Y = (V_Y(\cdot), E_Y(\cdot))$ be any two DGs. Let $\pi_0(\mathcal{G}_X)$ and $\pi_0(\mathcal{G}_Y)$ be the formigrams defined as in Proposition 5.16. Then,

$$d_1^F(\theta_X, \theta_Y) \leq d_1^{\text{dynG}}(\mathcal{G}_X, \mathcal{G}_Y).$$

Theorem 6.32 will be proved in Section 11.1.2.

7 The effect of smoothing operations

In this section we study the effect that the smoothing operation on formigrams (Definition 6.23) has on their barcodes. We will also see that the smoothing operations defined for DGs, formigrams, and Reeb graphs are compatible in a sense that we make clear in this section. Finally we see that each S_ε defined in Definitions 6.6 and 6.23 are nonexpansive for the metrics d_1^{dynG} and d_1^F (Definitions 6.9 and 6.26).

Figure 9 illustrates both the relationship between θ_X and $S_\varepsilon \theta_X$ and the relationship between their barcodes. The following proposition precisely explains the relationship between $\text{dgm}(\theta_X)$ and $\text{dgm}(S_\varepsilon \theta_X)$. For any $r \in \mathbf{R}$, we define $-\infty + r$ to be $-\infty$.

Proposition 7.1 (Effect of ε -smoothing a formigram on its barcode). Let θ_X be a formigram over X and let $\varepsilon \geq 0$. Then, there exists the following bijection between $\text{dgm}(\theta_X)$ and $\text{dgm}(S_\varepsilon \theta_X)$:

$\text{dgm}(\theta_X)$	\longleftrightarrow	$\text{dgm}(S_\varepsilon \theta_X)$	
(b, d)	\leftrightarrow	$(b + \varepsilon, d - \varepsilon)$	for $-\infty \leq b \leq b + \varepsilon < d - \varepsilon \leq +\infty$
(b, d)	\leftrightarrow	Nothing	for $b < d < b + 2\varepsilon$.
$[b, d)$	\leftrightarrow	$[b - \varepsilon, d - \varepsilon)$	
$(b, d]$	\leftrightarrow	$(b + \varepsilon, d + \varepsilon]$	
$[b, d]$	\leftrightarrow	$[b - \varepsilon, d + \varepsilon]$	

(10)

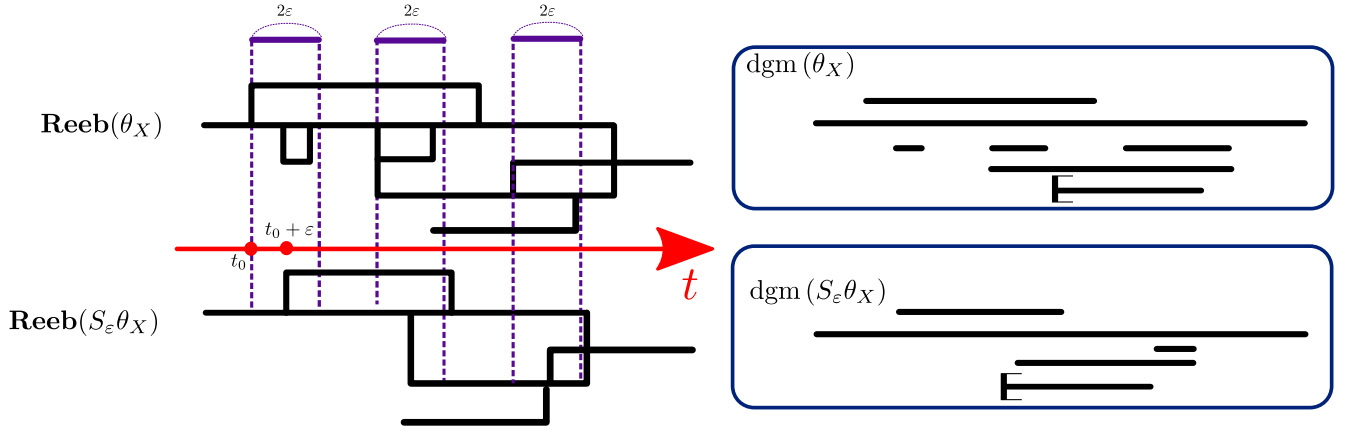


Figure 9: Top: The Reeb graph of a formigram θ_X and its barcode. Bottom: The Reeb graph of the formigram $S_\varepsilon \theta_X$ and its barcode. Small loops in $\mathbf{Reeb}(\theta_X)$ disappear in $\mathbf{Reeb}(S_\varepsilon \theta_X)$. In the barcodes, bars with “[” on the left stand for half-closed intervals of the form $[a, b)$. Open intervals in $\text{dgm}(\theta_X)$ that are shorter than 2ε do not have corresponding intervals in $\text{dgm}(S_\varepsilon \theta_X)$. Also, disbanding and merging events in θ_X which do not correspond to vertices on small loops in $\mathbf{Reeb}(\theta_X)$ are replicated in $S_\varepsilon \theta_X$: disbanding events in θ_X are reflected in $S_\varepsilon \theta_X$ but with delay ε , whereas merging events in θ_X are advanced by ε . For example, observe from the graphs $\mathbf{Reeb}(\theta_X)$ and $\mathbf{Reeb}(S_\varepsilon \theta_X)$ that the disbanding event in θ_X at $t = t_0$ is delayed to $t = t_0 + \varepsilon$ in $S_\varepsilon \theta_X$.

In words, (1) the ε -smoothing process erases open intervals shorter than 2ε , and (2) each (nonempty) interval in $\text{dgm}(S_\varepsilon \theta_X)$ is obtained by adjusting the endpoints of an interval in $\text{dgm}(\theta_X)$ according to ε as described in the table above.

The proof of Proposition 7.1 is in Section 11.3. The correspondence of barcodes given in Proposition 7.1 directly implies the following:

Corollary 7.2. Let θ_X be any formigram over X . Then, for $\varepsilon \geq 0$,

$$d_B(\text{dgm}(S_\varepsilon \theta_X), \text{dgm}(\theta_X)) \leq \varepsilon.$$

Recall the path component functor $\pi_0 : \mathbf{Graph} \rightarrow \mathbf{Sets}$ (Definition 5.15) and that its application to DGs results in formigrams (Proposition 5.16). We then have Proposition 7.3 below, which will be useful to prove some other propositions.

Proposition 7.3 (Commutativity). Let $\mathcal{G}_X = (V_X(\cdot), E_X(\cdot))$ be a DG and consider the formigram $\theta_X := \pi_0(\mathcal{G}_X)$ as in Proposition 5.16. Let $I \subset \mathbf{R}$ be any interval. Then,

$$\pi_0\left(\bigcup_I \mathcal{G}_X\right) = \bigvee_I \theta_X \text{ (see Definitions 6.6 and 6.23).}$$

Proposition 7.3 will be proved in Section 11.3. The smoothing operations defined for DGs, formigrams and Reeb graphs are compatible:

Proposition 7.4 (Compatibility between the smoothing operations). Let $\varepsilon \geq 0$. The ε -smoothing operations for DGs, formigrams, and Reeb graphs (Definitions 6.6, 6.23, and [22, Section 4.4]) are compatible to each other in the following sense:

(i) Let \mathcal{G}_X be a DG over X . Then,

$$\pi_0(S_\varepsilon \mathcal{G}_X) = S_\varepsilon(\pi_0(\mathcal{G}_X))$$

where S_ε on the LHS and the RHS are the smoothing operations for DGs and formigrams, respectively (Definitions 6.6 and 6.23).

(ii) Let θ_X be a formigram over X . Then,

$$\mathbf{Reeb}(S_\varepsilon \theta_X) = \mathcal{U}_\varepsilon \mathbf{Reeb}(\theta_X)$$

where S_ε and \mathcal{U}_ε on the LHS and the RHS are the smoothing operations for formigrams and Reeb graphs, respectively (Definition 6.23 and [22, Section 4.4]).

Proposition 7.4 will be proved in Section 11.3. The ε -smoothing operations make DGs and formigrams change continuously with respect to ε :

Proposition 7.5 (Continuity of smoothing operations). For any $\varepsilon \geq 0$, consider the smoothing operations S_ε of Definitions 6.6 and 6.23.

(i) For any DG \mathcal{G}_X over X ,

$$d_1^{\text{dynG}}(S_\varepsilon \mathcal{G}_X, \mathcal{G}_X) \leq \varepsilon.$$

(ii) For any formigram θ_X over X ,

$$d_1^{\text{F}}(S_\varepsilon \theta_X, \theta_X) \leq \varepsilon.$$

Proof. To prove (i), consider the tripod $R : X \xleftarrow{\text{id}_X} X \xrightarrow{\text{id}_X} X$ and check that R is an ε -tripod between $S_\varepsilon \mathcal{G}_X$ and \mathcal{G}_X . The same strategy can be applied for proving (ii). \square

The following proposition is analogous to [22, Proposition 4.14], which states that the ε -smoothing operation on cosheaves (i.e. functors from \mathbf{U} to \mathbf{Sets}) is non-expansive with respect to the interleaving distance for cosheaves. The proof directly follows from Propositions 6.8 and 6.25.

Proposition 7.6 (Non-expansiveness of smoothing operations). For any $\varepsilon \geq 0$, consider the smoothing operations S_ε of Definitions 6.6 and 6.23. Then, each S_ε is a contraction, i.e.

(i) for any DGs \mathcal{G}_X and \mathcal{G}_Y over X and Y respectively,

$$d_1^{\text{dynG}}(S_\varepsilon \mathcal{G}_X, S_\varepsilon \mathcal{G}_Y) \leq d_1^{\text{dynG}}(\mathcal{G}_X, \mathcal{G}_Y),$$

(ii) for any formigrams θ_X and θ_Y over X and Y respectively,

$$d_1^{\text{F}}(S_\varepsilon \theta_X, S_\varepsilon \theta_Y) \leq d_1^{\text{F}}(\theta_X, \theta_Y).$$

We also have:

Proposition 7.7. Let θ_X and θ_Y be formigrams over X and Y , respectively. Then, for any $\varepsilon \geq 0$,

$$d_{\text{B}}(\text{dgm}(S_\varepsilon \theta_X), \text{dgm}(S_\varepsilon \theta_Y)) \leq d_{\text{B}}(\text{dgm}(\theta_X), \text{dgm}(\theta_Y)) + 2\varepsilon.$$

Proof. By the triangle inequality for d_{B} , we have:

$$\begin{aligned} d_{\text{B}}(\text{dgm}(S_\varepsilon \theta_X), \text{dgm}(S_\varepsilon \theta_Y)) &\leq d_{\text{B}}(\text{dgm}(S_\varepsilon \theta_X), \text{dgm}(\theta_X)) + d_{\text{B}}(\text{dgm}(\theta_X), \text{dgm}(\theta_Y)) \\ &\quad + d_{\text{B}}(\text{dgm}(\theta_Y), \text{dgm}(S_\varepsilon \theta_Y)). \end{aligned}$$

Then, by invoking Corollary 7.2, we obtain the desired inequality. \square

Remark 7.8. Let θ_X and θ_Y be any two *saturated* formigrams over X and Y . Then, by invoking Remark 5.13 and Proposition 7.1, one can check that the inequality in Proposition 7.7 can be improved to

$$d_{\text{B}}(\text{dgm}(S_\varepsilon \theta_X), \text{dgm}(S_\varepsilon \theta_Y)) \leq d_{\text{B}}(\text{dgm}(\theta_X), \text{dgm}(\theta_Y)).$$

8 Dynamic directed graphs (DDGs)

In this section we extend our framework to the setting of dynamic directed graphs (DDGs).

Definition 8.1 (Dynamic directed graphs). A *dynamic directed graph* (DDG) $\overrightarrow{\mathcal{G}}_X$ over X consists of maps

$$V_X(\cdot) : \mathbf{R} \rightarrow \text{pow}(X) \quad \text{and} \quad A_X(\cdot) : \mathbf{R} \rightarrow \text{pow}(V_X(\cdot) \times V_X(\cdot)),$$

satisfying the conditions below. By $\text{crit}(\overrightarrow{\mathcal{G}}_X)$ we denote the union of the set of points of discontinuity of $V_X(\cdot)$ and the set of points of discontinuity of $A_X(\cdot)$. We call the elements of $\text{crit}(\overrightarrow{\mathcal{G}}_X)$ the *critical points* of $\overrightarrow{\mathcal{G}}_X$. We require $\overrightarrow{\mathcal{G}}_X = (V_X(\cdot), A_X(\cdot))$ to satisfy the following:

- (i) (Self-loops) For all $t \in \mathbf{R}$ and for all $x \in V_X(t)$, $(x, x) \in A_X(t)$.
- (ii) (Tameness) The set $\text{crit}(\overrightarrow{\mathcal{G}}_X)$ is locally finite.
- (iii) (Lifespan of vertices) for every $x \in X$, the set $I_x := \{t \in \mathbf{R} : x \in V_X(t)\}$, said to be the *lifespan* of x , is a non-empty interval.
- (iv) (Comparability) for every $t \in \mathbf{R}$, it holds that

$$V_X(t - \varepsilon) \subset V_X(t) \supset V_X(t + \varepsilon) \quad \text{and} \quad A_X(t - \varepsilon) \subset A_X(t) \supset A_X(t + \varepsilon)$$

for all sufficiently small $\varepsilon > 0$ (concisely, we can re-write this as $\overrightarrow{\mathcal{G}}_X(t - \varepsilon) \subset \overrightarrow{\mathcal{G}}_X(t) \supset \overrightarrow{\mathcal{G}}_X(t + \varepsilon)$).

In plain words, a DDG can be regarded as a digraph that is subject to a sequence of updates such as addition/deletion of vertices/arrows.

8.1 From DDGs to formigrams

We describe the process that associates a certain formigram to any DDG. Recall the category **Digraph** of directed graphs with digraph morphisms (Section 3.1, item 8).

Definition 8.2 (Clustering functors for DDGs). A functor $\overrightarrow{\pi}_0 : \mathbf{Digraph} \rightarrow \mathbf{Sets}$ is said to be a *clustering functor* if

- (i) Any digraph $\overrightarrow{G}_X = (X, A_X)$ is sent to a partition $\overrightarrow{\pi}_0(\overrightarrow{G}_X)$ of X , i.e. $\overrightarrow{\pi}_0(\overrightarrow{G}_X) \in \mathcal{P}(X)$.
- (ii) Any digraph morphism $f : \overrightarrow{G}_X = (X, A_X) \rightarrow \overrightarrow{G}_Y = (Y, A_Y)$ is also a partition morphism $\overrightarrow{\pi}_0(f)$ from $\overrightarrow{\pi}_0(\overrightarrow{G}_X)$ to $\overrightarrow{\pi}_0(\overrightarrow{G}_Y)$ (Definition 6.21). (f is identical to $\overrightarrow{\pi}_0(f)$ as a set map from X to Y .)

Remark 8.3. Let X be a non-empty finite set and let X' be a non-empty subset of X . Suppose that $\overrightarrow{G}_{X'} = (X', A_{X'})$ and $\overrightarrow{G}_X = (X, A_X)$ are any digraphs such that $A_{X'} \subset A_X$. Then the inclusion $\overrightarrow{G}_{X'} \hookrightarrow \overrightarrow{G}_X$ is a digraph morphism. Hence, for any clustering functor $\overrightarrow{\pi}_0 : \mathbf{Digraph} \rightarrow \mathbf{Sets}$, we have $\overrightarrow{\pi}_0(\overrightarrow{G}_{X'}) \leq \overrightarrow{\pi}_0(\overrightarrow{G}_X)$ in $\mathcal{P}^{\text{sub}}(X)$ (Definition 5.1).

Let $\overrightarrow{G}_X = (X, A_X)$ be a digraph and let $x, x' \in X$. A *directed path* p from x to x' refers to any sequence of directed edges $(x, x_1), (x_1, x_2), \dots, (x_n, x')$ in A_X . If the reverse directed edges $(x_1, x), (x_2, x_1), \dots, (x', x_n)$ are in A_X , then the path p admits a reverse path $p^{-1} : (x', x_n), (x_n, x_{n-1}), \dots, (x_1, x)$ from x' to x in \overrightarrow{G}_X , in which case we say that the directed path p is reversible.

Example 8.4 (Reciprocal and nonreciprocal clustering functors). Let $\overrightarrow{G}_X = (X, A_X)$ be any digraph.

- (i) Define the partition $\overrightarrow{\pi}_0^r(X, A_X) := X / \sim$ of X where \sim stands for the equivalence relation on X defined by $x \sim x'$ if and only if $x = x'$ or there exist a reversible directed path p from x to x' .

- (ii) Define the partition $\vec{\pi}_0^n(X, A_X) := X / \sim$ of X where \sim stands for the equivalence relation on X defined by $x \sim x'$ if and only if $x = x'$ or there are a directed path from x to x' and another direct path from x' to x .

Note that any digraph morphism $f : \vec{G}_X = (X, A_X) \rightarrow \vec{G}_Y = (Y, A_Y)$ is a set map from X to Y , which is a partition morphism between $\vec{\pi}_0^r(X, A_X)$, $\vec{\pi}_0^r(Y, A_Y)$ and between $\vec{\pi}_0^n(X, A_X)$, $\vec{\pi}_0^n(Y, A_Y)$. We call $\vec{\pi}_0^r$ and $\vec{\pi}_0^n$ the *reciprocal clustering functor* and the *nonreciprocal clustering functor*, respectively.¹⁰ It is noteworthy that $\vec{\pi}_0^r$ and $\vec{\pi}_0^n$ are analogous to the *reciprocal clustering method* the *nonreciprocal clustering method*, respectively for *weighted* directed graphs, i.e. networks [16].

Given a digraph $\vec{G}_X = (X, A_X)$, define $A_X^T := \{(x', x) \in X \times X : (x, x') \in A_X\}$.

Example 8.5 (Weakly connected component functor). Let $\vec{G}_X = (X, A_X)$ be any digraph. Define the partition $\vec{\pi}_0^w(X, A_X)$ of X to be $\vec{\pi}_0^r(X, A_X \cup A_X^T)$. It is not difficult to check that any digraph morphism $f : \vec{G}_X = (X, A_X) \rightarrow \vec{G}_Y = (Y, A_Y)$, a set map from X to Y , is a partition morphism between $\vec{\pi}_0^w(X, A_X)$ and $\vec{\pi}_0^w(Y, A_Y)$.

We can turn any DDG into a formigram via clustering functors (Definition 8.2):

Proposition 8.6. Let $\vec{\mathcal{G}}_X$ be a DDG over X and let $\vec{\pi}_0$ be any clustering functor. Then, the function $\vec{\pi}_0(\vec{\mathcal{G}}_X) : \mathbf{R} \rightarrow \mathcal{P}^{\text{sub}}(X)$ defined by $\vec{\pi}_0(\vec{\mathcal{G}}_X)(t) = \vec{\pi}_0(\vec{\mathcal{G}}_X(t))$ for $t \in \mathbf{R}$ satisfies all the conditions in Definition 5.4, therefore it is a formigram.

The proof of Proposition 8.6 is similar to that of Proposition 5.16, and thus we omit it.

8.2 A distance between DDGs

We define various notions that are necessary for defining the interleaving distance between DDGs. These notions are defined similarly to the ones for DGs in Section 6.1 via the following substitutions:

$$\mathcal{G}_X \leftarrow \vec{\mathcal{G}}_X, \quad \mathcal{G}_Y \leftarrow \vec{\mathcal{G}}_Y, \quad \text{“graph”} \leftarrow \text{“digraph”}.$$

The time-interlevel smoothing of DDG. This is defined in the same way as Definition 6.6.

Pullback of a (dynamic) digraph. Let $\vec{G}_X = (X, A_X)$ be any digraph and let Z be any set. For any map $\varphi : Z \rightarrow X$, the pullback $\vec{G}_Z := \varphi^* \vec{G}_X$ is the digraph on the vertex set Z with the directed edge set $A_Z = \{(z, z') : (\varphi(z), \varphi(z')) \in A_X\}$.

Definition 8.7 (Pullback of a DDG). Let $\vec{\mathcal{G}}_X$ be a DDG and let Z be any set. For any map $\varphi : Z \rightarrow X$, the pullback $\vec{\mathcal{G}}_Z := \varphi^* \vec{\mathcal{G}}_X$ of $\vec{\mathcal{G}}_X$ via φ is a DDG over Z defined as follows: for all $t \in \mathbf{R}$, $\vec{\mathcal{G}}_Z(t)$ is the digraph on the vertex set $V_Z(t) = \varphi^{-1}(V_X(t))$ with the directed edge set $A_Z(t) = \{(z, z') : (\varphi(z), \varphi(z')) \in A_X(t)\}$.

Interconnecting DDGs via tripods. Let $\vec{\mathcal{G}}_X = (V_X(\cdot), A_X(\cdot))$ and $\vec{\mathcal{G}}_Y = (V_Y(\cdot), A_Y(\cdot))$ be any two DDGs. Also, let $R : X \xleftarrow{\varphi_X} Z \xrightarrow{\varphi_Y} Y$ be any tripod between X and Y . By $\vec{\mathcal{G}}_X \xrightarrow{R} \vec{\mathcal{G}}_Y$ we mean the following: For all $t \in \mathbf{R}$, $\varphi_X^* \vec{\mathcal{G}}_X(t)$ is a sub-digraph of $\varphi_Y^* \vec{\mathcal{G}}_Y(t)$, i.e. the vertex set and the directed edge set of $\varphi_X^* \vec{\mathcal{G}}_X(t)$ are subsets of those of $\varphi_Y^* \vec{\mathcal{G}}_Y(t)$, respectively. (cf. Definition 6.3). We note:

Remark 8.8. Assuming $\vec{\mathcal{G}}_X \xrightarrow{R} \vec{\mathcal{G}}_Y$, let $f : X \rightarrow Y$ be any map such that $\{(x, f(x)) : x \in X\} \subset \varphi_Y \circ \varphi_X^{-1}$. Then, for all $t \in \mathbf{R}$, f is a digraph morphism from $\vec{\mathcal{G}}_X(t)$ to $\vec{\mathcal{G}}_Y(t)$, i.e. for any $(x, x') \in A_X(t)$, $(f(x), f(x')) \in A_Y(t)$.

The interleaving distance between DDGs. Definition 6.9 extends to the one for DDGs.

¹⁰The nonreciprocal clustering functor is often said to be the strongly connected component functor.

8.3 Stability of clustering

The following theorem is analogous to Theorem 6.32.

Theorem 8.9. Let $\overrightarrow{\mathcal{G}}_X, \overrightarrow{\mathcal{G}}_Y$ be any two DDGs over finite sets X and Y , respectively. Let $\overrightarrow{\pi}_0^w : \mathbf{Digraph} \rightarrow \mathbf{Sets}$ be the weakly connected component clustering functor (Example 8.5). Let $\theta_X := \overrightarrow{\pi}_0^w(\overrightarrow{\mathcal{G}}_X)$ and $\theta_Y := \overrightarrow{\pi}_0^w(\overrightarrow{\mathcal{G}}_Y)$ be the formigrams defined as in Proposition 8.6. Then,

$$d_1^F(\theta_X, \theta_Y) \leq d_1^{\text{dynG}}(\overrightarrow{\mathcal{G}}_X, \overrightarrow{\mathcal{G}}_Y).$$

Proof. Let $\varepsilon \geq 0$ and let $R : X \xleftarrow{\varphi_X} Z \xrightarrow{\varphi_Y} Y$ be an ε -tripod between $\overrightarrow{\mathcal{G}}_X$ and $\overrightarrow{\mathcal{G}}_Y$. We prove that R is also an ε -tripod between the formigrams θ_X and θ_Y . By symmetry, we will only prove that $\theta_X \xrightarrow{R} S_\varepsilon \theta_Y$. Let $z \in Z$ and let $\varphi_X(z) = x$, and $\varphi_Y(z) = y$. Fix $t \in \mathbf{R}$. Assume that x is in the underlying set of $\theta_X(t)$, which means that $x \in V_X(t)$. Since $\overrightarrow{\mathcal{G}}_X \xrightarrow{R} S_\varepsilon \overrightarrow{\mathcal{G}}_Y$, y must be in the vertex set of $S_\varepsilon \overrightarrow{\mathcal{G}}_Y(t)$, which is $\cup_{s \in [t]^\varepsilon} V_Y(s)$. It is easy to check that the underlying set of $(S_\varepsilon \theta_Y)(t) = \bigvee_{[t]^\varepsilon} \theta_Y$ is identical to $\cup_{s \in [t]^\varepsilon} V_Y(s)$ and therefore, y is in the underlying set of $S_\varepsilon \theta_Y(t)$.

Pick another $z' \in Z$ and let $\varphi_X(z') = x'$ and $\varphi_Y(z') = y'$. Suppose that x, x' belong to the same block of $\theta_X(t)$. Choose any map $\varphi : X \rightarrow Y$ such that $\{(x, \varphi(x)) : x \in X\} \subset \varphi_Y \circ \varphi_X^{-1}$ with $\varphi(x) = y$ and $\varphi(x') = y'$. By Remark 8.8, φ is a digraph morphism from $\overrightarrow{\mathcal{G}}_X(t)$ onto the image $\varphi(\overrightarrow{\mathcal{G}}_X(t))$ in $S_\varepsilon \overrightarrow{\mathcal{G}}_Y(t)$. By functoriality of $\overrightarrow{\pi}_0^w$, we have $\theta_X(t) = \overrightarrow{\pi}_0^w(\overrightarrow{\mathcal{G}}_X(t)) \leq_\varphi \overrightarrow{\pi}_0^w(\varphi(\overrightarrow{\mathcal{G}}_X(t)))$ (Definition 6.21), and thus y, y' belong to the same block of $\overrightarrow{\pi}_0^w(\varphi(\overrightarrow{\mathcal{G}}_X(t)))$. Also, by Remark 8.3, we know that $\overrightarrow{\pi}_0^w(\varphi(\overrightarrow{\mathcal{G}}_X(t))) \leq \overrightarrow{\pi}_0^w(S_\varepsilon \overrightarrow{\mathcal{G}}_Y(t))$ in $\mathcal{P}^{\text{sub}}(Y)$ and hence y, y' belong to the same block of $\overrightarrow{\pi}_0^w(S_\varepsilon \overrightarrow{\mathcal{G}}_Y(t))$. Since $\overrightarrow{\pi}_0^w(S_\varepsilon \overrightarrow{\mathcal{G}}_Y(t)) = \overrightarrow{\pi}_0^w(\bigcup_{[t]^\varepsilon} \overrightarrow{\mathcal{G}}_Y) = \bigvee_{[t]^\varepsilon} \theta_Y$, y, y' belong to the same block of $\bigvee_{[t]^\varepsilon} \theta_Y$. \square

Remark 8.10. It is noteworthy that Theorem 8.9 and its proof are valid even if $\overrightarrow{\pi}_0^w$ is replaced by any other clustering functor $\overrightarrow{\pi}_0$ (Definition 8.2) satisfying the following: For any $\varepsilon \geq 0$ and for any DDG $\overrightarrow{\mathcal{G}}_X = (V_X(\cdot), A_X(\cdot))$, $\overrightarrow{\pi}_0(S_\varepsilon \overrightarrow{\mathcal{G}}_X) = S_\varepsilon(\overrightarrow{\pi}_0(\overrightarrow{\mathcal{G}}_X))$.

The theorem below further implies that we can encode the clustering features of DDGs into barcodes in a stable manner, which is analogous to Theorem 1.1:

Theorem 8.11. Let $\overrightarrow{\mathcal{G}}_X, \overrightarrow{\mathcal{G}}_Y$ be any two DDGs over finite sets X and Y , respectively. For the weakly connected component clustering functor $\overrightarrow{\pi}_0^w$, let $\theta_X := \overrightarrow{\pi}_0^w(\overrightarrow{\mathcal{G}}_X)$ and $\theta_Y := \overrightarrow{\pi}_0^w(\overrightarrow{\mathcal{G}}_Y)$ be the formigrams defined as in Proposition 8.6. Then,

$$d_B(\text{dgm}(\theta_X), \text{dgm}(\theta_Y)) \leq 2 d_1^{\text{dynG}}(\overrightarrow{\mathcal{G}}_X, \overrightarrow{\mathcal{G}}_Y).$$

The proof of Theorem 8.11 is similar to that of Theorem 1.1 (see Section 2) except that we invoke Theorem 8.9 instead of Theorem 6.32, thus we omit it.

9 Analysis of dynamic metric spaces (DMSs)

Our work was first motivated by the desire to construct a well-defined summarization tool of clustering behavior of time-varying metric data, which will be said to be *dynamic metric spaces (DMSs)*. In this section, we introduce a method to turn DMSs into DGs (Proposition 9.5), which enables us to produce clustering barcodes derived from DMSs through the process that we have established in Propositions 5.10 and 5.16.

Besides permitting the simple visualization of clustering behaviors of DMS, one of the benefits of this summarization process is that we can quantify the degree of behavioral difference between two DMSs by computing the bottleneck distance between their clustering barcodes via efficient algorithm without incurring high cost.

9.1 DMSs

In this section we introduce definitions pertaining to our model for dynamic metric spaces (DMSs). In particular, *tameness* (Definition 9.4) is a crucial requirement on DMSs, which permits transforming DMSs into DGs, formigrams, Reeb graphs, and eventually barcodes. Details and omitted proofs can be found in Section 11.4.

Main definitions. Recall that a pseudo-metric space is a pair (X, d_X) where X is a (non-empty) set and $d_X : X \times X \rightarrow \mathbf{R}_+$ is a symmetric function which satisfies the triangle inequality, and such that $d_X(x, x) = 0$ for all $x \in X$. d_X is called the pseudo-metric. Note that one does not require that $d_X(x, x') = 0$ implies that $x = x'$ like in the case of standard metric spaces. Let \mathcal{M} (resp. \mathcal{M}_*) denote the collection of all finite (resp. pseudo-) metric spaces. Clearly, $\mathcal{M} \subset \mathcal{M}_*$. The *trivial* metric space $*$ is the one point metric space. We extend the definition of isometry to pseudo-metric spaces: two finite pseudo-metric spaces are called isometric if there exists a metric preserving bijection between them. Given a pseudo-metric space (X, d_X) one considers the equivalence relation \sim_X on X such that $x \sim_X x'$ if and only if $d_X(x, x') = 0$. By taking the quotient X'/\sim_X one obtains a metric space $(X', d_{X'})$ where $d_{X'}(p, p')$ is defined as $d_X(x, x')$ for any $x \in p$ and $x' \in p'$ for any equivalence classes $p, p' \in X'$ (using triangle inequalities, one can check that the choice of $x \in p$ and $x' \in p'$ does not affect the value of $d_X(x, x')$). We call the finite metric space $(X', d_{X'})$ thus obtained the *core* of (X, d_X) . For example, the core of the finite pseudo-metric space $(\{x_1, x_2\}, \begin{pmatrix} 0 & 0 \\ 0 & 0 \end{pmatrix})$ is the trivial metric space. We say that pseudo-metric spaces (X, d_X) and (Y, d_Y) are *equivalent* if their cores are isometric.

Definition 9.1 (Dynamic metric spaces). A *dynamic metric space* is a pair $\gamma_X = (X, d_X(\cdot))$ where X is a non-empty finite set and $d_X : \mathbf{R} \times X \times X \rightarrow \mathbf{R}_+$ satisfies:

- (i) For every $t \in \mathbf{R}$, $\gamma_X(t) = (X, d_X(t))$ is a pseudo-metric space.
- (ii) There exists $t_0 \in \mathbf{R}$ such that $\gamma_X(t_0)$ is a metric space.
- (iii) For fixed $x, x' \in X$, $d_X(\cdot)(x, x') : \mathbf{R} \rightarrow \mathbf{R}_+$ is continuous.

We refer to t as the *time* parameter.

We remark that a DMS γ_X is therefore to be regarded as a special type of continuous curve $\gamma_X : \mathbf{R} \rightarrow \mathcal{M}_*$, Condition 2 above is assumed since otherwise one could substitute the DMSs γ_X by another DMSs $\gamma_{X'}$ over a set X' which satisfies $|X'| < |X|$, and such that $\gamma_{X'}$ is point-wisely equivalent to γ_X .

Example 9.2 (Examples of DMSs). (i) As a first simple example consider the dynamic metric space $\gamma_* = (\{*\}, d_*)$ consisting of exactly one point. This means that the distance function $d_*(t)$ is exactly 0 for all $t \in \mathbf{R}$. We call γ_* the *trivial DMS*.

- (ii) Given a finite metric space (X, d'_X) , define the DMS $\gamma_X = (X, d_X(\cdot))$ where $d_X(\cdot)$ is the constant function on its first argument equal to d'_X . We refer to these as *constant* DMSs.
- (iii) A family of examples is given by n particles/animals moving continuously inside an environment $\Omega \subset \mathbf{R}^d$ where particles are allowed to coalesce. If the n trajectories are $p_1(t), \dots, p_n(t) \in \mathbf{R}^d$, then let $P := \{1, \dots, n\}$ and define a DMS $\gamma_P := (P, d_P(\cdot))$ as follows: for $t \in \mathbf{R}$ and $i, j \in \{1, \dots, n\}$, let $d_P(t)(i, j) := \|p_i(t) - p_j(t)\|$, where $\|\cdot\|$ denotes the Euclidean norm.
- (iv) Another example of a DMS is given by the following construction: Let $\psi : \mathbf{R} \rightarrow \mathbf{R}_+$ be any non identically zero continuous function. Then, for any finite metric space (X, d'_X) consider the DMS $\gamma_X^\psi = (X, d_X^\psi(\cdot))$ where for $t \in \mathbf{R}$, $d_X^\psi(t) := \psi(t) \cdot d'_X$.

We now introduce a notion of *equality* between two DMSs.

Definition 9.3 (Isomorphic DMSs). Let $\gamma_X = (X, d_X(\cdot))$ and $\gamma_Y = (Y, d_Y(\cdot))$ be two DMSs. We say that γ_X and γ_Y are isomorphic if there exists a bijection $\varphi : X \rightarrow Y$ such that φ is an isometry between $\gamma_X(t)$ and $\gamma_Y(t)$ across all $t \in \mathbf{R}$.

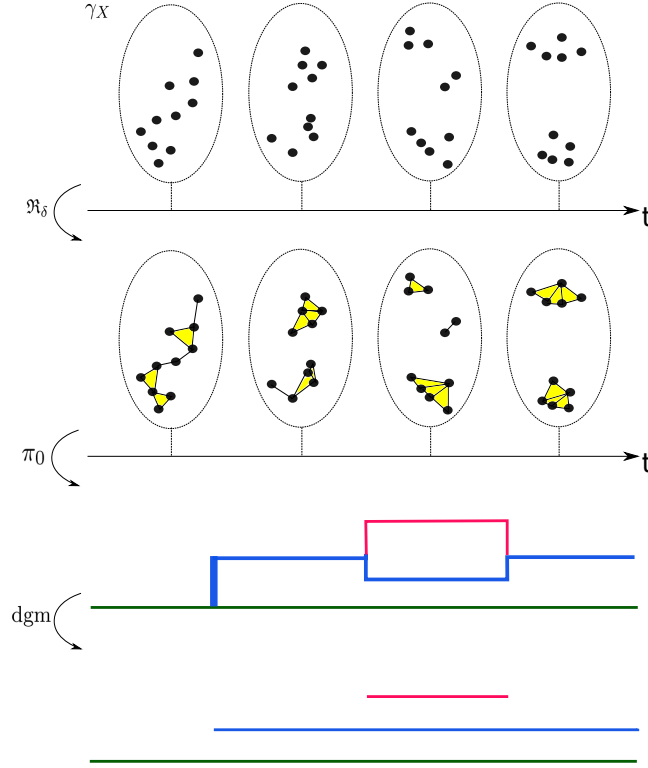


Figure 10: Summarization process of a DMS. A DMS, which is represented as a dynamic point cloud in the first row over the time axis, is converted into a zigzag simplicial complex (its 1-dimensional skeleton is a DG), into a formigram, and eventually into a barcode.

For example, when γ_X and γ_Y are constant DMSs, then they are isomorphic if and only if the underlying metric spaces are isometric.

Tame DMSs. We introduce a notion of *tameness* of DMS which will ultimately ensure that their zigzag persistent homology barcodes are well defined. We first define *tame* functions $f : \mathbf{R} \rightarrow \mathbf{R}$: a continuous function $f : \mathbf{R} \rightarrow \mathbf{R}$ is *tame*, if for any $c \in \mathbf{R}$ and any finite interval $I \subset \mathbf{R}$, the set $f^{-1}(c) \cap I \subset \mathbf{R}$ is empty or has only finitely many connected components. For instance, polynomial functions (in particular, constant functions) and Morse functions on \mathbf{R} are tame.

Definition 9.4 (Tame DMSs). We say that a DMS $\gamma_X = (X, d_X(\cdot))$ is *tame* if for any $x, x' \in X$ the function $d_X(\cdot)(x, x') : \mathbf{R} \rightarrow \mathbf{R}_+$ is tame.

9.2 From DMSs to DGs

In this section we propose a method to turn tame DMSs into DGs. Then, in turn, those DGs can be summarized further by converting them into formigrams and barcodes (see Figure 10) according to the method we have established (Proposition 5.16 and Definition 5.10).

Recall the Rips graph functor $\mathcal{R}_\delta^1 : \mathbf{Met} \rightarrow \mathbf{Graph}$ with threshold $\delta \geq 0$ from item 16 of Section 3.1 and the concept of tame DMSs from Definition 9.4. The following proposition establishes that the Rips graph functor turns a *tame* DMS into a DG.

Proposition 9.5 (From DMS to DG). Let γ_X be a *tame* DMS over X and let $\delta \geq 0$. Then, by defining $\mathcal{R}_\delta^1(\gamma_X)(t) := \mathcal{R}_\delta^1(\gamma_X(t))$ for $t \in \mathbf{R}$, $\mathcal{R}_\delta^1(\gamma_X)$ is a (saturated) DG over X .

The proof of Proposition 9.5 is given in Section 11.4.1. Let γ_X be a tame DMS over X . By Proposition 9.5 and Proposition 5.16, one can obtain a formigram $\theta_X := \pi_0(\mathcal{R}_\delta^1(\gamma_X))$. The following remark provides the complexity of computing the Reeb graph of θ_X for a certain case.

Remark 9.6 (Computing the Reeb graphs of formigrams in polynomial time). It is known from [10, Theorem 7] that if a DMS γ_X is given by a set of n points, in which each point travels along a linear trajectory with k edges in Euclidean space (\mathbf{R}^2), the Reeb graph $\mathbf{Reeb}(\theta_X)$ of the formigram $\theta_X := \pi_0(\mathcal{R}_\delta^1(\gamma_X))$ has $O(kn^2)$ edges, and can be computed in $O(kn^2 \log n)$ time.

9.3 The λ -slack interleaving distance between DMSs

The main goal of this section is to introduce a $[0, \infty)$ -parametrized family $\{d_{\lambda, \lambda}^{\text{dynM}}\}_{\lambda \in [0, \infty)}$ of extended metrics for DMSs. Each metric in this family is a hybrid between the Gromov-Hausdorff distance and the interleaving distance [9, 17] for Reeb graphs [22]. Specifically, we have a stability result with respect to the most stringent metric (the metric corresponding to $\lambda = 0$) in the family (Theorem 9.21). We begin with introducing new notation:

Definition 9.7. Let $\varepsilon \geq 0$. Given any map $d : X \times X \rightarrow \mathbf{R}$, by $d + \varepsilon$ we denote the map $X \times X \rightarrow \mathbf{R}$ defined as $(d + \varepsilon)(x, x') = d(x, x') + \varepsilon$ for all $(x, x') \in X \times X$.

Definition 9.8. Given any DMS $\gamma_X = (X, d_X(\cdot))$ and any interval $I \subset \mathbf{R}$, define the map $\bigvee_I d_X : X \times X \rightarrow \mathbf{R}_+$ by $(\bigvee_I d_X)(x, x') := \min_{t \in I} d_X(t)(x, x')$ for all $(x, x') \in X \times X$.

Given any map $d : X \times X \rightarrow \mathbf{R}$, let Z be any set and let $\varphi : Z \rightarrow X$ be any map. Then, we define $\varphi^* d : Z \times Z \rightarrow \mathbf{R}$ as

$$\varphi^* d(z, z') := d(\varphi(z), \varphi(z'))$$

for all $(z, z') \in Z \times Z$.

Definition 9.9 (Comparison of functions via tripods). Consider any two maps $d_1 : X \times X \rightarrow \mathbf{R}$ and $d_2 : Y \times Y \rightarrow \mathbf{R}$. Given a tripod

$R : X \xleftarrow{\varphi_X} Z \xrightarrow{\varphi_Y} Y$ between X and Y , by $d_1 \leq_R d_2$ we mean $\varphi_X^* d_1(z, z') \leq \varphi_Y^* d_2(z, z')$ for all $(z, z') \in Z \times Z$.

Recall that for any $t \in \mathbf{R}$, $[t]^\varepsilon := [t - \varepsilon, t + \varepsilon]$.

Definition 9.10 (λ -distortion of a tripod). Fix $\lambda \geq 0$. Let $\gamma_X = (X, d_X(\cdot))$ and $\gamma_Y = (Y, d_Y(\cdot))$ be any two DMSs. Let $R : X \xleftarrow{\varphi_X} Z \xrightarrow{\varphi_Y} Y$ be a tripod between X and Y such that

$$\text{for all } t \in \mathbf{R}, \bigvee_{[t]^\varepsilon} d_X \leq_R d_Y(t) + \lambda \varepsilon \text{ and } \bigvee_{[t]^\varepsilon} d_Y \leq_R d_X(t) + \lambda \varepsilon. \quad (11)$$

We call any such R a (λ, ε) -tripod between γ_X and γ_Y . Define the λ -distortion $\text{dis}_\lambda^{\text{dyn}}(R)$ of R to be the infimum of $\varepsilon \geq 0$ for which R is a (λ, ε) -tripod.

Remark 9.11. In Definition 9.10, if R is a (λ, ε) -tripod, then R is also a (λ, ε') -tripod for any $\varepsilon' > \varepsilon$: Fix any $t \in \mathbf{R}$. If for some $\varepsilon \geq 0$, $\bigvee_{[t]^\varepsilon} d_X \leq_R d_Y(t) + \lambda \varepsilon$, then for any $\varepsilon' > \varepsilon$,

$$\bigvee_{[t]^{\varepsilon'}} d_X \leq \bigvee_{[t]^\varepsilon} d_X \leq_R d_Y(t) + \lambda \varepsilon < d_Y(t) + \lambda \varepsilon'.$$

Example 9.12. For $\lambda > 0$, $\text{dis}_\lambda^{\text{dyn}}(R)$ in Definition 9.10 takes into account both spatial and temporal distortion of the tripod R between γ_X and γ_Y :

- (i) (Spatial distortion) Let $a, b \geq 0$. For the two metric spaces $(X, d_{X,a}) = (\{x, x'\}, \begin{pmatrix} 0 & a \\ a & 0 \end{pmatrix})$ and $(X, d_{X,b}) = (\{x, x'\}, \begin{pmatrix} 0 & b \\ b & 0 \end{pmatrix})$, consider the two constant DMSs $\gamma_{X,a} \equiv (X, d_{X,a})$ and $\gamma_{X,b} \equiv (X, d_{X,b})$ (Example 9.2 (ii)).

Take the tripod $R : X \xleftarrow{\text{id}_X} X \xrightarrow{\text{id}_X} X$. Then, for $\lambda > 0$, it is easy to check that $\text{dis}_\lambda^{\text{dyn}}(R) = \frac{|a-b|}{\lambda}$.

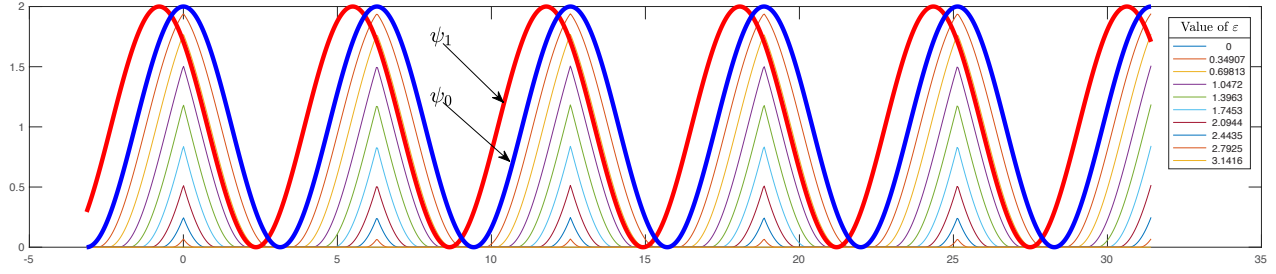


Figure 11: **The interleaving condition.** The thick blue curve and the thick red curve represent the graphs of $\psi_0(t) = 1 + \cos(t)$ and $\psi_1(t) = 1 + \cos(t + \pi/4)$, respectively. Fixing $\varepsilon \geq 0$, define a function $S_\varepsilon(\psi_0) : \mathbf{R} \rightarrow \mathbf{R}$ by $S_\varepsilon(\psi_0)(t) := \min_{s \in [t, t+\varepsilon]} \psi_0(s)$. The thin curves below the thick blue curve illustrate the graphs of $S_\varepsilon(\psi_0)$ for several different choices of ε . Note that for $\varepsilon \geq \pi/4 \approx 0.785$, it holds that $S_\varepsilon(\psi_0) \leq \psi_1$.

- (ii) (Temporal distortion) Fix $\tau \geq 0$. Let $\gamma_X = (X, d_X(\cdot))$ be any DMS and define any continuous map $\alpha : \mathbf{R} \rightarrow \mathbf{R}$ such that $\|\alpha - \text{id}_{\mathbf{R}}\|_\infty \leq \tau$. Define the DMS $\gamma_X \circ \alpha := (X, d_X(\alpha(\cdot)))$, i.e. for $t \in \mathbf{R}$, $\gamma_X \circ \alpha(t) = (X, d_X(\alpha(t)))$. Take the tripod $R : X \xleftarrow{\text{id}_X} X \xrightarrow{\text{id}_X} X$. Then, for any $\lambda \geq 0$, it is easy to check that $\text{dis}_\lambda^{\text{dyn}}(R) \leq \tau$.

Now we introduce a family of metrics for DMSs. Examples will be provided right after the definition.

Definition 9.13 (The λ -slack interleaving distance between DMSs). For each $\lambda \geq 0$, we define the λ -slack interleaving distance between any two DMSs $\gamma_X = (X, d_X(\cdot))$ and $\gamma_Y = (Y, d_Y(\cdot))$ as

$$d_{1,\lambda}^{\text{dynM}}(\gamma_X, \gamma_Y) := \min_R \text{dis}_\lambda^{\text{dyn}}(R)$$

where the minimum ranges over all tripods between X and Y . For simplicity, when $\lambda = 0$, we write d_1^{dynM} instead of $d_{1,0}^{\text{dynM}}$. If $d_{1,\lambda}^{\text{dynM}}(\gamma_X, \gamma_Y) \leq \varepsilon$ for some $\varepsilon \geq 0$, then we say that γ_X and γ_Y are ε -interleaved or simply interleaved.

By Definition 9.13, it is clear that for all $\lambda > 0$, $d_{1,\lambda}^{\text{dynM}} \leq d_1^{\text{dynM}}$. For $r > 0$, we call any DMS $\gamma_X = (X, d_X(\cdot))$ r -bounded if the distance between any pair of points in X does not exceed r across all $t \in \mathbf{R}$. If γ_X is r -bounded for some $r > 0$, then γ_X is said to be bounded.

Theorem 9.14. For each $\lambda \geq 0$, $d_{1,\lambda}^{\text{dynM}}$ is an extended metric between DMSs modulo isomorphism. In particular, for $\lambda > 0$, $d_{1,\lambda}^{\text{dynM}}$ is a metric between bounded DMSs modulo isomorphism.

The proof of Theorem 9.14 together with details pertaining to the following are deferred to Section 11.4.2:

- (i) For $\lambda > 0$, $d_{1,\lambda}^{\text{dynM}}$ generalizes the Gromov-Hausdorff distance (Remark 11.28).
- (ii) The metrics $d_{1,\lambda}^{\text{dynM}}$ for different $\lambda > 0$ are bilipschitz-equivalent (Proposition 11.29).
- (iii) In Proposition 11.31 we will elucidate a link between d_1^{dynM} and the Gromov-Hausdorff distance, which will be useful for determining the computational complexity of d_1^{dynM} (Theorem 9.25).

In the rest of this section, we investigate properties of d_1^{dynM} and provide some relevant examples. See Section 11.4.2 and [38] for details of the metrics $d_{1,\lambda}^{\text{dynM}}$ for $\lambda > 0$ and related stable signatures of DMSs.

Example 9.15 (An interleaved pair of DMSs I). This example refers to Figure 11. Fix the two-point metric space $(X, d_X) = (\{x, x'\}, \begin{pmatrix} 0 & 1 \\ 1 & 0 \end{pmatrix})$ and consider two DMSs $\gamma_X^{\psi_0} = (X, d_X^{\psi_0})$ and $\gamma_X^{\psi_1} = (X, d_X^{\psi_1})$ as in Example 9.2 (iv) where, for $t \in \mathbf{R}$, $\psi_0(t) = 1 + \cos(t)$, $\psi_1(t) = 1 + \cos(t + \pi/4)$. Then, $\gamma_X^{\psi_0}$ and $\gamma_X^{\psi_1}$ are ε -interleaved if and only if for $i, j \in \{0, 1\}$, $i \neq j$, and for all $t \in \mathbf{R}$, $S_\varepsilon(\psi_i)(t) := \min_{s \in [t, t+\varepsilon]} \psi_i(s) = \left(\bigvee_{[t, t+\varepsilon]} d_X^{\psi_i} \right)(x, x') \leq d_X^{\psi_j}(t)(x, x') = \psi_j(t)$. In fact, this inequality holds if and only if $\varepsilon \geq \pi/4$, and hence $d_1^{\text{dynM}}(\gamma_X^{\psi_0}, \gamma_X^{\psi_1}) = \pi/4$ (see Figure 11).

The following example generalizes the previous one. Details can be found in Section 11.4.2.

Example 9.16 (An interleaved pair of DMSs II). Fix the two-point metric space $(X, d_X) = (\{x, x'\}, \begin{pmatrix} 0 & 1 \\ 1 & 0 \end{pmatrix})$ and consider two DMSs $\gamma_X^{\psi_0} = (X, d_X^{\psi_0})$ and $\gamma_X^{\psi_1} = (X, d_X^{\psi_1})$ as in Example 9.2 (iv) where, for $t \in \mathbf{R}$, $\psi_0(t) = 1 + \cos(\omega t)$, $\psi_1(t) = 1 + \cos(\omega(t + \tau))$, for fixed $\omega > 0$ and $0 < \tau < \frac{2\pi}{\omega}$. Since in this case $\psi_1(t) = \psi_0(t + \tau)$ for all t , one would expect that the interleaving distance between $\gamma_X^{\psi_0}$ and $\gamma_X^{\psi_1}$ is able to uncover the precise value of τ . In this respect, we have: $d_1^{\text{dynM}}(\gamma_X^{\psi_0}, \gamma_X^{\psi_1}) = \min\left(\tau, \frac{2\pi}{\omega} - \tau\right) =: \eta(\omega, \tau)$.

Remark 9.17. There exist pairs of DMSs which are not ε -interleaved for any finite $\varepsilon \geq 0$. One simple example is given by γ_* , the trivial DMS, and any other constant non-trivial DMS γ_X . Note that in the context of persistent homology there also exist pairs of persistence modules which cannot be finitely interleaved [41]. In more generality we have Proposition 9.18 and Remark 9.19.

This is a necessary condition for two DMSs of different size to be interleaved (we omit its proof):

Proposition 9.18. Consider two DMSs $\gamma_X = (X, d_X(\cdot))$ and $\gamma_Y = (Y, d_Y(\cdot))$ with $|Y| < |X|$. Then γ_X and γ_Y can be interleaved only if the set $T(\gamma_X) := \{t \in \mathbf{R} : \exists x \neq x' \in X, d_X(t)(x, x') = 0\}$ is unbounded.

Remark 9.19 (Interleaving with constant DMSs). Let $\gamma_X = (X, d_X(\cdot))$, $\gamma_Y = (Y, d_Y(\cdot))$ be any two DMSs.

1. Suppose that both γ_X and γ_Y are constant DMSs and that they are ε -interleaved for some $0 \leq \varepsilon < +\infty$. Then they must be isomorphic. This implies that for constant DMSs, either $d_1^{\text{dynM}}(\gamma_X, \gamma_Y) = 0$ or $d_1^{\text{dynM}}(\gamma_X, \gamma_Y) = +\infty$.
2. Suppose that $\gamma_X(\cdot) \equiv (X, d_X)$ is constant where d_X is a metric, which is not just a pseudo-metric. Then, $d_1^{\text{dynM}}(\gamma_X, \gamma_Y) \leq \varepsilon$ for some $\varepsilon \geq 0$ if and only if there is a tripod $R : X \xleftarrow{\varphi_X} Z \xrightarrow{\varphi_Y} Y$ such that for all $t \in \mathbf{R}$, it holds that $\varphi_X^* d_X(t) = \varphi_Y^*(\bigvee_{[t]^\varepsilon} d_Y)$.

Stability results. The following proposition provides a gateway for extending the stability result (Theorem 1.1) to a similar result for DMSs.

Proposition 9.20 (\mathcal{R}_δ^1 is 1-Lipschitz). Let $\gamma_X = (X, d_X(\cdot))$ and $\gamma_Y = (Y, d_Y(\cdot))$ be any tame DMSs. Fix any $\delta \geq 0$. Consider saturated DGs $\mathcal{G}_X := \mathcal{R}_\delta^1(\gamma_X)$, $\mathcal{G}_Y := \mathcal{R}_\delta^1(\gamma_Y)$, as in Proposition 9.5. Then,

$$d_1^{\text{dynG}}(\mathcal{G}_X, \mathcal{G}_Y) \leq d_1^{\text{dynM}}(\gamma_X, \gamma_Y).$$

Proof. The proof can be completed by checking that for any $\varepsilon \geq 0$, any $(0, \varepsilon)$ -tripod R between γ_X and γ_Y (Definition 9.13) is also an ε -tripod between \mathcal{G}_X and \mathcal{G}_Y (Definition 6.9). \square

Proposition 9.20 together with Theorem 1.1 directly imply:

Theorem 9.21. Let $\gamma_X = (X, d_X(\cdot))$ and $\gamma_Y = (Y, d_Y(\cdot))$ be any two tame DMSs. Fix any $\delta \geq 0$. Consider the saturated formigrams $\theta_X := \pi_0(\mathcal{R}_\delta^1(\gamma_X))$ and $\theta_Y := \pi_0(\mathcal{R}_\delta^1(\gamma_Y))$.¹¹ Then,

$$d_B(\text{dgm}(\theta_X), \text{dgm}(\theta_Y)) \leq 2 d_1^{\text{dynM}}(\gamma_X, \gamma_Y).$$

Remark 9.22. Suppose $\gamma_X = (X, d_X(\cdot))$ and $\gamma_Y = (Y, d_Y(\cdot))$ are DMSs with $m = |X| \neq |Y| = n$ such that $d_X(\cdot)$ and $d_Y(\cdot)$ are proper metrics (not just pseudo-metrics) at all times. Then, for $\delta = 0$, the DGs $\mathcal{R}_\delta^1(\gamma_X)$ and $\mathcal{R}_\delta^1(\gamma_Y)$ are constant DGs over X and Y which have no edges other than self-loops. Therefore, for the formigrams θ_X and θ_Y defined as in Theorem 9.21, their respective diagrams $\text{dgm}(\theta_X)$ and $\text{dgm}(\theta_Y)$ consist solely of the infinite interval $(-\infty, \infty)$ with (different) multiplicities m and n (Remark 5.11); therefore the bottleneck distance between them is $+\infty$. This would seem to suggest that Theorem 9.21 could be falsified. However, Proposition 9.18 implies that $d_1^{\text{dynM}}(\gamma_X, \gamma_Y) = +\infty$ in this case as well so Theorem 9.21 does not contradict this example.

¹¹These are formigrams by Propositions 9.5 and 5.16.

Remark 9.23. Recall Example 9.16. For $\delta \in [0, 2)$, the lower bound for $d_1^{\text{dynM}}(\gamma_X^{\psi_0}, \gamma_X^{\psi_1})$ given by Theorem 9.21 equals $\frac{1}{2} \min(\eta(\omega, \tau), \frac{1}{\omega} \arccos(\delta - 1))$ (see Section 11.4.2 for details). Thus, for δ small enough, the actual interleaving distance between the two spaces and the lower bound given by Theorem 9.21 will be the same up to a factor of 2.

We will discuss the generalization of Theorem 9.21 to higher dimensional homology barcodes in Section 10.

The following corollary is a generalization of Theorem 9.21: The barcodes of ε -smoothed out formigram obtained from tame DMSs are stable with respect to the bottleneck d_B and the interleaving d_1^{dynM} . This is directly obtained by combining Theorem 9.21 with Remark 7.8.

Corollary 9.24. Let $\varepsilon \geq 0$. With the same assumptions of Theorem 9.21,

$$d_B(\text{dgm}(S_\varepsilon \theta_X), \text{dgm}(S_\varepsilon \theta_Y)) \leq 2 d_1^{\text{dynM}}(\gamma_X, \gamma_Y).$$

Computational complexity. A DMS $\gamma_X = (X, d_X(\cdot))$ is said to be *piecewise linear* if for all $x, x' \in X$, the function $d_X(\cdot)(x, x') : \mathbf{R} \rightarrow \mathbf{R}_+$ is piecewise linear. We denote by S_X the set of all breakpoints of all distance functions $d_X(\cdot)(x, x'), x, x' \in X$.

Theorem 9.25 (Complexity of d_1^{dynM}). Fix $\rho \in (1, 6)$ and let γ_X and γ_Y be piecewise linear DMSs. Then, it is not possible to compute a ρ -approximation to $d_1^{\text{dynM}}(\gamma_X, \gamma_Y)$ in time polynomial in $|X|, |Y|, |S_X|$, and $|S_Y|$, unless $P = NP$.

Theorem 9.25 will be proved in Section 11.4.2. The theorem above further indicates that computing the lower bound for d_1^{dynM} given by Theorem 9.21 is a realistic approach to comparing DMSs.

10 Discussion

In this section we discuss extendibility of Theorem 9.21 (Section 10) and introduce to the reader computational experiments that we carried out (Section 10).

Higher dimensional persistent homology barcodes of DMSs. Proposition 9.20 provides a method for turning any tame DMS into a DG. In turn, this DG can be further summarized as a clustering barcode by invoking Proposition 5.16 and Definition 5.10. This resulting barcode encodes the clustering behavior of the given DMS for a fixed scale $\delta \geq 0$.

However, we do not need to restrict ourselves to clustering features of DMSs. Imagine that a flock of birds flies while keeping a circular arrangement from time $t = 0$ to $t = 1$. Regarding this flock as a DMS (trajectory data in \mathbf{R}^3), we may want to have an interval containing $[0, 1]$ in its *1-dimensional homology barcode*. This idea can actually be implemented as follows (see Section 11.5 for details).

For a fixed $\delta \geq 0$, we substitute the Rips functor \mathcal{R}_δ (item 15 in Section 3.1) for the Rips graph functor \mathcal{R}_δ^1 in Proposition 9.20. What we obtain is a *dynamic simplicial complex or zigzag simplicial filtration*, a generalization of Definition 4.1, induced from any tame DMS γ_X (see the first two rows of Figure 10). We then can apply the k -th homology functor to this zigzag simplicial filtration for each $k \geq 0$ in order to obtain a zigzag module. This zigzag module will be a signature summarizing the time evolution of k -dimensional homological features of γ_X . By virtue of the standard decomposability results [7, 12], we eventually obtain the *k-th homology barcode* $\text{dgm}(H_k(\mathcal{R}_\delta(\gamma_X)))$ of γ_X with respect to the fixed scale $\delta \geq 0$. In particular, the 0-th homology barcode of the resulting zigzag module coincides with $\text{dgm}(\pi_0(\mathcal{R}_\delta^1(\gamma_X)))$ as defined in Theorem 9.21.

A natural question is then to ask whether our stability theorem (Theorem 9.21) can be extended to higher dimensional homology barcodes:

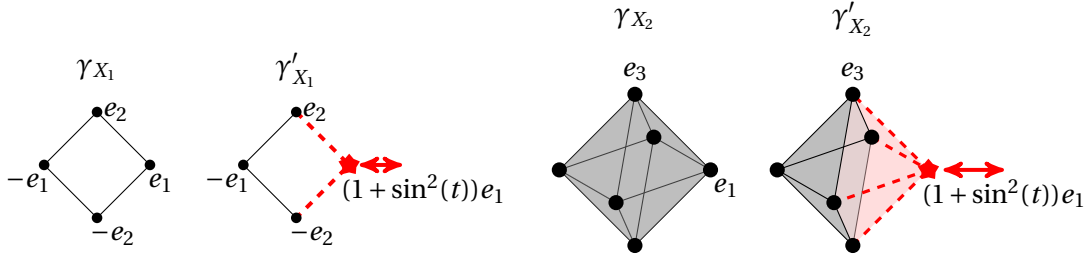


Figure 12: Pairs of DMSs $(\gamma_{X_i}, \gamma'_{X_i})$ for $i = 1, 2$ such that $d_1^{\text{dynM}}(\gamma_{X_i}, \gamma'_{X_i}) \leq \pi/2$. In contrast, for $k = 1$ (or $k = 2$), the bottleneck distance between their k -dimensional zigzag-persistence barcodes is infinite for $\delta \in [\sqrt{2}, 2)$. DMS γ_{X_1} , described as the left-most figure, $(\gamma_{X_2}$, the third figure from the left) consists of four (eight) static points located at $\pm e_1 = (\pm 1, 0, 0)$ and $\pm e_2 = (0, \pm 1, 0)$ (and $\pm e_3 = (0, 0, \pm 1)$), respectively. On the other hand, DMS γ'_{X_1} , illustrated at the second from the left (γ'_{X_2} , at the right-most), contains a single oscillating point, denoted by a star shape, with trace $(1 + \sin^2(t))e_1$ for $t \in \mathbf{R}$ along with three (five) static points located at $-e_1, +e_2$ and $-e_2$, (and $\pm e_3$), respectively. Then, the 1-dimensional (2-dimensional) zigzag-persistent homology barcode for γ_{X_1} (for γ_{X_2}) consists of exactly one interval $(-\infty, \infty)$, indicating the presence of a loop (a void) for all time. However, the barcode of γ'_{X_1} (γ'_{X_2}) consists of an infinite number of ephemeral intervals $[n\pi, n\pi]$, $n \in \mathbf{Z}$, indicating the on-and-off presence of a loop (a void) that exists only at $t = n\pi$ for $n \in \mathbf{Z}$ in its configuration.

Question 10.1. For any pair of tame DMSs $\gamma_X = (X, d_X(\cdot))$ and $\gamma_Y = (Y, d_Y(\cdot))$, is it true that for any $\delta \geq 0$ and for any $k \geq 1$,

$$d_B(\text{dgm}(H_k(\mathcal{R}_\delta(\gamma_X))), \text{dgm}(H_k(\mathcal{R}_\delta(\gamma_Y)))) \leq 2 d_1^{\text{dynM}}(\gamma_X, \gamma_Y) ?$$

Interestingly, we found a family of counter-examples that indicates that stability, as expressed by Theorem 9.21, is a phenomenon which seems to be essentially tied to clustering (i.e. H_0) information.

Theorem 10.2. For each integer $k \geq 1$ there exist two different tame DMSs γ_{X_k} and γ_{Y_k} , and $\delta_k \geq 0$ such that $d_1^{\text{dynM}}(\gamma_{X_k}, \gamma_{Y_k}) < \infty$ but such that the bottleneck distance between the barcodes of $H_k(\mathcal{R}_{\delta_k}(\gamma_{X_k}))$ and $H_k(\mathcal{R}_{\delta_k}(\gamma_{Y_k}))$ is unbounded.

Proof. Fix any $k \geq 1$. We will illustrate DMSs γ_{X_k} and γ_{Y_k} as collections of trajectories of points in \mathbf{R}^{k+1} , with the metric inherited from the Euclidean metric of \mathbf{R}^{k+1} across all $t \in \mathbf{R}$. For $k = 1$ or $k = 2$, see Figure 12.

Define γ_{X_k} to be the constant DMS consisting of $2(k+1)$ points $\pm e_i = (0, \dots, 0, \pm 1, 0, \dots, 0) \in \mathbf{R}^{k+1}$ for $i = 1, 2, \dots, k+1$. On the other hand, define γ_{Y_k} to be obtained from γ_{X_k} by substituting the still point $+e_1$ of γ_{X_k} by the oscillating point $(1 + \sin^2(t))e_1 = (1 + \sin^2(t), 0, \dots, 0)$ for $t \in \mathbf{R}$.

It is not difficult to check that $d_1^{\text{dynM}}(\gamma_{X_k}, \gamma_{Y_k}) \leq \pi/2$. However, with the connectivity parameter $\delta = \sqrt{2}$, their barcodes of the k -th zigzag persistent homology are $\text{dgm}(H_k(\mathcal{R}_\delta(X_k))) = \{(-\infty, \infty)\}$ and $\text{dgm}(H_k(\mathcal{R}_\delta(Y_k))) = \{[n\pi, n\pi] : n \in \mathbf{Z}\}$, respectively (we omit the details on this computation). Therefore, $d_B(\text{dgm}(H_k(\mathcal{R}_\delta(X_k))), \text{dgm}(H_k(\mathcal{R}_\delta(Y_k)))) = +\infty$. \square

Computational experiments. See [39] for computational experiments related to the techniques developed in this paper. In that experiments we classify different flocking behaviors by analyzing their 0-th homology barcodes.

11 Details and Proofs

In this section we discuss details on Sections 6-10.

11.1 Details from Section 6

11.1.1 Details from Section 6.1

For any non-empty set $A \subset \mathbf{R}$ and $t \in \mathbf{R}$, let $A - t := \{a - t : a \in A\}$.

Proof of Proposition 6.7. We first claim that $S_\varepsilon \mathcal{G}_X$ satisfies Definition 4.1 (ii).¹² The set $\text{crit}(\mathcal{G}_X)$ is locally finite by Definition 4.1 (ii). The tameness of $S_\varepsilon \mathcal{G}_X$ follows from the observation that $\text{crit}(S_\varepsilon \mathcal{G}_X)$ is a subset of $(\text{crit}(\mathcal{G}_X) - \varepsilon) \cup (\text{crit}(\mathcal{G}_X) + \varepsilon)$, which is locally finite.

Next, we check Definition 4.1 (iii). For each $x \in X$, let I_x be the lifespan of x in \mathcal{G}_X . By the definition of $S_\varepsilon \mathcal{G}_X$, the lifespan of x in $S_\varepsilon \mathcal{G}_X$ becomes the ε -thickening $(I_x)^\varepsilon$ of I_x . Lastly, we check Definition 4.1 (iv). Pick any $t \in \mathbf{R}$. We wish to prove that for all sufficiently small $\varepsilon \geq 0$, it holds that $S_\varepsilon \mathcal{G}_X(t - \varepsilon) \subset S_\varepsilon \mathcal{G}_X(t) \supset S_\varepsilon \mathcal{G}_X(t + \varepsilon)$.

Since the set $\text{crit}(\mathcal{G}_X)$ is locally finite by definition, one can choose $r > 0$ such that $\text{crit}(\mathcal{G}_X) \cap [t - \varepsilon, t + \varepsilon]^r = \text{crit}(\mathcal{G}_X) \cap [t - \varepsilon, t + \varepsilon]$. Pick any $0 \leq \eta < r$. We will verify that $S_\varepsilon \mathcal{G}_X(t - \eta) \subset S_\varepsilon \mathcal{G}_X(t)$. Note that the set $\text{crit}(\mathcal{G}_X) \cap ([t - \varepsilon, t + \varepsilon] - \eta)$ is contained in the set $\text{crit}(\mathcal{G}_X) \cap [t - \varepsilon, t + \varepsilon]$. Assuming that $\text{crit}(\mathcal{G}_X) \cap ([t - \varepsilon, t + \varepsilon] - \eta)$ is not empty, we have

$$S_\varepsilon \mathcal{G}_X(t - \eta) = \bigcup_{[t - \varepsilon, t + \varepsilon] - \eta} \mathcal{G}_X \stackrel{(*)}{=} \bigcup_{c \in \text{crit}(\mathcal{G}_X) \cap ([t - \varepsilon, t + \varepsilon] - \eta)} \mathcal{G}_X(c) \subset \bigcup_{c \in \text{crit}(\mathcal{G}_X) \cap [t - \varepsilon, t + \varepsilon]} \mathcal{G}_X(c) \stackrel{(*)}{=} \bigcup_{[t - \varepsilon, t + \varepsilon]} \mathcal{G}_X = S_\varepsilon \mathcal{G}_X(t),$$

where the equalities marked with $(*)$ hold since \mathcal{G}_X is locally maximal at critical points. Even if $\text{crit}(\mathcal{G}_X) \cap ([t - \varepsilon, t + \varepsilon] - \eta)$ is empty, one can check that $S_\varepsilon \mathcal{G}_X(t - \eta) \subset \mathcal{G}_X(t)$. In the same way, the containment $S_\varepsilon \mathcal{G}_X(t) \supset S_\varepsilon \mathcal{G}_X(t + \eta)$ can be established. \square

Proof of Theorem 6.10. Reflexivity and symmetry of d_1^{dynG} are clear and thus we only show the triangle inequality: Let X, Y and W be some finite sets and let $\mathcal{G}_X = (V_X(\cdot), E_X(\cdot))$, $\mathcal{G}_Y = (V_Y(\cdot), E_Y(\cdot))$ and $\mathcal{G}_W = (V_W(\cdot), E_W(\cdot))$ be any DGs. We wish to prove $d_1^{\text{dynG}}(\mathcal{G}_X, \mathcal{G}_W) \leq d_1^{\text{dynG}}(\mathcal{G}_X, \mathcal{G}_Y) + d_1^{\text{dynG}}(\mathcal{G}_Y, \mathcal{G}_W)$. We assume that $d_1^{\text{dynG}}(\mathcal{G}_X, \mathcal{G}_Y)$ and $d_1^{\text{dynG}}(\mathcal{G}_Y, \mathcal{G}_W)$ are finite because otherwise there is nothing to prove. Let $0 < \varepsilon_1, \varepsilon_2 < \infty$, and suppose that there are an ε_1 -tripod $R_1 : X \xleftarrow{\varphi_X} Z_1 \xrightarrow{\varphi_Y} Y$ between \mathcal{G}_X and \mathcal{G}_Y and an ε_2 -tripod $R_2 : Y \xleftarrow{\psi_Y} Z_2 \xrightarrow{\psi_W} W$ between \mathcal{G}_Y and \mathcal{G}_W . Consider the set $Z := \{(z_1, z_2) \in Z_1 \times Z_2 : \varphi_Y(z_1) = \psi_Y(z_2)\}$ and let $\pi_1 : Z \rightarrow Z_1$ and $\pi_2 : Z \rightarrow Z_2$ be the canonical projections to the first and the second coordinate, respectively. Recall the tripod $R_2 \circ R_1$ between X and W from equation (9).

It suffices to prove that $R_2 \circ R_1$ is an $(\varepsilon_1 + \varepsilon_2)$ -tripod between \mathcal{G}_X and \mathcal{G}_W . We will only show that $\mathcal{G}_X \xrightarrow{R_2 \circ R_1} S_{\varepsilon_1 + \varepsilon_2} \mathcal{G}_W$. By the choice of R_1 and R_2 , we have $\mathcal{G}_X \xrightarrow{R_1} S_{\varepsilon_1} \mathcal{G}_Y$ and $\mathcal{G}_Y \xrightarrow{R_2} S_{\varepsilon_2} \mathcal{G}_W$. Then by Proposition 6.8, we have $S_{\varepsilon_1} \mathcal{G}_Y \xrightarrow{R_2} S_{\varepsilon_1} (S_{\varepsilon_2} \mathcal{G}_W) = S_{\varepsilon_1 + \varepsilon_2} \mathcal{G}_W$ and in turn by Remark 6.5, we have $\mathcal{G}_X \xrightarrow{R_2 \circ R_1} S_{\varepsilon_1 + \varepsilon_2} \mathcal{G}_W$, as desired. \square

From [11, Section 7.3], we recall the *Gromov-Hausdorff distance* between metric spaces. Let (X, d_X) and (Y, d_Y) be any two metric spaces and let $R : X \xleftarrow{\varphi_X} Z \xrightarrow{\varphi_Y} Y$ be a tripod between X and Y . Then, the *distortion* of R is defined as

$$\text{dis}(R) := \sup_{z, z' \in Z} |d_X(\varphi_X(z), \varphi_X(z')) - d_Y(\varphi_Y(z), \varphi_Y(z'))|.$$

Definition 11.1 (The Gromov-Hausdorff distance [11, Section 7.3.3]). Let (X, d_X) and (Y, d_Y) be any two metric spaces. Then,

$$d_{\text{GH}}((X, d_X), (Y, d_Y)) = \frac{1}{2} \inf_R \text{dis}(R)$$

where the infimum is taken over all tripods R between X and Y . In particular, any tripod R between X and Y is said to be an ε -tripod between (X, d_X) and (Y, d_Y) if $\text{dis}(R) \leq \varepsilon$.

¹²This claim is an analogue to [22, Proposition 4.16] and the proof is essentially the same.

Proposition 11.2. Let (X, d_X) and (Y, d_Y) be any two finite metric spaces. Then, there exist two dynamic graphs $\mathcal{G}_X = (V_X(\cdot), E_X(\cdot))$ and $\mathcal{G}_Y = (V_Y(\cdot), E_Y(\cdot))$ corresponding to (X, d_X) and (Y, d_Y) respectively such that

$$d_1^{\text{dynG}}(\mathcal{G}_X, \mathcal{G}_Y) = 2 \cdot d_{\text{GH}}((X, d_X), (Y, d_Y)).$$

Proof. We define \mathcal{G}_X by specifying the two maps $V_X(\cdot) : \mathbf{R} \rightarrow \text{pow}(X)$ and $E_X(\cdot) : \mathbf{R} \rightarrow \text{pow}(\text{pow}_2(X))$ as follows (Definition 4.1):

$$V_X(t) := \begin{cases} \emptyset, & t \in (-\infty, 0) \\ X, & t \in [0, \infty), \end{cases} \quad E_X(t) := \begin{cases} \emptyset, & t \in (-\infty, 0) \\ \{\{x, x'\} : d_X(x, x') \leq t\}, & t \in [0, \infty). \end{cases}$$

Define \mathcal{G}_Y similarly. We verify that $d_1^{\text{dynG}}(\mathcal{G}_X, \mathcal{G}_Y) \geq 2 \cdot d_{\text{GH}}((X, d_X), (Y, d_Y))$. To this end, suppose that for some $\varepsilon \geq 0$, $R : X \xleftarrow{\varphi_X} Z \xrightarrow{\varphi_Y} Y$ is any ε -tripod between \mathcal{G}_X and \mathcal{G}_Y (Definition 6.9). Then, by the construction of $\mathcal{G}_X, \mathcal{G}_Y$, it must hold that $|d_X(\varphi_X(z), \varphi_X(z')) - d_Y(\varphi_Y(z), \varphi_Y(z'))| \leq \varepsilon$ for all $z, z' \in Z$. The other inequality $d_1^{\text{dynG}}(\mathcal{G}_X, \mathcal{G}_Y) \leq 2 \cdot d_{\text{GH}}((X, d_X), (Y, d_Y))$ can be similarly proved. \square

Proof of Theorem 6.11. Pick any two non-trivial ultrametric spaces (X, u_X) and (Y, u_Y) . Then, by Proposition 11.2, there exist DGs $\mathcal{G}_X = (V_X(\cdot), E_X(\cdot))$ and $\mathcal{G}_Y = (V_Y(\cdot), E_Y(\cdot))$ such that the interleaving distance between \mathcal{G}_X and \mathcal{G}_Y is identical to twice the Gromov-Hausdorff distance $\Delta := d_{\text{GH}}((X, u_X), (Y, u_Y))$ between (X, u_X) and (Y, u_Y) . However, according to [51, Corollary 3.8], Δ cannot be approximated within any factor less than 3 in polynomial time, unless $P = NP$. The author shows this by observing that any instance of the 3-partition problem can be reduced to an instance of the bottleneck ∞ -Gromov-Hausdorff distance (∞ -BGHD) problem between ultrametric spaces (see [51, p.865]). The proof follows. \square

11.1.2 Details from Section 6.2

Given a dendrogram $\theta_X : \mathbf{R}_+ \rightarrow \mathcal{P}(X)$ (Definition 5.2) on a set X , we will consider it as a formigram $\theta_X : \mathbf{R} \rightarrow \mathcal{P}^{\text{sub}}(X)$ by extending the domain of θ_X trivially: for all $t \in (-\infty, 0)$, let $\theta_X(t) := \emptyset$.

Remark 11.3 (Interleaving between dendrograms). When θ_X, θ_Y are dendrograms over sets X and Y respectively, let $R : X \xleftarrow{\varphi_X} Z \xrightarrow{\varphi_Y} Y$ be an ε -tripod between θ_X and θ_Y . Since both θ_X and θ_Y get coarser as $t \in \mathbf{R}$ increases, the interleaving condition in Definition 6.26 can be re-written as follows: Letting $\varphi := \varphi_Y \circ \varphi_X^{-1} : X \rightrightarrows Y$, for all $t \in \mathbf{R}$ it holds that $\theta_X(t) \leq_\varphi \theta_Y(t + \varepsilon)$ and $\theta_Y(t) \leq_{\varphi^{-1}} \theta_X(t + \varepsilon)$ (Definition 6.21). In particular, this ε -tripod between dendrograms induces ε -compatible maps between their underlying merge trees [46].

Let X be a finite set and let $\theta_X : \mathbf{R}_+ \rightarrow \mathcal{P}(X)$ be a dendrogram over X (Definition 5.2). Recall from [14] that this θ_X induces a canonical ultrametric $u_X : X \times X \rightarrow \mathbf{R}_+$ on X defined by

$$u_X(x, x') := \inf\{\varepsilon \geq 0 : x, x' \text{ belong to the same block of } \theta_X(\varepsilon)\}.$$

Proposition 11.4 (d_1^{F} and the Gromov-Hausdorff distance). Given any two dendrograms θ_X, θ_Y over sets X, Y , respectively, let u_X, u_Y be the canonical ultrametrics on X and Y , respectively. Then, $d_1^{\text{F}}(\theta_X, \theta_Y) = 2 \cdot d_{\text{GH}}((X, u_X), (Y, u_Y))$.

Proof. First we show “ \geq ”. Let $\varepsilon \geq 0$ and let $R : X \xleftarrow{\varphi_X} Z \xrightarrow{\varphi_Y} Y$ be any ε -tripod between the two dendrograms θ_X and θ_Y . Pick any $z, z' \in Z$ and let $x = \varphi_X(z)$, $x' = \varphi_X(z')$, $y = \varphi_Y(z)$, and $y' = \varphi_Y(z')$. Let $t := u_X(x, x')$. This implies that x, x' belong to the same block of the partition $\theta_X(t)$. For the multivalued map $\varphi := \varphi_Y \circ \varphi_X^{-1}$, since $\theta_X(t) \leq_\varphi \theta_Y(t + \varepsilon)$ (Remark 11.3), y, y' must belong to the same block of $\theta_Y(t + \varepsilon)$, and in turn this implies that $u_Y(y, y') \leq t + \varepsilon = u_X(x, x') + \varepsilon$. By symmetry, we also have $u_Y(y, y') \leq u_X(x, x') + \varepsilon$ and in turn $|u_X(x, x') - u_Y(y, y')| \leq \varepsilon$. By Definition 11.1, this implies that $d_{\text{GH}}((X, u_X), (Y, u_Y)) \leq \varepsilon/2$.

Next, we prove “ \leq ”. Let $R : X \xleftarrow{\varphi_X} Z \xrightarrow{\varphi_Y} Y$ be a tripod between X and Y such that $\text{dis}(R) = \varepsilon$. Let

$\varphi := \varphi_Y \circ \varphi_X^{-1}$. By Remark 11.3, it suffices to show that for all $t \in \mathbf{R}$, $\theta_X(t) \leq_\varphi \theta_Y(t + \varepsilon)$ and $\theta_Y(t) \leq_{\varphi^{-1}} \theta_X(t + \varepsilon)$. By symmetry, we only prove that $\theta_X(t) \leq_\varphi \theta_Y(t + \varepsilon)$ for all $t \in \mathbf{R}$. For $t < 0$, since $\theta_X(t) = \emptyset$, $\theta_X(t) \leq_\varphi \theta_Y(t + \varepsilon)$ trivially holds. Now pick any $t \geq 0$ and pick any $z, z' \in Z$ and let $x = \varphi_X(z)$, $x' = \varphi_X(z')$, $y = \varphi_Y(z)$, and $y' = \varphi_Y(z')$. Assume that x, x' belong to the same block of $\theta_X(t)$, implying that $u_X(x, x') \leq t$. Since $|u_X(x, x') - u_Y(y, y')| \leq \varepsilon$, we know $u_Y(y, y') \leq t + \varepsilon$, and hence y, y' belong to the same block of $\theta_Y(t + \varepsilon)$. Therefore, $\theta_X(t) \leq_\varphi \theta_Y(t + \varepsilon)$ for all $t \in \mathbf{R}$. \square

Computational complexity of d_1^F .

Theorem 11.5 (Complexity of computing d_1^F). Fix $\rho \in (1, 6)$. It is not possible to obtain a ρ approximation to the distance $d_1^F((X, \theta_X), (Y, \theta_Y))$ between formigrams in time polynomial on $|X|, |Y|, |\text{crit}(\theta_X)|, |\text{crit}(\theta_Y)|$ unless $P = NP$.

Proof. Pick any two dendrograms and invoke Proposition 11.4 to reduce the problem to the computation of the Gromov-Hausdorff distance between the ultrametric spaces associated to the dendrograms. The rest of the proof follows along the same lines as that of Theorem 6.11. \square

Proof of Proposition 6.31. Suppose that $d_1^F(\theta_X, \theta_Y) < \infty$. By the definition of d_1^F , there is an ε -tripod

$R : X \xleftarrow{\varphi_X} Z \xrightarrow{\varphi_Y} Y$ between θ_X and θ_Y for some $\varepsilon \geq 0$. Since θ_X and θ_Y are constant, $S_\varepsilon \theta_X = \theta_X$ and $S_\varepsilon \theta_Y = \theta_Y$, and thus $\theta_X \xrightarrow{R} \theta_Y$ and $\theta_Y \xrightarrow{R} \theta_X$, implying that R is a 0-tripod. This implies that for the multivalued maps $\varphi := \varphi_Y \circ \varphi_X^{-1} : X \rightrightarrows Y$ and $\varphi^{-1} := \varphi_X \circ \varphi_Y^{-1} : Y \rightrightarrows X$, we have $P_X \leq_\varphi P_Y$ and $P_Y \leq_{\varphi^{-1}} P_X$. Then, for any $(x, y), (x', y') \in \varphi$, x, x' belong to the same block of P_X if and only if y, y' belong to the same block of P_Y , which implies that $|P_X| = |P_Y|$.

Conversely, assuming that $|P_X| = |P_Y|$, take any bijection $f : P_X \rightarrow P_Y$. Let $Z := \bigsqcup_{\substack{B \in P_X \\ f(B) = C}} (B \times C) \subset X \times Y$ and

let $\pi_X : Z \rightarrow X$ and $\pi_Y : Z \rightarrow Y$ be the canonical projections to the first and the second coordinate, respectively. Then the tripod $R : X \xleftarrow{\pi_X} Z \xrightarrow{\pi_Y} Y$ is a 0-tripod between θ_X and θ_Y . \square

Proof of Theorem 6.32. Let $\varepsilon \geq 0$ and let $R : X \xleftarrow{\varphi_X} Z \xrightarrow{\varphi_Y} Y$ be an ε -tripod between \mathcal{G}_X and \mathcal{G}_Y . We prove that R is also an ε -tripod between the formigrams θ_X and θ_Y . By symmetry, we only prove that $\theta_X \xrightarrow{R} S_\varepsilon \theta_Y$. Let $z \in Z$ and let $\varphi_X(z) = x$, and $\varphi_Y(z) = y$. Fix $t \in \mathbf{R}$. Suppose that x is in the underlying set $V_X(t)$ of $\theta_X(t)$. Since $\mathcal{G}_X \xrightarrow{R} S_\varepsilon \mathcal{G}_Y$, we have $y \in \cup_{s \in [t]^\varepsilon} V_Y(s)$, which is the underlying set of $\bigvee_{[t]^\varepsilon} \theta_Y$. Pick another $z' \in Z$ and let $\varphi_X(z') = x'$ and $\varphi_Y(z') = y'$. Assume that x, x' belong to the same block of $\theta_X(t)$, meaning that there is a sequence $x = x_0, x_1, \dots, x_n = x'$ in X such that $\{x_i, x_{i+1}\} \in E_X(t)$ for $0 \leq i \leq n-1$. Consider the multivalued map $\varphi := \varphi_Y \circ \varphi_X^{-1} : X \rightrightarrows Y$. For each $1 \leq i \leq n-1$, pick $y_i \in \varphi(x_i) \subset Y$ and let $y_0 = y \in \varphi(x)$, and $y_n = y' \in \varphi(x')$. Since R is an ε -tripod between \mathcal{G}_X and \mathcal{G}_Y , we have $\{y_i, y_{i+1}\} \in \cup_{s \in [t]^\varepsilon} E_Y(s)$ (Remark 6.12). Then, y, y' belong to the same connected component of the graph $\bigcup_{[t]^\varepsilon} \mathcal{G}_Y$ and in turn, by Proposition 7.3, the same block of $\bigvee_{[t]^\varepsilon} \theta_Y$. \square

11.2 Details from Section 2

In this section we rigorously prove Theorem 1.1, complementing Section 2. The central idea in the proof of Theorem 1.1 is to extend the domain of definition of formigrams to the upper-half of the Euclidean plane and interpret it as a signature of their Reeb graphs. This idea was inspired by the work [8] of M. Botnan and M. Lesnick.

In Section 11.2.1, we review the definitions of the interleaving distance, and the bottleneck distance. In Section 11.2.2, we introduce a simple way to turn formigrams into 2-dimensional **Sets**-valued diagrams and exploit it to prove some stability results. In Section 11.2.4, we show that those **Sets**-valued diagrams can be interpreted as signatures of the Reeb graphs of formigrams. Along the way, in Section 11.2.3, we clarify that the notion of finest common coarsening of partitions coincides with the colimit in the category of **Sets**, which will be useful in Section 11.2.4.

11.2.1 Interleavings and the bottleneck distance

Recall that for a poset \mathbf{P} , any functor $F : \mathbf{P} \rightarrow \mathbf{Vec}$ is said to be a \mathbf{P} -indexed module (Section 3.2). The interleaving distance is used in the topological data analysis (TDA) community for measuring distance between multidimensional persistence modules [41], i.e. \mathbf{R}^n -indexed module. However, in this paper, we are mainly interested in diagrams indexed by \mathbf{U} (Item 11 in Section 3.1). Hence we restrict ourselves to the settings of interest to us in the following definition. For $\varepsilon \geq 0$, let $\vec{\varepsilon} := (-\varepsilon, \varepsilon)$.

Definition 11.6 (Interleaving distance, [8]). Let $\varepsilon \geq 0$ and \mathbf{C} be an arbitrary category. Two functors $F, G : \mathbf{U} \rightarrow \mathbf{C}$ are said to be ε -interleaved if there exist collections of morphisms $f = (f_{\mathbf{u}} : F_{\mathbf{u}} \rightarrow G_{\mathbf{u}+\vec{\varepsilon}})_{\mathbf{u} \in \mathbf{U}}$ and $g = (g_{\mathbf{w}} : G_{\mathbf{w}} \rightarrow F_{\mathbf{w}+\vec{\varepsilon}})_{\mathbf{w} \in \mathbf{U}}$ satisfying the following:

1. For all $\mathbf{u}, \mathbf{w} \in \mathbf{U}$, $g_{\mathbf{u}+\vec{\varepsilon}} \circ f_{\mathbf{u}} = \varphi_F(\mathbf{u}, \mathbf{u} + 2\vec{\varepsilon})$ and $f_{\mathbf{w}+\vec{\varepsilon}} \circ g_{\mathbf{w}} = \varphi_G(\mathbf{w}, \mathbf{w} + 2\vec{\varepsilon})$.
2. For all $\mathbf{u} \leq \mathbf{w} \in \mathbf{U}$,
 $\varphi_G(\mathbf{u} + \vec{\varepsilon}, \mathbf{w} + \vec{\varepsilon}) \circ f_{\mathbf{u}} = f_{\mathbf{w}} \circ \varphi_F(\mathbf{u}, \mathbf{w})$ and $\varphi_F(\mathbf{u} + \vec{\varepsilon}, \mathbf{w} + \vec{\varepsilon}) \circ g_{\mathbf{u}} = g_{\mathbf{w}} \circ \varphi_G(\mathbf{u}, \mathbf{w})$.

In this case, we call (f, g) an ε -interleaving pair. For $F, G \in \text{Ob}(\mathbf{C}^{\mathbf{U}})$, the interleaving distance is defined as follows:

$$d_1(F, G) := \inf\{\varepsilon \geq 0 : F \text{ and } G \text{ are } \varepsilon\text{-interleaved}\}.$$

If F and G are not ε -interleaved for any $\varepsilon \geq 0$, then $d_1(F, G) = +\infty$ by definition. We will use this definition of interleaving distance when \mathbf{C} is either **Sets** or **Vec**.

Recall that injective partial functions are said to be *matchings* and the category **Mch** consists of finite sets as objects and matchings as morphisms [26]. We use $\sigma : A \rightarrowtail B$ to denote a matching $\sigma \subset A \times B$ and the canonical projections of σ onto A and B are denoted by $\text{coim}(\sigma)$ and $\text{im}(\sigma)$, respectively.

Many equivalent representations of the *bottleneck distance* have been given in TDA community. We adopt the following form from [3]: First we introduce some notation. By $\langle b, d \rangle$ for $b \in \{-\infty\} \cup \mathbf{R}$ and $d \in \mathbf{R} \cup \{\infty\}$, we denote any of the intervals (b, d) , $[b, d)$, $(b, d]$ or $[b, d]$ in \mathbf{R} . Letting \mathcal{A} be a multiset of intervals in \mathbf{R} and $\varepsilon \geq 0$,

$$\mathcal{A}^\varepsilon := \{\langle b, d \rangle \in \mathcal{A} : b + \varepsilon < d\} = \{I \in \mathcal{A} : [t, t + \varepsilon] \subset I \text{ for some } t \in \mathbf{R}\}.$$

Note that $\mathcal{A}^0 = \mathcal{A}$.

Definition 11.7 (δ -matchings and bottleneck distance [3]). Let \mathcal{A} and \mathcal{B} be multisets of intervals in \mathbf{R} . We define a δ -matching between \mathcal{A} and \mathcal{B} to be a matching $\sigma : \mathcal{A} \rightarrowtail \mathcal{B}$ such that $\mathcal{A}^{2\delta} \subset \text{coim}(\sigma)$, $\mathcal{B}^{2\delta} \subset \text{im}(\sigma)$, and if $\sigma\langle b, d \rangle = \langle b', d' \rangle$, then

$$\langle b, d \rangle \subset \langle b' - \delta, d' + \delta \rangle, \quad \langle b', d' \rangle \subset \langle b - \delta, d + \delta \rangle.$$

with the convention $+\infty + \delta = +\infty$ and $-\infty - \delta = -\infty$. We define the bottleneck distance d_B by

$$d_B(\mathcal{A}, \mathcal{B}) := \inf\{\delta \in [0, \infty) : \exists \delta\text{-matching between } \mathcal{A} \text{ and } \mathcal{B}\}.$$

We declare $d_B(\mathcal{A}, \mathcal{B}) = +\infty$ when there is no δ -matching between \mathcal{A} and \mathcal{B} for any $\delta \in [0, \infty)$.

11.2.2 \mathbf{U} -indexed diagrams induced by formigrams

In this section we study the relationship between the distance on formigrams and the distance on their Reeb graphs. Recall that \mathbf{U} is the sub-poset of $\mathbf{R}^{\text{op}} \times \mathbf{R}$ consisting of pairs (a, b) with $a \leq b$ (Item 11 in Section 3.1) and the notion of finest common coarsening and time-interlevel smoothing of formigrams (Definitions 6.17 and 6.23).

Definition 11.8 (\mathbf{U} -indexed **Sets**-valued diagrams induced by formigrams). Given a formigram θ_X over X , define a functor $E_{\mathbf{Sets}}(\theta_X) : \mathbf{U} \rightarrow \mathbf{Sets}$ as follows:

- Each point $\mathbf{u} = (u, u') \in \mathbf{U}$ is sent to the sub-partition $\bigvee_{[u, u']} \theta_X$ of X .
- Each arrow $\mathbf{u} = (u, u') \leq \mathbf{w} = (w, w')$ in \mathbf{U} is sent to the canonical map from $\bigvee_{[u, u']} \theta_X$ to $\bigvee_{[w, w']} \theta_X$, i.e. each block $A \in \bigvee_{[u, u']} \theta_X$ is sent to the unique block $B \in \bigvee_{[w, w']} \theta_X$ such that $A \subset B$.

Recall the notion of partition morphisms from Definition 6.21. Whenever $f : X \rightarrow Y$ is a partition morphism between $P_X \in \mathcal{P}(X)$ and $P_Y \in \mathcal{P}(Y)$, there is an obvious induced map $f^* : P_X \rightarrow P_Y$. Namely, any block B of P_X is sent by f^* to the block C in P_Y which contains the image of B . Also, recall that for $\varepsilon \geq 0$, $\vec{\varepsilon} := (-\varepsilon, \varepsilon)$. Now we prove that $E_{\mathbf{Sets}}$ is 1-Lipschitz.

Proposition 11.9 ($E_{\mathbf{Sets}}$ is 1-Lipschitz). Let θ_X and θ_Y be any formigrams over X and Y , respectively. Then,

$$d_1(E_{\mathbf{Sets}}(\theta_X), E_{\mathbf{Sets}}(\theta_Y)) \leq d_1^F(\theta_X, \theta_Y). \quad (12)$$

We will provide a geometric interpretation of the LHS of (12) in Remark 11.18.

Proof. If the RHS is $+\infty$, there is nothing to prove. Let $\varepsilon \geq 0$ and assume that $R : X \xleftarrow{\varphi_X} Z \xrightarrow{\varphi_Y} Y$ is an ε -tripod between θ_X and θ_Y . Let $\mathcal{P}_X := E_{\mathbf{Sets}}(\theta_X)$ and $\mathcal{Q}_Y := E_{\mathbf{Sets}}(\theta_Y)$, which are functors from \mathbf{U} to \mathbf{Sets} . It suffices to construct an ε -interleaving pair between $\mathcal{P}_X := E_{\mathbf{Sets}}(\theta_X)$ and $\mathcal{Q}_Y := E_{\mathbf{Sets}}(\theta_Y)$ (Definition 11.6).

Claim 1. Let $z \in Z$ and let $\varphi_X(z) = x$, and $\varphi_Y(z) = y$. Also suppose that for some $\mathbf{u} \in \mathbf{U}$, x is in the underlying set of $\mathcal{P}_X(\mathbf{u}) \in \mathcal{P}^{\text{sub}}(X)$. Then, for any $\mathbf{w} = (w, w') \in \mathbf{U}$ with $\mathbf{w} \geq \mathbf{u} + \vec{\varepsilon}$, y belong to the underlying set of $\mathcal{P}_X(\mathbf{w})$.

Proof of Claim 1. Since x is in the underlying set of $\mathcal{P}_X(\mathbf{u}) = \bigvee_{[u, u']} \theta_X$, there must be a time $t \in [u, u']$ when x is in the underlying set of the sub-partition $\theta_X(t) \in \mathcal{P}^{\text{sub}}(X)$. Then, by Proposition 6.30 (i), there is $s \in [t]^\varepsilon \subset [u, u']^\varepsilon$ such that y belongs to the underlying set of $\theta_Y(s) \in \mathcal{P}^{\text{sub}}(Y)$, which in turn implies that y is in the underlying set of $\mathcal{P}_X(\mathbf{w}) = \bigvee_{[w, w']} \theta_Y$ since $s \in [u, u']^\varepsilon \subset [w, w']$. \square

Claim 2. For some $z, z' \in Z$, let $x := \varphi_X(z)$, $x' := \varphi_X(z')$ and assume that $\varphi_Y(z) = \varphi_Y(z') =: y$. Suppose that for some $\mathbf{u} \in \mathbf{U}$, y is in the underlying set of $\mathcal{Q}_Y(\mathbf{u})$. Then, for any $\mathbf{w} = (w, w') \in \mathbf{U}$ with $\mathbf{w} \geq \mathbf{u} + \vec{\varepsilon}$, x and x' belong to the same block in $\mathcal{P}_X(\mathbf{w})$.

Proof of Claim 2. Since $y \in \mathcal{Q}_Y(\mathbf{u}) = \bigvee_{[u, u']} \theta_Y$, there must be a time $t \in [u, u'] \subset \mathbf{R}$ such that $y \in \theta_Y(t)$. Because $\theta_Y \xrightarrow{R} S_\varepsilon \theta_X$, x and x' must be in the same block of $\bigvee_{[t]^\varepsilon} \theta_X$. Invoking that $[t]^\varepsilon \subset [u, u']^\varepsilon \subset [w, w'] \subset \mathbf{R}$, we have $\bigvee_{[t]^\varepsilon} \theta_X \leq \bigvee_{[w, w']} \theta_X = \mathcal{P}_X(\mathbf{w})$, which implies in turn that x and x' belong to the same block of $\mathcal{P}_X(\mathbf{w})$. \square

Take any maps $\phi : X \rightarrow Y$ and $\psi : Y \rightarrow X$ such that $\{(x, \phi(x)) : x \in X\} \cup \{(\psi(y), y) : y \in Y\} \subset \varphi_Y \circ \varphi_X^{-1}$.

Fix any $\mathbf{u} \in \mathbf{U}$. By **Claims 1 and 2**, the restriction of $\phi : X \rightarrow Y$ to the underlying set of $\mathcal{P}_X(\mathbf{u})$ is the partition morphism between $\mathcal{P}_X(\mathbf{u})$ and $\mathcal{Q}_Y(\mathbf{u} + \vec{\varepsilon})$ (Definition 6.21) and hence we have the induced map $\phi_{\mathbf{u}}^* : \mathcal{P}_X(\mathbf{u}) \rightarrow \mathcal{Q}_Y(\mathbf{u} + \vec{\varepsilon})$ sending each block B in $\mathcal{P}_X(\mathbf{u})$ to the block C in $\mathcal{Q}_Y(\mathbf{u} + \vec{\varepsilon})$ to which the image of B via ϕ belongs. Similarly, we also have the induced map $\psi_{\mathbf{u}}^* : \mathcal{Q}_Y(\mathbf{u}) \rightarrow \mathcal{P}_X(\mathbf{u} + \vec{\varepsilon})$ from $\psi : Y \rightarrow X$. Consider the collections of set maps $\phi^* := (\phi_{\mathbf{u}}^*)_{\mathbf{u} \in \mathbf{U}}$ and $\psi^* = (\psi_{\mathbf{u}}^*)_{\mathbf{u} \in \mathbf{U}}$.

Claim 3. The pair (ϕ^*, ψ^*) is an ε -interleaving pair between the functors $\mathcal{P}_X : \mathbf{U} \rightarrow \mathbf{Sets}$ and $\mathcal{Q}_Y : \mathbf{U} \rightarrow \mathbf{Sets}$.

Proof of Claim 3. We wish to show that

- (i) for all $\mathbf{u} \in \mathbf{U}$, $\mathcal{P}_X(\mathbf{u} \leq \mathbf{u} + 2\vec{\varepsilon}) = \psi_{\mathbf{u} + \vec{\varepsilon}}^* \circ \phi_{\mathbf{u}}^*$ and $\mathcal{Q}_Y(\mathbf{u} \leq \mathbf{u} + 2\vec{\varepsilon}) = \phi_{\mathbf{u} + \vec{\varepsilon}}^* \circ \psi_{\mathbf{u}}^*$,
- (ii) for all $\mathbf{u} \leq \mathbf{w} \in \mathbf{U}$,
 $\mathcal{Q}_Y(\mathbf{u} + \vec{\varepsilon}, \mathbf{w} + \vec{\varepsilon}) \circ \phi_{\mathbf{u}}^* = \phi_{\mathbf{w}}^* \circ \mathcal{P}_X(\mathbf{u} \leq \mathbf{w})$ and $\mathcal{P}_X(\mathbf{u} + \vec{\varepsilon}, \mathbf{w} + \vec{\varepsilon}) \circ \psi_{\mathbf{u}}^* = \psi_{\mathbf{w}}^* \circ \mathcal{Q}_Y(\mathbf{u} \leq \mathbf{w})$.

We prove the first equality of (i). Let $\mathbf{u} \in \mathbf{U}$ and take any $x \in X$ that belongs to the underlying set of $\mathcal{P}_X(\mathbf{u})$. Then, by the definition of \mathcal{P}_X , the block containing x in $\mathcal{P}_X(\mathbf{u})$ is sent to the block containing x in $\mathcal{P}_X(\mathbf{u} + 2\tilde{\varepsilon})$ via $\mathcal{P}_X(\mathbf{u} \leq \mathbf{u} + 2\tilde{\varepsilon})$. Hence, it suffices to prove that x and $\psi \circ \phi(x)$ belong to the same block in $\mathcal{P}_X(\mathbf{u} + 2\tilde{\varepsilon})$. By definition of ϕ and ψ , (1) there are $z, z' \in Z$, such that $\varphi_X(z) = x$, $\varphi_X(z') = \psi \circ \phi(x)$, and $\varphi_Y(z) = \varphi_Y(z') = \phi(x)$, and (2) $\phi(x)$ is in the underlying set of $\mathcal{Q}_Y(\mathbf{u} + \tilde{\varepsilon})$. Therefore, since $\mathbf{u} + 2\tilde{\varepsilon} = (\mathbf{u} + \tilde{\varepsilon}) + \tilde{\varepsilon}$, by **Claim 2**, x and $\psi \circ \phi(x)$ belong to the same block of $\mathcal{P}_X(\mathbf{u} + 2\tilde{\varepsilon})$.

Next, we show the first equality of (ii). Fix any $\mathbf{u} \leq \mathbf{w} \in \mathbf{U}$ and any $x \in X$ that belongs to the underlying set of $\mathcal{P}_X(\mathbf{u})$. Then it is easy to check that the block containing x in $\mathcal{P}_X(\mathbf{u})$ is sent to the block containing $\phi(x)$ in $\mathcal{Q}_Y(\mathbf{w} + \tilde{\varepsilon})$ by both maps $\mathcal{Q}_Y(\mathbf{u} + \tilde{\varepsilon}, \mathbf{w} + \tilde{\varepsilon}) \circ \phi_{\mathbf{u}}^*$ and $\phi_{\mathbf{w}}^* \circ \mathcal{P}_X(\mathbf{u} \leq \mathbf{w})$. \square

Definition 11.10 (Equivalent tripods). Let X, Y be any two sets. For any two tripods $R : X \xleftarrow{\varphi_X} Z \xrightarrow{\varphi_Y} Y$ and $S : X \xleftarrow{\psi_X} Z \xrightarrow{\psi_Y} Y$ between X and Y , we say that R and S are *equivalent* if the two multivalued maps $\varphi_Y \circ \varphi_X^{-1}$ and $\psi_Y \circ \psi_X^{-1}$ from X to Y are identical.

Remark 11.11. Let θ_X and θ_Y be any two formigrams over X and Y , respectively. Suppose that R and S are equivalent tripods between X and Y . Then, it is not difficult to check that for any $\varepsilon \geq 0$, R is an ε -tripod between θ_X and θ_Y if and only if S is an ε -tripod between θ_X and θ_Y .

Example 11.12. Let $X = \{x\}$ and $Y = \{y_1, y_2\}$. Define saturated formigrams θ_X, θ_Y over X, Y as follows: $\theta_X(t) := \{\{x\}\}$ for all $t \in \mathbf{R}$, and $\theta_Y(t) := \begin{cases} \{\{y_1\}, \{y_2\}\}, & t \in (-1, 1) \\ \{\{y_1, y_2\}\}, & \text{otherwise.} \end{cases}$ Let $c : Y \rightarrow X$ be the unique constant map. Then

$R : X \xleftarrow{c} Y \xrightarrow{\text{id}_Y} Y$ is the unique tripod between X and Y up to equivalence (Definition 11.10). By Remark 11.11, noting that the minimal $\varepsilon \geq 0$ for which $\text{id}_Y \circ c^{-1} = \{(x, y_1), (x, y_2)\} \subset X \times Y$ becomes a *partition morphism* from $\theta_X(0)$ to $\bigvee_{[-\varepsilon, \varepsilon]} \theta_Y$ (Definition 6.21) is $\varepsilon = 1$, one can check that $d_1^F(\theta_X, \theta_Y) = 1$. On the other hand, one can also check that $d_1(E_{\mathbf{Sets}}(\theta_X), E_{\mathbf{Sets}}(\theta_Y)) = 1/2$.

11.2.3 Colimits of diagrams induced by formigrams

In this section we interpret the finest common coarsening of partitions on a specific set X as a colimit in the category **Sets**.

We introduce a succinct version of the definition of colimit, by restricting ourselves to the category **Sets**, which is enough for this paper. Consult [43] for general definition of the colimit. By \leftrightarrow we will mean either \leftarrow or \rightarrow .

Definition 11.13 (Colimit). Given a diagram

$$\mathcal{D} : \quad A_1 \xrightarrow{f_1} A_2 \xleftarrow{f_2} A_3 \xrightarrow{f_3} \cdots \xleftarrow{f_{n-1}} A_n$$

of sets and set maps, the colimit of \mathcal{D} is a pair $(B, (\phi_i)_{i=1}^n)$ consisting of a set B and a collection of maps $\phi_i : A_i \rightarrow B$ for $i = 1, \dots, n$ satisfying the following:

1. $(B, (\phi_i)_{i=1}^n)$ is a co-cone over \mathcal{D} , i.e. the diagram below commutes.

$$\begin{array}{ccccccc} & & & & B & & \\ & \nearrow \phi_1 & & \nearrow \phi_2 & \uparrow \phi_3 & \nwarrow \phi_n & \\ A_1 & \xrightarrow{f_1} & A_2 & \xleftarrow{f_2} & A_3 & \xrightarrow{f_3} & \cdots \xleftarrow{f_{n-1}} A_n \end{array}$$

2. (Universal property) If there is another co-cone $(C, (\psi_i)_{i=1}^n)$ over \mathcal{D} , then there exists a unique map $u : B \rightarrow C$ such that $\psi_i = u \circ \phi_i$ for all $i = 1, \dots, n$.

In fact: (1) the colimit is well-defined regardless of the direction of arrows in the diagram \mathcal{D} in Definition 11.13 and (2) the colimit is unique (up to isomorphism).

Let X be a non-empty set. Let \sim, \sim' be two sub-equivalence relations on X such that \sim is contained in \sim' . Then, the *canonical map* $X/\sim \rightarrow X/\sim'$ sends each block B in X/\sim to the block containing B in X/\sim' . Let $\{\sim_i\}_{i=1}^n$ be an *alternating sequence of equivalence relations* on X , i.e. either $\sim_1 \subset \sim_2 \supset \sim_3 \subset \dots \sim_n$ or $\sim_1 \supset \sim_2 \subset \sim_3 \supset \dots \sim_n$. For each $i = 1, 2, \dots, n$, let X_i be the underlying set \sim_i . Then, we have the *induced diagram of canonical maps*

$$X_1/\sim_1 \longrightarrow X_2/\sim_2 \longleftarrow X_3/\sim_3 \longrightarrow \dots \longleftrightarrow X_n/\sim_n \quad (13)$$

from $\{\sim_i\}_{i=1}^n$. Note that diagram (5) has this structure (with infinite length).

Proposition 11.14. Consider diagram (13) and let \sim be the sub-equivalence closure (Definition 6.16) of the collection $\{\sim_i\}_{i=1}^n$. Then \sim is an equivalence relation on $X := \cup_{i=1}^n X_i$. For each $i = 1, \dots, n$, let $\phi_i : X_i/\sim_i \rightarrow X/\sim$ be the canonical map. The colimit of diagram (13) is equal to the pair

$$(X/\sim, (\phi_i)_{i=1}^n).$$

Proposition 11.14 can be proved in a routine (but lengthy) way so we omit its proof. But, appealing to the universal property of colimit, what the statement tells us is inherently expected: any co-cone over the diagram factors through the co-cone described in the statement of Proposition 11.14.

Remark 11.15. Proposition 11.14 implies that the colimit of a diagram of canonical maps between sub-partitions $(P_i)_{i=1}^n$ of a set X is nothing but the finest common coarsening $Q = \bigvee_{i=1}^n P_i$ of $\{P_i\}_{i=1}^n$ with the canonical maps $P_i \rightarrow Q$ (see Definition 6.17).

11.2.4 The Reeb cosheaf functor \mathcal{C}

In this section we re-interpret Definition 11.8 as cosheaves in the category **Sets** over **R**. Let **Top** denote the category of topological spaces with continuous maps. In this section, π_0 is not the one defined in Definition 5.15 but stands for the path connected component functor $\pi_0 : \mathbf{Top} \rightarrow \mathbf{Sets}$. Let T be a topological space and let $f : T \rightarrow \mathbf{R}$ be a continuous map. We call the pair (T, f) an **R-space** [22]. Specifically, every **R-graph** is an **R-space** (Definition 5.17). The *Reeb cosheaf functor* \mathcal{C} converts an **R-space** to its *Reeb cosheaf*:

Definition 11.16 (The Reeb cosheaf functor [22, Section 3.4]). Let (T, f) be an **R-space**. Then $\mathcal{C}(T, f) = F$ is the functor $F : \mathbf{U} \rightarrow \mathbf{Sets}$ defined by¹³ for all $\mathbf{u} = (u, u') \leq \mathbf{w} = (w, w')$ in \mathbf{U} ,

$$F(\mathbf{u}) = \pi_0 f^{-1}([u, u']), \quad F(\mathbf{u} \leq \mathbf{w}) = \pi_0 [f^{-1}([u, u']) \subset f^{-1}([w, w'])].$$

Recall the notion of Reeb graphs of formigrams from Definition 5.18. Reeb graphs of formigrams are **R-spaces** and thus one can apply the Reeb cosheaf \mathcal{C} functor to the Reeb graphs of formigrams.

Proposition 11.17 (Interpretation of $E_{\mathbf{Sets}}(\theta_X)$ as a Reeb cosheaf). Let θ_X be a formigram over X . Then, $\mathcal{C}(\mathbf{Reeb}(\theta_X))$ and $E_{\mathbf{Sets}}(\theta_X)$ are *naturally isomorphic* (Item 14 in Section 3.1).

Proof. Recall from Definition 5.18 that all the edges and vertices of $\mathbf{Reeb}(\theta_X)$ can be labeled by sub-partitions of X in $\{\theta_X(t) : t \in \mathbf{R}\}$ and keeping those labels enables us to rebuild the original formigram $\theta_X : \mathbf{R} \rightarrow \mathcal{P}^{\text{sub}}(X)$. Let $F := \mathcal{C}(\mathbf{Reeb}(\theta_X)) : \mathbf{U} \rightarrow \mathbf{Sets}$ and fix any $\mathbf{u} = (u, u') \in \mathbf{U}$.

Let $\text{crit}(\theta_X) = \{c_i : i \in \mathbf{Z}\}$ such that $\dots < c_{i-1} < c_i < c_{i+1} < \dots$, $\lim_{i \rightarrow +\infty} c_i = +\infty$, and $\lim_{i \rightarrow -\infty} c_i = -\infty$ (if $\text{crit}(\theta_X)$ is finite, then choose $\{c_i : i \in \mathbf{Z}\}$ to be any superset of $\text{crit}(\theta_X)$). Without loss of generality, assume that $[u, u'] \cap \text{crit}(\theta_X) = \{c_1 < c_2 < \dots < c_n\}$ for some $n \in \mathbf{N}$. Pick $s_i \in (c_i, c_{i+1})$ for each $i = 1, \dots, n-1$. Then, the set $F(\mathbf{u}) = \pi_0 f^{-1}([u, u'])$ is identical (up to isomorphic) to the colimit of the diagram

$$\theta_X(c_1) \leftarrow \theta_X(s_1) \rightarrow \theta_X(c_2) \leftarrow \theta_X(s_2) \rightarrow \dots \leftarrow \theta_X(s_{n-1}) \rightarrow \theta_X(c_n) \quad (14)$$

¹³In [22], the authors consider the preimages of bounded *open* intervals, not bounded closed intervals as above. But, this difference is negligible in terms of computing the interleaving distance of Reeb graphs, which is already noted in [8, Remark 4.12].

in the category **Sets** where all the arrows are the canonical maps (see page 15 for the meaning of ‘canonical’). Note that this diagram is of the form (13). By Remark 11.15, the colimit of diagram (14) is the finest common coarsening of the sub-partitions of X that are present in diagram (14). By Definition 11.8, $E_{\mathbf{Sets}}(\theta_X)(\mathbf{u}) = \bigvee_{[u,u']} \theta_X$ and it is not difficult to check that $E_{\mathbf{Sets}}(\theta_X)(\mathbf{u})$ is also the finest common coarsening of the collection of the sub-partitions of X that are present in diagram (14). Therefore, $F(\mathbf{u})$ is isomorphic to $E_{\mathbf{Sets}}(\mathbf{u})$ in the category **Sets**.

Pick any $\mathbf{w} = (w, w') \in \mathbf{U}$ such that $\mathbf{w} \geq \mathbf{u}$. By computing $F(\mathbf{w})$ in the same way as in the computation of $F(\mathbf{u})$ above, one can prove that the map $F(\mathbf{u} \leq \mathbf{w}) = \pi_0 [f^{-1}([u, u']) \subset f^{-1}([w, w'])]$ is identical to the canonical map $E_{\mathbf{Sets}}(\theta_X)(\mathbf{u} \leq \mathbf{w}) : \bigvee_{[u,u']} \theta_X \rightarrow \bigvee_{[w,w']} \theta_X$, completing the proof. \square

Remark 11.18 (Geometric interpretation of the LHS of (12)). By Proposition 11.17, the LHS of (12) is identical to the interleaving distance between the Reeb graphs $\mathbf{Reeb}(\theta_X), \mathbf{Reeb}(\theta_Y)$ of θ_X and θ_Y [22]. The pair of formigrams θ_X and θ_Y in Example 5.20 is an instance of the case $E_{\mathbf{Sets}}(\theta_X) \cong E_{\mathbf{Sets}}(\theta_Y)$, which was roughly discussed in Remark 6.28.

By Proposition 11.17 and [8, Theorem 4.13] together with [5, Corollary 5.5], we have:

Corollary 11.19. Let θ_X and θ_Y be any formigrams over X and Y , respectively. Then,

$$d_B(\mathcal{L}_0(\mathbf{Reeb}(\theta_X)), \mathcal{L}_0(\mathbf{Reeb}(\theta_Y))) \leq 2 d_I(E_{\mathbf{Sets}}(\theta_X), E_{\mathbf{Sets}}(\theta_Y)).$$

Proof. By [8, Theorem 4.13] together with [5, Corollary 5.5], we have

$$d_B(\mathcal{L}_0(\mathbf{Reeb}(\theta_X)), \mathcal{L}_0(\mathbf{Reeb}(\theta_Y))) \leq 2 d_I(\mathcal{C}(\mathbf{Reeb}(\theta_X)), \mathcal{C}(\mathbf{Reeb}(\theta_Y))).$$

Invoking that $\mathcal{C}(\mathbf{Reeb}(\theta_X)) \cong E_{\mathbf{Sets}}(\theta_X)$ and $\mathcal{C}(\mathbf{Reeb}(\theta_Y)) \cong E_{\mathbf{Sets}}(\theta_Y)$ from Proposition 11.17, we have the desired inequality. \square

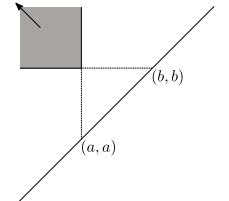
Remark 11.20. In Corollary 11.19, recalling that $\text{dgm}(\theta_X) = \mathcal{L}_0(\mathbf{Reeb}(\theta_X))$ and $\text{dgm}(\theta_Y) = \mathcal{L}_0(\mathbf{Reeb}(\theta_Y))$ from Proposition 5.22, we have

$$d_B(\text{dgm}(\theta_X), \text{dgm}(\theta_Y)) \leq 2 d_I(E_{\mathbf{Sets}}(\theta_X), E_{\mathbf{Sets}}(\theta_Y)).$$

11.3 Details from Section 7

In order to prove Proposition 7.1, we need Propositions 11.21, 11.22, 11.23, and 11.24 below. In what follows, we use the notation $\langle b, d \rangle_{\text{BL}}$ as defined in [8, p.12] for $b, d \in \mathbf{R}$: $\langle b, d \rangle_{\text{BL}}$ denotes a *block* of the form $(a, b)_{\text{BL}}, [a, b)_{\text{BL}}, (a, b]_{\text{BL}}$ or $[a, b]_{\text{BL}}$, each standing for a convex region of \mathbf{U} .¹⁴ Among others, we recall that for $a, b \in \mathbf{R}$ with $a < b$, $[b, a]_{\text{BL}} = \{(x, y) \in \mathbf{U} : x \leq a < b \leq y\}$ (see figure on the right).

Any block $\langle a, b \rangle_{\text{BL}}$ of \mathbf{U} is an interval of \mathbf{U} (Definition 3.1) and thus the \mathbf{U} -indexed module $I^{\langle a, b \rangle_{\text{BL}}}$ is indecomposable (Proposition 3.2). A \mathbf{U} -indexed module F is said to be *block decomposable* if for some index set J and blocks $\langle b_j, d_j \rangle_{\text{BL}}$, $j \in J$, one has $F \cong \bigoplus_{j \in J} I^{\langle b_j, d_j \rangle_{\text{BL}}}$. In this case, the multiset $\text{dgm}^{\text{BL}}(F) := \{\langle b_j, d_j \rangle_{\text{BL}} : j \in J\}$ is said to be the *block barcode* of F . Recall the Reeb cosheaf functor \mathcal{C} (Definition 11.16) and the free functor $\mathfrak{V}_{\mathbb{F}}$ (item 18 in Section 3.1).



Proposition 11.21. Let (T, f) be any \mathbf{R} -graph (Definition 5.17 (i)) and consider the functor $\mathcal{C}(T, f) : \mathbf{U} \rightarrow \mathbf{Sets}$.

- (i) The \mathbf{U} -indexed module $F := \mathfrak{V}_{\mathbb{F}}(\mathcal{C}(T, f))$ is *block decomposable*, and thus F admits its block barcode $\text{dgm}^{\text{BL}}(F)$.
- (ii) The block barcode $\text{dgm}^{\text{BL}}(F)$ of F does not contain a block of the form $[b, a]_{\text{BL}}$ for $b > a$.

¹⁴Note that $\langle b, d \rangle_{\text{BL}}$ is different from intervals $\langle b, d \rangle_{\mathbf{ZZ}}$ of \mathbf{ZZ} defined in Remark 3.4 or real intervals $\langle b, d \rangle$ defined in p. 42.

Proof. First, we show (i). Consider the *interlevel filtration functor* $S(f) : \mathbf{U} \rightarrow \mathbf{Top}$ defined by $S(f)(u_1, u_2) = f^{-1}([u_1, u_2])$ and $S(f)((u_1, u_2) \leq (w_1, w_2)) = f^{-1}([u_1, u_2]) \hookrightarrow f^{-1}([w_1, w_2])$. Then, F is naturally isomorphic to $G = H_0 \circ S(f)$ where H_0 is the 0-th singular homology functor (item 17 in Section 3.1). Then, (i) directly follows from [8, Theorem 4.7, (i)].

Next we prove (ii). It suffices to show that for $b > a$ in \mathbf{R} , the block $[b, a]_{\text{BL}}$ cannot be in $\text{dgm}^{\text{BL}}(G)$. Fix $b > a$ in \mathbf{R} and pick $\varepsilon > 0$ such that $b - 2\varepsilon > a$. To obtain a contradiction, suppose that $G \cong I^{[b, a]_{\text{BL}}} \oplus G'$ for some \mathbf{U} -indexed module G' . Consider the sub-diagram of G indexed by the four points $(a + \varepsilon, b - \varepsilon), (a, b - \varepsilon), (a + \varepsilon, b), (a, b)$ in \mathbf{U} :

$$\begin{array}{ccc} H_0(f^{-1}([a + \varepsilon, b - \varepsilon])) & \xrightarrow{i_*} & H_0(f^{-1}([a, b - \varepsilon])) \\ \downarrow j_* & & \downarrow k_* \\ H_0(f^{-1}([a + \varepsilon, b])) & \xrightarrow{l_*} & H_0(f^{-1}([a, b])), \end{array} \quad (15)$$

where the arrows are obtained by applying the (singular) homology functor H_0 to the canonical inclusions. Then by the Mayer-Vietoris sequence

$$\cdots H_0(f^{-1}([a + \varepsilon, b - \varepsilon])) \xrightarrow{(i_*, j_*)} H_0(f^{-1}([a, b - \varepsilon])) \oplus H_0(f^{-1}([a + \varepsilon, b])) \xrightarrow{k_* - l_*} H_0(f^{-1}([a, b])) \xrightarrow{0} 0,$$

diagram (15) is a *push-out* diagram ([43, Ch. III]), implying that any element in $H_0(f^{-1}([a, b]))$ is a sum of $v \in \text{im}(k_*)$ and $w \in \text{im}(l_*)$. However, the element $u \in H_0(f^{-1}([a, b]))$ corresponding to $(1, 0) \in (I^{[b, a]_{\text{BL}}} \oplus G')_{(a, b)} = \mathbb{F} \oplus G'_{(a, b)}$ cannot be expressed as a sum of elements in $\text{im}(k_*)$ and $\text{im}(l_*)$, which is a contradiction. Therefore, G cannot admit $[b, a]_{\text{BL}}$ in its block barcode, as desired. \square

Given a formigram θ_X over X , recall the functor $E_{\mathbf{Sets}}(\theta_X) : \mathbf{U} \rightarrow \mathbf{Sets}$ from Definition 11.8.

Proposition 11.22. Let θ_X be a formigram over X and fix $\varepsilon \geq 0$. Then, for all $\mathbf{u} \in \mathbf{U}$,

$$E_{\mathbf{Sets}}(S_\varepsilon \theta_X)(\mathbf{u}) = E_{\mathbf{Sets}}(\theta_X)(\mathbf{u} + \vec{\varepsilon}).$$

Proof. By definition, $E_{\mathbf{Sets}}(S_\varepsilon \theta_X)(\mathbf{u}) = \bigvee_{[u, u']} S_\varepsilon \theta_X$ and $E_{\mathbf{Sets}}(\theta_X)(\mathbf{u} + \vec{\varepsilon}) = \bigvee_{[u - \varepsilon, u' + \varepsilon]} \theta_X$. We first show that $\bigvee_{[u, u']} S_\varepsilon \theta_X \leq \bigvee_{[u - \varepsilon, u' + \varepsilon]} \theta_X$. Note that for each $t \in [u, u']$, the interval $[t - \varepsilon, t + \varepsilon]$ is a subset of $[u - \varepsilon, u' + \varepsilon]$ and thus $S_\varepsilon \theta_X(t) = \bigvee_{[t - \varepsilon, t + \varepsilon]} \theta_X \in \mathcal{P}^{\text{sub}}(X)$ refines $\bigvee_{[u - \varepsilon, u' + \varepsilon]} \theta_X \in \mathcal{P}^{\text{sub}}(X)$. Since this holds for each $t \in [u, u']$, it must be that $\bigvee_{[u, u']} S_\varepsilon \theta_X \leq \bigvee_{[u - \varepsilon, u' + \varepsilon]} \theta_X$ (Remark 6.19 (ii)).

Next we verify that $\bigvee_{[u - \varepsilon, u' + \varepsilon]} \theta_X \leq \bigvee_{[u, u']} S_\varepsilon \theta_X$. Pick any $t \in [u - \varepsilon, u' + \varepsilon]$. Then, there is $s \in [u, u']$ such that the subinterval $[s - \varepsilon, s + \varepsilon] \subset [u - \varepsilon, u' + \varepsilon]$ contains t . Then, we have $\theta_X(t) \leq S_\varepsilon \theta_X(s) \leq \bigvee_{[u, u']} S_\varepsilon \theta_X$. Since this holds for any $t \in [u - \varepsilon, u' + \varepsilon]$, the finest common coarsening $\bigvee_{[u - \varepsilon, u' + \varepsilon]} \theta_X$ refines $\bigvee_{[u, u']} S_\varepsilon \theta_X$, as desired. \square

Let $\pi_2 : \mathbf{R}^2 \rightarrow \mathbf{R}$ be the canonical projection map to the second coordinate. Let B be any subset of the upper-half plane $\mathbf{U} = \{(x, y) \in \mathbf{R}^2 : y \geq x\}$ and let $\varepsilon \geq 0$. Define $\text{diag}^\varepsilon(B) := \pi_2(B \cap \{(t - \varepsilon, t + \varepsilon) \in \mathbf{U} : t \in \mathbf{R}\})$. In words, $\text{diag}^\varepsilon(B)$ is the image of the intersection of B and the line $y = x + 2\varepsilon$ under the projection π_2 . Also given a multiset \mathcal{B} of subsets of \mathbf{U} , let

$$\text{diag}^\varepsilon(\mathcal{B}) := \{\{\text{diag}^\varepsilon(B) : B \in \mathcal{B} \text{ and } B \cap \{(t - \varepsilon, t + \varepsilon) \in \mathbf{R}^2 : t \in \mathbf{R}\} \neq \emptyset\}\}.$$

For ease of notation, we set $\text{diag}(\mathcal{B}) := \text{diag}^0(\mathcal{B})$.

For any formigram θ_X over X , consider its Reeb graph $\mathbf{Reeb}(\theta_X) =: (\mathbb{X}_{\theta_X}, f_{\theta_X})$ (Definition 5.18). Then, f_{θ_X} is of Morse type (Definition 3.6) and $\mathbf{Reeb}(\theta_X)$ is an \mathbf{R} -graph. By Proposition 11.21 (i), $\mathfrak{V}_{\mathbb{F}}(\mathcal{C}(\mathbf{Reeb}(\theta_X))) : \mathbf{U} \rightarrow \mathbf{Vec}$ is *block decomposable* and thus admits its *block barcode* $\text{dgm}^{\text{BL}}(\mathfrak{V}_{\mathbb{F}}(\mathcal{C}(\mathbf{Reeb}(\theta_X))))$. Moreover, by the construction of $\text{dgm}^{\text{BL}}(\mathfrak{V}_{\mathbb{F}}(\mathcal{C}(\mathbf{Reeb}(\theta_X))))$ in [8], we have

$$\mathcal{L}_0(\mathbf{Reeb}(\theta_X)) = \text{diag}\left(\text{dgm}^{\text{BL}}(\mathfrak{V}_{\mathbb{F}}(\mathcal{C}(\mathbf{Reeb}(\theta_X))))\right) \text{ (see [8, p.3]).}$$

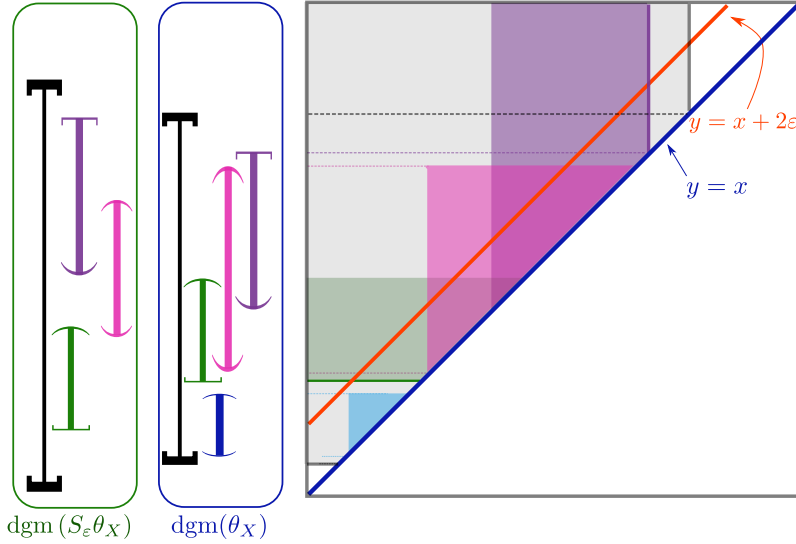


Figure 13: Assuming that the 2D-barcode of an \mathbf{U} -indexed module $E_{\mathbf{Vec}}(\theta_X)$ consists of five blocks (gray, purple, pink green, blue) as described to the left, the barcode $\text{dgm}(\theta_X)$ is obtained by projecting the intersections of those blocks with the line $y = x$ down onto the y -axis. On the other hand, $\text{dgm}(S_\epsilon \theta_X)$ is obtained by projecting the intersections of blocks with the line $y = x + 2\epsilon$ onto the y -axis and then moving downward by ϵ . In this process, all the open intervals that are shorter than 2ϵ disappear.

Let $E_{\mathbf{Vec}}(\theta_X) := \mathfrak{V}_{\mathbb{F}} \circ E_{\mathbf{Sets}}(\theta_X) : \mathbf{U} \rightarrow \mathbf{Vec}$. By Proposition 11.17, we know the natural equivalence $E_{\mathbf{Vec}}(\theta_X) \cong \mathfrak{V}_{\mathbb{F}}(\mathcal{C}(\mathbf{Reeb}(\theta_X)))$, which implies that:

$$\mathcal{L}_0(\mathbf{Reeb}(\theta_X)) = \text{diag}\left(\text{dgm}^{\text{BL}}(E_{\mathbf{Vec}}(\theta_X))\right).$$

From Proposition 5.22, we know that $\mathcal{L}_0(\mathbf{Reeb}(\theta_X)) = \text{dgm}(\theta_X)$ and hence we have:

Proposition 11.23. For any formigram θ_X over X , we have

$$\text{dgm}(\theta_X) = \text{diag}\left(\text{dgm}^{\text{BL}}(E_{\mathbf{Vec}}(\theta_X))\right) \text{ (see Figure 13).}$$

By Proposition 11.21 (ii), the natural equivalence $E_{\mathbf{Vec}}(\theta_X) \cong \mathfrak{V}_{\mathbb{F}}(\mathcal{C}(\mathbf{Reeb}(\theta_X)))$ implies that $\text{dgm}^{\text{BL}}(E_{\mathbf{Vec}}(\theta_X))$ does not contain any block of the type $[b, a]_{\text{BL}}$ for $b > a$. This implies that every block $\langle a, b \rangle_{\text{BL}}$ in $\text{dgm}^{\text{BL}}(E_{\mathbf{Vec}}(\theta_X))$ intersects the diagonal line $y = x$ and the following proposition immediately follows from the definitions of $(a, b)_{\text{BL}}$, $[a, b]_{\text{BL}}$, $(a, b]_{\text{BL}}$, and $[a, b)_{\text{BL}}$ (see [8, p.12-13]):

Proposition 11.24 (Correspondence between barcodes). Let θ_X be a formigram over X . There exists the bijection between $\text{dgm}(\theta_X)$ and $\text{dgm}^{\text{BL}}(E_{\mathbf{Vec}}(\theta_X))$ as follows (see Figure 13):

$\text{dgm}(\theta_X)$		$\text{dgm}^{\text{BL}}(E_{\mathbf{Vec}}(\theta_X))$	
$[c_i, c_j]$	\leftrightarrow	$[c_i, c_j]_{\text{BL}}$	for $i \leq j$
$[c_i, c_{j+1})$	\leftrightarrow	$[c_i, c_{j+1})_{\text{BL}}$	for $i \leq j$
$(c_i, c_j]$	\leftrightarrow	$(c_i, c_j]_{\text{BL}}$	for $i < j$
(c_i, c_{j+1})	\leftrightarrow	$(c_i, c_{j+1})_{\text{BL}}$	for $i \leq j$.

Proof of Proposition 7.1. Consider the two \mathbf{U} -indexed modules $\mathcal{P}_X := E_{\mathbf{Vec}}(\theta_X) = \mathfrak{V}_{\mathbb{F}} \circ E_{\mathbf{Sets}}(\theta_X)$ and $\mathcal{P}_X^\epsilon := E_{\mathbf{Vec}}(S_\epsilon \theta_X) = \mathfrak{V}_{\mathbb{F}} \circ E_{\mathbf{Sets}}(S_\epsilon \theta_X)$. For any multiset A of real numbers \mathbf{R} and any $t \in \mathbf{R}$, let $A - t$ to be the multiset obtained by subtracting t from all the elements in A . We have:

$$\begin{aligned} \text{dgm}(S_\epsilon \theta_X) &= \text{diag}(\text{dgm}^{\text{BL}}(\mathcal{P}_X^\epsilon)) && \text{Proposition 11.23} \\ &= \text{diag}^\epsilon(\text{dgm}^{\text{BL}}(\mathcal{P}_X)) - \epsilon && \text{Proposition 11.22 (see Figure 13).} \end{aligned}$$

Invoking the bijection between $\text{dgm}(\theta_X)$ and $\text{dgm}^{\text{BL}}(\mathcal{P}_X)$ (Proposition 11.24) and the definitions of blocks $(a, b)_{\text{BL}}$, $[a, b)_{\text{BL}}$, $(a, b]_{\text{BL}}$, $[a, b]_{\text{BL}}$ in \mathbf{U} for $a, b \in \mathbf{R}$, we have the correspondence described as in table (10). \square

Proposition 7.3 will be proved by making use of the lemma below. For a non-empty set X , let R be a relation on X . We denote the sub-equivalence closure of R by \overline{R} , i.e. \overline{R} is the smallest equivalence relation on $X' = \{x \in X : \exists x' \in X, (x, x') \in R, \text{ or } (x', x) \in R\}$ containing R (Definition 6.16).

Lemma 11.25. Let X be a non-empty set. For any index set I , let $\{R_i\}_{i \in I}$ be a collection of relations on X . Then, one has $\overline{\bigcup_{i \in I} R_i} = \bigcup_{i \in I} \overline{R_i}$.

Proof. Since $R_i \subset \overline{R_i}$ for each $i \in I$, \subset is clear. On the other hand, as $R_i \subset \bigcup_{i \in I} R_i$ for each $i \in I$, one has $\overline{R_i} \subset \overline{\bigcup_{i \in I} R_i}$ and hence $\bigcup_{i \in I} \overline{R_i} \subset \overline{\bigcup_{i \in I} R_i}$. Therefore, $\overline{\bigcup_{i \in I} R_i} \subset \overline{\bigcup_{i \in I} \overline{R_i}} = \bigcup_{i \in I} \overline{R_i}$, completing the proof. \square

Proof of Proposition 7.3. For each $t \in \mathbf{R}$, we have the sub-partition $\theta_X(t) = \pi_0(\mathcal{G}_X(t))$ of X . This sub-partition is identical to the quotient set of $V_X(t) \subset X$ by the equivalence relation $\overline{R(t)}$ on $V_X(t)$, which is the transitive closure of $R(t)$ where $(x, x') \in R(t)$ if and only if $\{x, x'\} \in E_X(t)$. Note that the sub-partition $\pi_0(\bigcup_I \mathcal{G}_X)$ is the quotient set of $\bigcup_{s \in I} V_X(s)$ by the equivalence relation $\overline{\bigcup_{s \in I} R(s)}$ on $\bigcup_{s \in I} V_X(s)$, whereas $\bigvee_I \theta_X$ is the quotient set of $\bigcup_{s \in I} V_X(s)$ by the equivalence relation $\overline{\bigcup_{s \in I} \overline{R(s)}}$ on $\bigcup_{s \in I} V_X(s)$. Therefore, $\pi_0(\bigcup_I \mathcal{G}_X) = \bigvee_I \theta_X$ by virtue of Lemma 11.25. \square

Proof of Proposition 7.4. (i) follows directly from Proposition 7.3. Let us show (ii). To this end, we will verify that the Reeb cosheaves corresponding to $\mathbf{Reeb}(S_\varepsilon \theta_X)$ and $\mathcal{U}_\varepsilon \mathbf{Reeb}(\theta_X)$ are naturally isomorphic. In other words, for the Reeb cosheaf functor \mathcal{C} (Definition 11.16), we will prove that $\mathcal{C}(\mathbf{Reeb}(S_\varepsilon \theta_X))$ and $\mathcal{C}(\mathcal{U}_\varepsilon \mathbf{Reeb}(\theta_X))$ are naturally isomorphic as functors $\mathbf{U} \rightarrow \mathbf{Sets}$. Then the Reeb graphs $\mathbf{Reeb}(S_\varepsilon \theta_X)$ and $\mathcal{U}_\varepsilon \mathbf{Reeb}(\theta_X)$ are isomorphic by the equivalence between the category of Reeb graphs and the category of constructible cosheaves [22, Theorem 3.20]. We have

$$\begin{aligned} \mathcal{C}(\mathbf{Reeb}(S_\varepsilon \theta_X)) &\cong E_{\mathbf{Sets}}(S_\varepsilon \theta_X) && \text{Proposition 11.17} \\ &\cong S_\varepsilon E_{\mathbf{Sets}}(\theta_X) && \text{see below} \\ &\cong S_\varepsilon \mathcal{C}(\mathbf{Reeb}(\theta_X)) && \text{Proposition 11.17} \\ &\cong \mathcal{C} \mathcal{U}_\varepsilon(\mathbf{Reeb}(\theta_X)) && [22, \text{Proposition 4.29}], \end{aligned}$$

where the smooth operation S_ε on the second line above is the one for (pre-)cosheaves defined in [22, Definition 4.11]. We show the second “ \cong ”: Pick any $\mathbf{u} = (u, u') \in \mathbf{U}$. Then

$$E_{\mathbf{Sets}}(S_\varepsilon \theta_X)(\mathbf{u}) \stackrel{(1)}{=} E_{\mathbf{Sets}}(\theta_X)(\mathbf{u} + \vec{\varepsilon}) \stackrel{(2)}{=} S_\varepsilon E_{\mathbf{Sets}}(\theta_X)(\mathbf{u}),$$

where (1) follows from Proposition 11.22 and (2) holds by the definition of $S_\varepsilon E_{\mathbf{Sets}}(\theta_X)$. In addition, for any $\mathbf{w} \in \mathbf{U}$ with $\mathbf{w} \geq \mathbf{u}$,

$$E_{\mathbf{Sets}}(S_\varepsilon \theta_X)(\mathbf{u} \leq \mathbf{w}) = E_{\mathbf{Sets}}(\theta_X)(\mathbf{u} + \vec{\varepsilon} \leq \mathbf{w} + \vec{\varepsilon}) = S_\varepsilon E_{\mathbf{Sets}}(\theta_X)(\mathbf{u} \leq \mathbf{w}),$$

completing the proof. \square

11.4 Details from Section 9

11.4.1 Details from Section 9.2

Proof of Proposition 9.5. First note that, by the definition of the Rips graph functor \mathcal{R}_δ^1 , $\mathcal{R}_\delta^1(\gamma_X)$ is a function from \mathbf{R} to the set of graphs on the vertex set X . By the definition of DMSs, this $\mathcal{R}_\delta^1(\gamma_X)$ clearly satisfies Definition 4.1, (iii) since every $x \in X$ lives over the whole \mathbf{R} .

We show that Definition 4.1, (iv) holds. For simplicity, assume that $X = \{1, 2, \dots, n\}$ for some $n \in \mathbf{N}$. Fix $c \in \mathbf{R}$ and consider the following two subsets of $X \times X$:

$$A(c, \delta) := \{(i, j) : i < j \in X, d_X(c)(i, j) \leq \delta\},$$

$$B(c, \delta) := \{(i, j) : i < j \in X, d_X(c)(i, j) > \delta\}.$$

The continuity of $d_X(\cdot)(i, j)$ for each $(i, j) \in X \times X$ guarantees that there exists $\varepsilon > 0$ such that

$$B(t, \delta) \supset B(c, \delta) \quad \text{for all } t \in (c - \varepsilon, c + \varepsilon)$$

and in turn

$$A(t, \delta) \subset A(c, \delta) \quad \text{for all } t \in (c - \varepsilon, c + \varepsilon)$$

since $A(t, \delta) \cup B(t, \delta) = \{(i, j) : i < j \in X\}$ for all $t \in \mathbf{R}$. This implies that the graph $\mathcal{R}_\delta^1(\gamma_X(c))$ contains $\mathcal{R}_\delta^1(\gamma_X(t))$ as a subgraph for each $t \in (c - \varepsilon, c + \varepsilon)$, which means that $\mathcal{R}_\delta^1(\gamma_X)$ satisfies Definition 4.1 (iv).

We only need to verify additionally that the time-varying graph $\mathcal{R}_\delta^1(\gamma_X)$ is tame (Definition 4.1, (ii)). For $i, j \in X$, let $f_{i,j} := d_X(\cdot)(i, j) : \mathbf{R} \rightarrow \mathbf{R}_+$ and let $I \subset \mathbf{R}$ be any finite interval. Note that discontinuity points of $\mathcal{R}_\delta^1(\gamma_X)$ can occur only at endpoints of connected components of the set $f_{i,j}^{-1}(\delta)$ for some $i, j \in X$. Fix any $i, j \in X$. Then, by Definition 9.4, the set $f_{i,j}^{-1}(\delta) \cap I$ has only finitely many connected components and thus there are only finitely many endpoints arising from those components. Since the set X is finite, this implies that $\mathcal{R}_\delta^1(\gamma_X)$ can have only finitely many critical points in I . \square

11.4.2 Details from Section 9.3

Details about $d_{1,\lambda}^{\text{dynM}}$. We further investigate properties of the metrics in the family $\{d_{1,\lambda}^{\text{dynM}}\}_{\lambda \in [0, \infty)}$. In particular, stable invariants of DMSs with regard to the metrics $d_{1,\lambda}^{\text{dynM}}$ for $\lambda > 0$ can be found in [38].

Recall that for $r > 0$, we call any DMS $\gamma_X = (X, d_X(\cdot))$ *r-bounded* if the distance between any pair of points in X does not exceed r across all $t \in \mathbf{R}$. If γ_X is *r-bounded* for some $r > 0$, then γ_X is said to be *bounded*.

Remark 11.26. Let $\lambda > 0$. The distance $d_{1,\lambda}^{\text{dynM}}$ between any two bounded DMSs is finite. More specifically, for any *r-bounded* DMSs $\gamma_X = (X, d_X(\cdot))$ and $\gamma_Y = (Y, d_Y(\cdot))$ for some $r > 0$, any tripod R between X and Y is a $(\lambda, \frac{r}{\lambda})$ -tripod between γ_X and γ_Y . This implies that

$$d_{1,\lambda}^{\text{dynM}}(\gamma_X, \gamma_Y) \leq \frac{r}{\lambda}.$$

Remark 11.27. Let $\gamma_X = (X, d_X(\cdot))$ and $\gamma_Y = (Y, d_Y(\cdot))$ be any two DMSs. Suppose that R and S are equivalent tripods between X and Y (Definition 11.10). Then, it is not difficult to check that for any $\lambda, \varepsilon \geq 0$, R is a (λ, ε) -tripod between γ_X and γ_Y if and only if S is a (λ, ε) -tripod between γ_X and γ_Y .

Proof of Theorem 9.14. We prove the triangle inequality. Take any DMSs γ_X, γ_Y and γ_W over X, Y and W , respectively. For some $\varepsilon, \varepsilon' > 0$, let $R_1 : X \xleftarrow{\varphi_X} Z_1 \xrightarrow{\varphi_Y} Y$ and $R_2 : Y \xleftarrow{\psi_Y} Z_2 \xrightarrow{\psi_W} W$ be any (λ, ε) -tripod between γ_X and γ_Y and (λ, ε') -tripod between γ_Y and γ_W (Definition 9.10), respectively. Consider the set $Z := \{(z_1, z_2) \in Z_1 \times Z_2 : \varphi_Y(z_1) = \psi_Y(z_2)\}$ and let $\pi_1 : Z \rightarrow Z_1$ and $\pi_2 : Z \rightarrow Z_2$ be the canonical projections to the first and the second coordinate, respectively. Define the tripod $R_2 \circ R_1$ between X and W as in equation (9). It is not difficult to check that $R_2 \circ R_1$ is a $(\lambda, \varepsilon + \varepsilon')$ -tripod between γ_X and γ_W and thus we have $d_{1,\lambda}^{\text{dynM}}(\gamma_X, \gamma_W) \leq d_{1,\lambda}^{\text{dynM}}(\gamma_X, \gamma_Y) + d_{1,\lambda}^{\text{dynM}}(\gamma_Y, \gamma_W)$.

Next assume that $d_{1,\lambda}^{\text{dynM}}(\gamma_X, \gamma_Y) = 0$. We outline the proof of that γ_X and γ_Y are isomorphic (Definition 9.3). Because there are only finitely many tripods between X and Y up to equivalence (Definition 11.10), $d_{1,\lambda}^{\text{dynM}}(\gamma_X, \gamma_Y) = 0$ implies that there must be a certain tripod $R : X \xleftarrow{\varphi_X} Z \xrightarrow{\varphi_Y} Y$ between X and Y such that R becomes an (λ, ε) -tripod between γ_X and γ_Y for *any* $\varepsilon > 0$. In order to show that γ_X and γ_Y are isomorphic, one needs to prove that R is in fact $(\lambda, 0)$ -tripod. After that, invoke Definition 9.1, (ii) and (iii) to verify that the multivalued map $\varphi_Y \circ \varphi_X^{-1} : X \rightrightarrows Y$ is in fact a bijection from X to Y .

In particular, by Remark 11.26, for $\lambda > 0$, $d_{1,\lambda}^{\text{dynM}}$ is finite between bounded DMSs modulo isomorphism. \square

Remark 11.28 (For $\lambda > 0$, $d_{\mathbf{l},\lambda}^{\text{dynM}}$ generalizes the Gromov-Hausdorff distance). Let $\lambda > 0$. Given any two constant DMSs $\gamma_X \equiv (X, d_X)$ and $\gamma_Y \equiv (Y, d_Y)$, the metric $d_{\mathbf{l},\lambda}^{\text{dynM}}$ recovers the Gromov-Hausdorff distance between (X, d_X) and (Y, d_Y) up to multiplicative constant $\frac{\lambda}{2}$. Indeed, for any tripod $R: X \xleftarrow{\varphi_X} Z \xrightarrow{\varphi_Y} Y$ between X and Y , condition (11) reduces to

$$|d_X(\varphi_X(z), \varphi_X(z')) - d_Y(\varphi_Y(z), \varphi_Y(z'))| \leq \lambda \varepsilon \text{ for all } z, z' \in Z.$$

Therefore,

$$d_{\text{GH}}((X, d_X), (Y, d_Y)) = \frac{\lambda}{2} \cdot d_{\mathbf{l},\lambda}^{\text{dynM}}(\gamma_X, \gamma_Y).$$

We have the following bilipschitz-equivalence relation between the metrics $d_{\mathbf{l},\lambda}^{\text{dynM}}$ for different $\lambda > 0$.

Proposition 11.29 (Bilipschitz-equivalence). For all $0 < \lambda < \lambda'$,

$$d_{\mathbf{l},\lambda'}^{\text{dyn}} \leq d_{\mathbf{l},\lambda}^{\text{dynM}} \leq \frac{\lambda'}{\lambda} \cdot d_{\mathbf{l},\lambda'}^{\text{dyn}}.$$

Proof. Fix any two DMSs γ_X and γ_Y over X and Y . That $d_{\mathbf{l},\lambda'}^{\text{dynM}}(\gamma_X, \gamma_Y) \leq d_{\mathbf{l},\lambda}^{\text{dynM}}(\gamma_X, \gamma_Y)$ follows from the observation that any (λ, ε) -tripod R between γ_X and γ_Y is also a (λ', ε) -tripod (Definition 9.10). We next prove $d_{\mathbf{l},\lambda}^{\text{dynM}}(\gamma_X, \gamma_Y) \leq \frac{\lambda'}{\lambda} \cdot d_{\mathbf{l},\lambda'}^{\text{dyn}}(\gamma_X, \gamma_Y)$. For some $\varepsilon \geq 0$ let R be any (λ', ε) -tripod between γ_X and γ_Y . It suffices to show that R is also a $(\lambda, \frac{\lambda'}{\lambda} \varepsilon)$ -tripod. Fix any $t \in T$. Then,

$$\bigvee_{[t] \left(\frac{\lambda'}{\lambda} \varepsilon \right)} d_X \leq \bigvee_{[t]^\varepsilon} d_X \leq_R d_Y(t) + \lambda' \varepsilon = d_Y(t) + \lambda \left(\frac{\lambda'}{\lambda} \varepsilon \right).$$

By symmetry, we also have $\bigvee_{[t] \left(\frac{\lambda'}{\lambda} \varepsilon \right)} d_Y \leq_R d_X(t) + \lambda \left(\frac{\lambda'}{\lambda} \varepsilon \right)$, as desired. \square

Computational details from examples. What follows complements Example 9.16 and Remark 9.23.

Details from Example 9.16. First, we show that $d_1^{\text{dynM}}(\gamma_X^{\psi_0}, \gamma_X^{\psi_1}) \leq \min(\tau, \frac{2\pi}{\omega} - \tau)$. Consider the tripod $R: X \xleftarrow{\text{id}_X} X \xrightarrow{\text{id}_X} X$ and define $\alpha, \beta: \mathbf{R} \rightarrow \mathbf{R}$ to be $\alpha(t) = t - \tau$ and $\beta(t) = t + \tau$ for all $t \in \mathbf{R}$. Then, since $\|\alpha - \text{id}_{\mathbf{R}}\|_\infty = \|\beta - \text{id}_{\mathbf{R}}\|_\infty = \tau$, it follows that for all $t \in \mathbf{R}$, $\min_{s \in [t]^\tau} d_X^{\psi_1}(s)(x, x') \leq d_X^{\psi_1}(\alpha(t))(x, x') = d_X^{\psi_0}(t)(x, x')$, and $\min_{s \in [t]^\tau} d_X^{\psi_0}(s)(x, x') \leq d_X^{\psi_0}(\beta(t))(x, x') = d_X^{\psi_1}(t)(x, x')$. Therefore, $d_1^{\text{dynM}}(\gamma_X^{\psi_0}, \gamma_X^{\psi_1}) \leq \tau$. On the other hand, letting $\tilde{\alpha}, \tilde{\beta}: \mathbf{R} \rightarrow \mathbf{R}$ be $\tilde{\alpha}(t) = t + \frac{2\pi}{\omega} - \tau$ and $\tilde{\beta}(t) = t - \frac{2\pi}{\omega} + \tau$, one can check that $d_1^{\text{dynM}}(\gamma_X^{\psi_0}, \gamma_X^{\psi_1}) \leq \frac{2\pi}{\omega} - \tau$ in the same way and this completes the proof for $d_1^{\text{dynM}}(\gamma_X^{\psi_0}, \gamma_X^{\psi_1}) \leq \min(\tau, \frac{2\pi}{\omega} - \tau)$. Next, we prove that $\min(\tau, \frac{2\pi}{\omega} - \tau) \leq d_1^{\text{dynM}}(\gamma_X^{\psi_0}, \gamma_X^{\psi_1})$. Pick any $t_0 \in \mathbf{R}$ such that $d_X^{\psi_0}(t_0)(x, x') = 0$. Then the nearest $s \in \mathbf{R}$ from t_0 such that $d_X^{\psi_1}(s)(x, x') = 0$ is at distance $\min(\tau, \frac{2\pi}{\omega} - \tau)$ from t_0 . This leads to the conclusion that the value of $d_1^{\text{dynM}}(\gamma_X^{\psi_0}, \gamma_X^{\psi_1})$ is at least $\min(\tau, \frac{2\pi}{\omega} - \tau)$, as desired. \square

Recall the notion of δ -matching and bottleneck distance from Definition 11.7.

Details from Remark 9.23. Consider DMSs $\gamma_X^{\psi_0}(t) := (X, \psi_0(t) \cdot d_X)$ and $\gamma_X^{\psi_1}(t) := (X, \psi_1(t) \cdot d_X)$ as in Example 9.16. For simplicity, let $\omega = 1$. We will compute the barcodes of the saturated formigrams $\theta_{X,\delta}^0 := \pi_0(\mathcal{R}_\delta^1(\gamma_X^{\psi_0}))$ and $\theta_{X,\delta}^1 := \pi_0(\mathcal{R}_\delta^1(\gamma_X^{\psi_1}))$ and the bottleneck distance between them for all possible choices of the connectivity parameter $\delta \geq 0$.

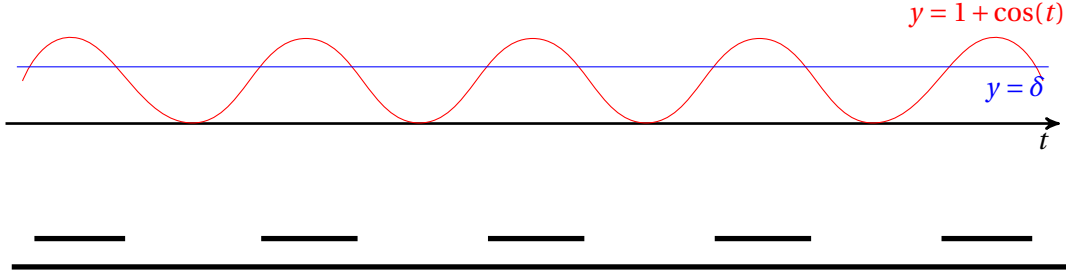


Figure 14: The upper picture represents the graph of $y = 1 + \cos(t)$ and $y = \delta$. Below is the graphical representation of the barcode $\text{dgm}(\theta_{X,\delta}^0)$. Here we depict the regime $\delta \in [0, 2)$. Since the set $\{t \in \mathbf{R} : 1 + \cos(t) > \delta\}$ consists of intervals of length $2\arccos(\delta - 1)$, the barcode $\text{dgm}(\theta_{X,\delta}^0)$ consists of infinitely many intervals of length $2\arccos(\delta - 1)$ plus one copy of $(-\infty, \infty)$.

Case 1. $\delta \geq 2$. Observe that if the connectivity parameter δ is ≥ 2 , then both $\mathcal{R}_\delta^1(\gamma_X^{\psi_0})$ and $\mathcal{R}_\delta^1(\gamma_X^{\psi_1})$ are identical to the constant DG $\mathcal{G}_X = (V_X(\cdot), E_X(\cdot))$ such that for all $t \in \mathbf{R}$, $\mathcal{G}_X(t)$ is the graph on the vertex set $X = \{x, x'\}$ with the edge set $E_X = \{\{x, x'\}, \{x, x\}, \{x', x'\}\}$. Hence, both $\theta_{X,\delta}^0$ and $\theta_{X,\delta}^1$ are constant formigrams defined by $\theta_{X,\delta}^0(t) = \theta_{X,\delta}^1(t) = \{\{x, x'\}\}$ for all $t \in \mathbf{R}$. By Remark 5.11, in this case both barcodes of θ_X^0 and θ_X^1 consist solely of the interval $(-\infty, \infty)$ with multiplicity 1, and thus $d_B(\text{dgm}(\theta_{X,\delta}^0), \text{dgm}(\theta_{X,\delta}^1)) = 0$.

Case 2. $0 < \delta < 2$. In this case, we shall check that

$$d_B(\text{dgm}(\theta_{X,\delta}^0), \text{dgm}(\theta_{X,\delta}^1)) = \min(\tau, 2\pi - \tau, \arccos(\delta - 1)). \quad (16)$$

First, we compute the barcodes $\text{dgm}(\theta_{X,\delta}^0)$ and $\text{dgm}(\theta_{X,\delta}^1)$. Notice that the formigram $\theta_{X,\delta}^0 : \mathbf{R} \rightarrow \mathcal{P}(X)$ is defined by

$$\theta_{X,\delta}^0(t) = \begin{cases} \{\{x\}, \{x'\}\}, & \text{if } 1 + \cos(t) > \delta, \\ \{\{x, x'\}\}, & \text{otherwise.} \end{cases}$$

Define any strictly increasing function $\mathcal{G} : \mathbf{Z} \rightarrow \mathbf{R}$ such that $\text{im}(\mathcal{G})$ becomes the solution set of the equation $1 + \cos(t) = \delta$. Let $c_i := \mathcal{G}(i)$ for $i \in \mathbf{Z}$. Then, the zigzag module $\mathbb{V}_{\theta_{X,\delta}^0}$ defined as in equation (6) is isomorphic to

$$\begin{array}{ccccccc} \cdots & & \mathbb{F} & & \mathbb{F} & & \mathbb{F} & & \cdots \\ & \nwarrow (1\ 0) & \nearrow & \nwarrow & \nearrow & \nwarrow (1\ 0) & \nearrow & \nwarrow & \nearrow \\ & \mathbb{F}^2 & & \mathbb{F} & & \mathbb{F}^2 & & \mathbb{F} & \\ & \nearrow & \nwarrow 1 & \nearrow & \nwarrow & \nearrow & \nwarrow 1 & \nearrow & \nwarrow \end{array}$$

and in turn $\text{dgm}(\theta_{X,\delta}^0)$ consists of infinitely many intervals of length $2\arccos(\delta - 1)$ and one copy of $(-\infty, \infty)$ (see Figure 14). Also, the barcode $\text{dgm}(\theta_{X,\delta}^1)$ is obtained by parallel translation of all the intervals in $\text{dgm}(\theta_{X,\delta}^0)$ by $-\tau$ (or equivalently by $2\pi - \tau$).

Then one can easily check that the bottleneck distance $d_B(\text{dgm}(\theta_{X,\delta}^0), \text{dgm}(\theta_{X,\delta}^1))$ is the smallest number among $\tau, 2\pi - \tau$ and $\arccos(\delta - 1)$ (see Figure 15). In Example 9.16, we already saw that $d_I^{\text{dynM}}(\gamma_X^{\psi_0}, \gamma_X^{\psi_1}) = \min(\tau, 2\pi - \tau)$. Therefore, if $0 < \delta < 2$ is a value such that $\arccos(\delta - 1)$ is greater than either of τ and $2\pi - \tau$, then we have $d_I^{\text{dynM}}(\gamma_X^{\psi_0}, \gamma_X^{\psi_1}) = d_B(\text{dgm}(\theta_{X,\delta}^0), \text{dgm}(\theta_{X,\delta}^1))$.

Case 3. $\delta = 0$. In a similar way to *Case 2*, one can check that

$$d_B(\text{dgm}(\theta_{X,\delta}^0), \text{dgm}(\theta_{X,\delta}^1)) = \min(\tau, 2\pi - \tau).$$

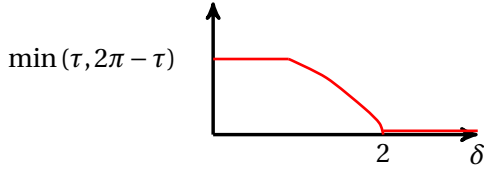


Figure 15: Given a fixed $\tau \in (0, 2\pi)$ this figure shows the graph of the function $f(\delta) := \min(\tau, 2\pi - \tau, \arccos(\delta - 1))$ for $\delta \geq 0$.

Since $\arccos(-1) = \pi \geq \min(\tau, 2\pi - \tau)$ for any $\tau \in (0, 2\pi)$, and $\arccos(1) = 0$, equation (16) holds for all $\delta \in [0, 2]$. \square

Remark 11.30 (Tightness of the bound in Theorem 9.21). Recall that in the inequality of Theorem 9.21, the coefficient 2 was placed in front of the interleaving distance d_1^{dynM} . We conjecture that this coefficient 2 can be reduced to 1. We have not found a proof nor a counter-example for this yet.

Computational complexity of d_1^{dynM} . We relate the Gromov-Hausdorff distance between two given ultrametric spaces to the interleaving distance d_1^{dynM} between certain derived DMSs. Then, invoking results from F. Schmiedl's PhD thesis we obtain the claim of Theorem 9.25.

Given a nontrivial ultrametric space (X, u_X) , define a DMS $\mathcal{D}(X, u_X) := (X, d_X(\cdot))$ where for all $x, x' \in X$ and for all $t \in \mathbf{R}$, $d_X(t)(x, x') := \max(0, u_X(x, x') - t)$. It is noteworthy that for any $x, x' \in X$, $d_X(\cdot)(x, x') : \mathbf{R} \rightarrow \mathbf{R}_+$ is decreasing down to zero and that $d_X(0) = u_X$, a legitimate metric (i.e. not just pseudo-metric), satisfying the second item of Definition 9.1. Furthermore, note that $\mathcal{D}(X, u_X)$ is clearly piecewise linear and that the set of breakpoints is $S_{\mathcal{D}(X, u_X)} = \{u_X(x, x'), x, x' \in X\}$. Recall Definition 11.1.

Proposition 11.31. For any two nontrivial ultrametric spaces (X, u_X) and (Y, u_Y) we have

$$d_1^{\text{dynM}}(\mathcal{D}(X, u_X), \mathcal{D}(Y, u_Y)) = 2 d_{\text{GH}}((X, u_X), (Y, u_Y)).$$

Proof. Let $\mathcal{D}(X, u_X) = (X, d_X(\cdot))$ and $\mathcal{D}(Y, u_Y) = (Y, d_Y(\cdot))$. Observe that for any $x, x' \in X$, any $t \in \mathbf{R}$, and any $\varepsilon \geq 0$, $\min_{s \in [t, t+\varepsilon]} d_X(s)(x, x') = d_X(t+\varepsilon)(x, x')$ since d_X is decreasing over time. Thus, for some $\varepsilon \geq 0$, a tripod $R : X \xleftarrow{\varphi_X} Z \xrightarrow{\varphi_Y} Y$ is an ε -tripod between (X, d_X) and (Y, d_Y) (Definition 11.1) if and only if for all $z, z' \in Z$ and for all $t \in \mathbf{R}$, $d_X(t+\varepsilon)(\varphi_X(z), \varphi_X(z')) \leq d_Y(t)(\varphi_Y(z), \varphi_Y(z'))$ and $d_Y(t+\varepsilon)(\varphi_Y(z), \varphi_Y(z')) \leq d_X(t)(\varphi_X(z), \varphi_X(z'))$, if and only if for all $z, z' \in Z$ and for all $t \in \mathbf{R}$, $\max(0, u_X(\varphi_X(z), \varphi_X(z')) - t - \varepsilon) \leq \max(0, u_Y(\varphi_Y(z), \varphi_Y(z')) - t)$ and $\max(0, u_Y(\varphi_Y(z), \varphi_Y(z')) - t - \varepsilon) \leq \max(0, u_X(\varphi_X(z), \varphi_X(z')) - t)$ if and only if for all $z, z' \in Z$, $|u_X(\varphi_X(z), \varphi_X(z')) - u_Y(\varphi_Y(z), \varphi_Y(z'))| \leq \varepsilon$, completing the proof. \square

Proof of Theorem 9.25. Pick any two non-trivial ultrametric spaces (X, u_X) and (Y, u_Y) . Then, by Proposition 11.31, the interleaving distance between $\mathcal{D}(X, u_X)$ and $\mathcal{D}(Y, u_Y)$ is identical to twice the Gromov-Hausdorff distance $\Delta := d_{\text{GH}}((X, u_X), (Y, u_Y))$ between (X, u_X) and (Y, u_Y) . The rest of the proof follows along the same lines as that of Theorem 6.11. \square

11.4.3 The maximal groups [10] of DMSs and their clustering barcodes

In this section we investigate the connection between the maximal groups and the barcode of formigrams derived from DMSs. Let γ_X be a tame DMS and fix $\delta \geq 0$. Consider the barcode $\text{dgm}(\theta_X)$ of the formigram $\theta_X := \pi_0(\mathcal{R}_\delta^1(\gamma_X))$ (Propositions 9.20 and 5.16). This θ_X is saturated and thus by Remark 5.13, the barcode of θ_X consists solely of open intervals. For any finite open interval $(a, b) \subset \mathbf{R}$, we call a and b the *left endpoint* and the *right endpoint* of (a, b) , respectively.

Proposition 11.32. For $m \in \mathbf{N}$, if some $t \in \mathbf{R}$ is a left endpoint of m distinct intervals in $\text{dgm}(\theta_X)$, then this signifies a disbanding event of some $(1, \delta, 0)$ -maximal group[s] so that the number of clusters increases by m at time t . On the other hand, if $t \in \mathbf{R}$ is a right endpoint of m distinct intervals in $\text{dgm}(\theta_X)$, then this indicates a merging event of some $(1, \delta, 0)$ -maximal groups so that the number of clusters decreases by m at time t .

For $n \geq 2$, the connection between $(n, \delta, 0)$ -maximal groups and the barcode $\text{dgm}(\theta_X)$ is slightly opaque, compared to the one in the case $n = 1$: for $n \geq 2$, if $t \in \mathbf{R}$ is the left endpoint of an interval in $\text{dgm}(\theta_X)$, some of $(n, \delta, 0)$ -maximal groups may perish at time t because of a disbanding event of some clusters. Conversely, if $t \in \mathbf{R}$ is the right endpoint of an interval in $\text{dgm}(\theta_X)$, some of $(n, \delta, 0)$ -maximal groups can be born at $t \in \mathbf{R}$ out of a merging event of groups.

11.5 Details from Section 10

11.5.1 Zigzag simplicial filtrations and their barcodes

Consult [48] for the notions of abstract simplicial complex, simplicial map and homology. Given a finite non-empty set X , we denote the set of all the (abstract) simplicial complexes on any non empty vertex set $X' \subset X$ by $\mathcal{S}(X)$. We refer to any monotonic function $f: \mathbf{R} \rightarrow \mathcal{S}(X)$ as a *standard simplicial filtration on X* . That f is monotonic means that $f(a)$ is a subcomplex of $f(b)$, denoted by $f(a) \hookrightarrow f(b)$, whenever $a \leq b$. We generalize this familiar object in TDA by allowing the simplicial complexes to sometimes become “smaller”.

Definition 11.33 (Zigzag simplicial filtration). Let X be a non-empty finite set. A *zigzag simplicial filtration* on X is any function $f: \mathbf{R} \rightarrow \mathcal{S}(X)$ with some conditions below. Let $\text{crit}(f)$ denote that set of points of discontinuity of the zigzag simplicial filtration f . We call the elements of $\text{crit}(f)$ *the critical points of f* . We require f to satisfy the following:

- (i) (Tameness) The set $\text{crit}(f)$ is locally finite.
- (ii) (Comparability) For any point $c \in \mathbf{R}$, it holds that $f(c - \varepsilon) \hookrightarrow f(c) \hookleftarrow f(c + \varepsilon)$ for all sufficiently small $\varepsilon > 0$.¹⁵

Remark 11.34. (i) In Definition 11.33, when f is right-continuous, f is a standard simplicial filtration. The Rips filtration on a finite metric space is an example of standard simplicial filtration.

- (ii) Let $F: \mathbf{Graph} \rightarrow \mathbf{Simp}$ be the functor that sends each graph $G_X = (X, E_X)$ to the 1-dimensional simplicial complex obtained by getting rid of all self-loops in G_X . Given a DG $\mathcal{G}_X = (V_X(\cdot), E_X(\cdot))$, it is not difficult to check that the map $F \circ \mathcal{G}_X: \mathbf{R} \rightarrow \mathcal{S}(X)$ defined as $t \mapsto F(\mathcal{G}_X(t))$ is a zigzag simplicial filtration on X .

Barcode of a zigzag simplicial filtration. We define the homology barcode of zigzag simplicial filtrations (Definition 11.33).

Let $f: \mathbf{R} \rightarrow \mathcal{S}(X)$ be a zigzag simplicial filtration on X . We wish to keep track of the homological features of f . Let $\text{crit}(f) = \{c_i : i \in \mathbf{Z}\}$ such that $\dots < c_{i-1} < c_i < c_{i+1} < \dots$, $\lim_{i \rightarrow +\infty} c_i = +\infty$, and $\lim_{i \rightarrow -\infty} c_i = -\infty$ (if $\text{crit}(f)$ is finite, then choose $\{c_i : i \in \mathbf{Z}\}$ to be any superset of $\text{crit}(f)$). For each $i \in \mathbf{Z}$, pick any $s_i \in (c_i, c_{i+1})$. Then we have the following chain of inclusion maps:

$$\mathbb{S}_f: \quad \cdots \quad \begin{array}{ccccc} & f(c_{i-1}) & & f(c_i) & & f(c_{i+1}) & \\ & \nearrow & \nwarrow & \nearrow & \nwarrow & \nearrow & \\ & & f(s_{i-1}) & & f(s_i) & & \end{array} \quad \cdots \quad (17)$$

Note that different choices of $s_i \in (c_i, c_{i+1})$ do not change the structure of this diagram. This diagram is a diagram in the category **Simp**. For any $k \in \mathbf{Z}_+$, by applying the simplicial homology functor H_k (with coefficients in the field \mathbb{F}) to this diagram, we obtain the following diagram in **Vec**.

$$H_k(\mathbb{S}_f): \quad \cdots \quad \begin{array}{ccccc} & V_{c_{i-1}} & & V_{c_i} & & V_{c_{i+1}} & \\ & \nearrow & \nwarrow & \nearrow & \nwarrow & \nearrow & \\ & & V_{s_{i-1}} & & V_{s_i} & & \end{array} \quad \cdots \quad (18)$$

¹⁵If c is a point of discontinuity, then at least one of the inclusions of $f(c - \varepsilon) \hookrightarrow f(c) \hookleftarrow f(c + \varepsilon)$ would be strict for small $\varepsilon > 0$. But, if f is continuous at c , then both inclusions are actually the identity map for small $\varepsilon > 0$.

where V_{c_j}, V_{s_j} are the vector spaces $H_k(f(c_j))$ and $H_k(f(s_j))$, respectively and the arrows are the linear maps obtained by applying H_k to the inclusions in (17). Then the k -th homology barcode of f is defined as in the same way as the barcode of a formigram (see table (7)).

Remark 11.35. Recall that any DG \mathcal{G}_X can be mapped to a (1-dimensional) zigzag simplicial filtration $F \circ \mathcal{G}_X$ (Remark 11.34, (ii)). For any DG \mathcal{G}_X , it is not difficult to check that the barcode of the formigram $\theta_X = \pi_0(\mathcal{G}_X)$ (Proposition 5.16) is identical to the 0-th homology barcode of $F \circ \mathcal{G}_X$.

References

- [1] G. Azumaya et al. Corrections and supplementaries to my paper concerning krull-remak-schmidt's theorem. *Nagoya Mathematical Journal*, 1:117–124, 1950.
- [2] U. Bauer, C. Landi, and F. Memoli. The reeb graph edit distance is universal. *arXiv preprint arXiv:1801.01866*, 2018.
- [3] U. Bauer and M. Lesnick. Induced matchings and the algebraic stability of persistence barcodes. *Journal of Computational Geometry*, 6(2):162–191, 2015.
- [4] M. Benkert, J. Gudmundsson, F. Hübner, and T. Wollé. Reporting flock patterns. *Computational Geometry*, 41(3):111–125, 2008.
- [5] H. B. Bjerkevik. Stability of higher-dimensional interval decomposable persistence modules. *arXiv preprint arXiv:1609.02086*, 2016.
- [6] J. Bondy and U. Murty. *Graph theory (graduate texts in mathematics)*. Springer New York, 2008.
- [7] M. B. Botnan. Interval decomposition of infinite zigzag persistence modules. *Proceedings Of The American Mathematical Society*, 145(8):3571–3577, 2017.
- [8] M. B. Botnan and M. Lesnick. Algebraic stability of persistence modules. *arXiv preprint arXiv:1604.00655*, 2016.
- [9] P. Bubenik and J. A. Scott. Categorification of persistent homology. *Discrete & Computational Geometry*, 51(3):600–627, 2014.
- [10] K. Buchin, M. Buchin, M. J. van Kreveld, B. Speckmann, and F. Staals. Trajectory grouping structure. *JoCG*, 6(1):75–98, 2015.
- [11] D. Burago, Y. Burago, and S. Ivanov. *A course in metric geometry*, volume 33.
- [12] G. Carlsson and V. De Silva. Zigzag persistence. *Foundations of computational mathematics*, 10(4):367–405, 2010.
- [13] G. Carlsson, V. De Silva, and D. Morozov. Zigzag persistent homology and real-valued functions. In *Proceedings of the twenty-fifth annual symposium on Computational geometry*, pages 247–256. ACM, 2009.
- [14] G. Carlsson and F. Mémoli. Characterization, stability and convergence of hierarchical clustering methods. *Journal of Machine Learning Research*, 11:1425–1470, 2010.
- [15] G. Carlsson and F. Mémoli. Classifying clustering schemes. *Foundations of Computational Mathematics*, 13(2):221–252, 2013.
- [16] G. Carlsson, F. Mémoli, A. Ribeiro, and S. Segarra. Axiomatic construction of hierarchical clustering in asymmetric networks. In *Acoustics, Speech and Signal Processing (ICASSP), 2013 IEEE International Conference on*, pages 5219–5223. IEEE, 2013.

- [17] F. Chazal, D. Cohen-Steiner, M. Glisse, L. J. Guibas, and S. Oudot. Proximity of persistence modules and their diagrams. In *Proc. 25th ACM Sympos. on Comput. Geom.*, pages 237–246, 2009.
- [18] F. Chazal, D. Cohen-Steiner, L. J. Guibas, F. Mémoli, and S. Y. Oudot. Gromov-Hausdorff stable signatures for shapes using persistence. In *Proc. of SGP*, 2009.
- [19] D. Cohen-Steiner, H. Edelsbrunner, and J. Harer. Stability of persistence diagrams. *Discrete & Computational Geometry*, 37(1):103–120, 2007.
- [20] D. Cohen-Steiner, H. Edelsbrunner, and D. Morozov. Vines and vineyards by updating persistence in linear time. In *Proceedings of the twenty-second annual symposium on Computational geometry*, pages 119–126. ACM, 2006.
- [21] P. Corcoran and C. B. Jones. Modelling topological features of swarm behaviour in space and time with persistence landscapes. *IEEE Access*, 5:18534–18544, 2017.
- [22] V. De Silva, E. Munch, and A. Patel. Categorified reeb graphs. *Discrete & Computational Geometry*, 55(4):854–906, 2016.
- [23] T. K. Dey, A. Rossi, and A. Sidiropoulos. Temporal clustering. *arXiv preprint arXiv:1704.05964*, 2017.
- [24] T. K. Dey, A. Rossi, and A. Sidiropoulos. Temporal hierarchical clustering. *arXiv preprint arXiv:1707.09904*, 2017.
- [25] H. Edelsbrunner, J. Harer, A. Mascarenhas, V. Pascucci, and J. Snoeyink. Time-varying reeb graphs for continuous space-time data. *Computational Geometry*, 41(3):149–166, 2008.
- [26] H. Edelsbrunner, G. Jabłoński, and M. Mrozek. The persistent homology of a self-map. *Foundations of Computational Mathematics*, 15(5):1213–1244, 2015.
- [27] R. Gonzalez-Diaz, M.-J. Jimenez, and B. Medrano. Spatiotemporal barcodes for image sequence analysis. In *International Workshop on Combinatorial Image Analysis*, pages 61–70. Springer, 2015.
- [28] J. Gudmundsson and M. van Kreveld. Computing longest duration flocks in trajectory data. In *Proceedings of the 14th annual ACM international symposium on Advances in geographic information systems*, pages 35–42. ACM, 2006.
- [29] J. Gudmundsson, M. van Kreveld, and B. Speckmann. Efficient detection of patterns in 2d trajectories of moving points. *Geoinformatica*, 11(2):195–215, 2007.
- [30] M. Hajij, B. Wang, C. Scheidegger, and P. Rosen. Visual detection of structural changes in time-varying graphs using persistent homology. arxiv preprint. *arXiv preprint arXiv:1707.06683*, 3, 2017.
- [31] A. Hatcher. *Algebraic Topology*. Cambridge U. Press, New York, 2002.
- [32] Y. Huang, C. Chen, and P. Dong. Modeling herds and their evolvments from trajectory data. In *International Conference on Geographic Information Science*, pages 90–105. Springer, 2008.
- [33] S.-Y. Hwang, Y.-H. Liu, J.-K. Chiu, and E.-P. Lim. Mining mobile group patterns: A trajectory-based approach. In *PAKDD*, volume 3518, pages 713–718. Springer, 2005.
- [34] N. Jardine and R. Sibson. *Mathematical taxonomy*. John Wiley & Sons Ltd., London, 1971. Wiley Series in Probability and Mathematical Statistics.
- [35] H. Jeung, M. L. Yiu, X. Zhou, C. S. Jensen, and H. T. Shen. Discovery of convoys in trajectory databases. *Proceedings of the VLDB Endowment*, 1(1):1068–1080, 2008.

- [36] P. Kalnis, N. Mamoulis, and S. Bakiras. On discovering moving clusters in spatio-temporal data. In *SSTD*, volume 3633, pages 364–381. Springer, 2005.
- [37] W. Kim and F. Mémoli. Formigrams: Clustering summaries of dynamic data. In *Proceedings of 30th Canadian Conference on Computational Geometry (CCCG18)*.
- [38] W. Kim and F. Mémoli. Stable invariants of dynamic metric spaces. *In preparation*, 2018.
- [39] W. Kim, F. Mémoli, and Z. Smith. <https://research.math.osu.edu/networks/formigrams>.
- [40] I. Kostitsyna, M. J. van Kreveld, M. Löffler, B. Speckmann, and F. Staals. Trajectory grouping structure under geodesic distance. In *31st International Symposium on Computational Geometry, SoCG 2015, June 22–25, 2015, Eindhoven, The Netherlands*, pages 674–688, 2015.
- [41] M. Lesnick. The theory of the interleaving distance on multidimensional persistence modules. *Found. Comput. Math.*, 15(3):613–650, June 2015.
- [42] Z. Li, B. Ding, J. Han, and R. Kays. Swarm: Mining relaxed temporal moving object clusters. *Proceedings of the VLDB Endowment*, 3(1-2):723–734, 2010.
- [43] S. Mac Lane. *Categories for the working mathematician*, volume 5. Springer Science & Business Media, 2013.
- [44] F. Mémoli. A distance between filtered spaces via tripods. *arXiv preprint arXiv:1704.03965*, 2017.
- [45] N. Milosavljević, D. Morozov, and P. Skraba. Zigzag persistent homology in matrix multiplication time. In *Proceedings of the Twenty-seventh Annual Symposium on Computational Geometry, SoCG ’11*, pages 216–225, New York, NY, USA, 2011. ACM.
- [46] D. Morozov, K. Beketayev, and G. Weber. Interleaving distance between merge trees. *Discrete and Computational Geometry*, 49:22–45, 2013.
- [47] E. Munch. *Applications of persistent homology to time varying systems*. PhD thesis, 2013.
- [48] J. R. Munkres. *Elements of algebraic topology*, volume 2. Addison-Wesley Menlo Park, 1984.
- [49] P. Oesterling, C. Heine, G. H. Weber, D. Morozov, and G. Scheuermann. Computing and visualizing time-varying merge trees for high-dimensional data. In *Topological Methods in Data Analysis and Visualization*, pages 87–101. Springer, 2015.
- [50] J. K. Parrish and W. M. Hamner. *Animal groups in three dimensions: how species aggregate*. Cambridge University Press, 1997.
- [51] F. Schmedl. Computational aspects of the gromov–hausdorff distance and its application in non-rigid shape matching. *Discrete & Computational Geometry*, 57(4):854–880, 2017.
- [52] Z. Smith, S. Chowdhury, and F. Mémoli. Hierarchical representations of network data with optimal distortion bounds. In *Signals, Systems and Computers, 2016 50th Asilomar Conference on*, pages 1834–1838. IEEE, 2016.
- [53] D. J. Sumpter. *Collective animal behavior*. Princeton University Press, 2010.
- [54] C. M. Topaz, L. Ziegelmeier, and T. Halverson. Topological data analysis of biological aggregation models. *PloS one*, 10(5):e0126383, 2015.

- [55] A. van Goethem, M. J. van Kreveld, M. Löffler, B. Speckmann, and F. Staals. Grouping time-varying data for interactive exploration. In *32nd International Symposium on Computational Geometry, SoCG 2016, June 14-18, 2016, Boston, MA, USA*, pages 61:1–61:16, 2016.
- [56] M. J. van Kreveld, M. Löffler, and F. Staals. Central trajectories. *Journal of Computational Geometry*, 8(1):366–386, 2017.
- [57] M. J. van Kreveld, M. Löffler, F. Staals, and L. Wiratma. A refined definition for groups of moving entities and its computation. In *27th International Symposium on Algorithms and Computation, ISAAC 2016, December 12-14, 2016, Sydney, Australia*, pages 48:1–48:12, 2016.
- [58] M. R. Vieira, P. Bakalov, and V. J. Tsotras. On-line discovery of flock patterns in spatio-temporal data. In *Proceedings of the 17th ACM SIGSPATIAL international conference on advances in geographic information systems*, pages 286–295. ACM, 2009.
- [59] Y. Wang, E.-P. Lim, and S.-Y. Hwang. Efficient algorithms for mining maximal valid groups. *The VLDB Journal—The International Journal on Very Large Data Bases*, 17(3):515–535, 2008.
- [60] W. Widanagamaachchi, C. Christensen, V. Pascucci, and P.-T. Bremer. Interactive exploration of large-scale time-varying data using dynamic tracking graphs. In *Large data analysis and visualization (LDAV), 2012 IEEE Symposium on*, pages 9–17. IEEE, 2012.
- [61] Wikipedia. Formicarium — Wikipedia, the free encyclopedia, 2017. [Online; accessed 03-June-2017].